



Application of Cementitious Materials and Fiber Reinforcement to Enhance Lime Stabilization for Nebraska Shale Soils

Jongwan Eun, PhD, PE

Assistant Professor
Department of Civil and Environmental Engineering
University of Maryland

Laith Ibdah

Graduate Research Assistant
Department of Civil and Environmental Engineering
University of Maryland

Seunghee Kim, PhD, PE

Associate Professor
Department of Civil and Environmental Engineering
University of Nebraska-Lincoln

Chung R. Song, PhD

Associate Professor
Department of Civil and Environmental Engineering
University of Nebraska-Lincoln

Kenaz Owusu

Graduate Research Assistant
Department of Civil and Environmental Engineering
University of Nebraska-Lincoln

Nebraska Department of Transportation Research

Headquarters Address (402) 479-4697
1400 Nebraska Parkway <https://dot.nebraska.gov/business-center/research/>
Lincoln, NE 68509 ndot.research@nebraska.gov

Nebraska Transportation Center

262 Prem S. Paul Research (402) 472-1932
Center at Whittier School <http://ntc.unl.edu>
2200 Vine Street
Lincoln, NE 68583-0851

This report was funded in part through grant from the U.S. Department of Transportation Federal Highway Administration. The views and opinions of the authors expressed herein do not necessarily state or reflect those of the U.S. Department of Transportation.

Application of Cementitious Materials and Fiber Reinforcement to Enhance Lime
Stabilization for Nebraska Shale Soils

Jongwan Eun, Ph.D., P.E.
Assistant Professor
Department of Civil and Environmental
Engineering
University of Maryland

Chung R. Song, Ph.D.
Associate Professor
Department of Civil and Environmental
Engineering
University of Nebraska-Lincoln

Laith Ibdah
Graduate Research Assistant
Department of Civil and Environmental
Engineering
University of Maryland

Kenaz Owusu
Graduate Research Assistant
Department of Civil and Environmental
Engineering
University of Nebraska-Lincoln

Seunghee Kim, Ph.D., P.E.
Associate Professor
Department of Civil and Environmental
Engineering
University of Nebraska-Lincoln

Sponsored By
Nebraska Department of Transportation and U.S. Department of Transportation Federal
Highway Administration

February 2025

TECHNICAL REPORT DOCUMENTATION PAGE

1. Report No. SPR-FY23(015)	2. Government Accession No.		3. Recipient's Catalog No.	
4. Title and Subtitle Application of Cementitious Materials and Fiber Reinforcement to Enhance Lime Stabilization for Nebraska Shale Soils			5. Report Date February 2025	
			6. Performing Organization Code	
7. Author(s) Jongwan Eun, Seunghye Kim, Chung R. Song, Laith Ibdah, Kenaz Owusu			8. Performing Organization Report No. If applicable, enter any/all unique numbers assigned to the performing organization.	
9. Performing Organization Name and Address Board of Regents, University of Nebraska-Lincoln			10. Work Unit No.	
			11. Contract	
12. Sponsoring Agency Name and Address Nebraska Department of Transportation Research Section 1400 Nebraska Parkway Lincoln, NE 68502			13. Type of Report and Period Covered Final Report July 2022 to February 2025	
			14. Sponsoring Agency Code	
15. Supplementary Notes If applicable, enter information not included elsewhere, such as translation of (or by), report supersedes, old edition number, alternate title (e.g. project name), or hypertext links to documents or related information.				
16. Abstract Lime stabilization is a widely used technique to improve weak subgrades; however, its effectiveness under freeze-thaw cycles remains a critical challenge. This study investigates the incorporation of cementitious materials and fiber to enhance the mechanical properties and environmental resistance of lime-stabilized soils under such conditions. Two types of soil, gray shale (plasticity index of 37.8) and clay soil (plasticity index of 19.0) from Nebraska, were used. Stabilization mixtures included lime dosages of 0%, 3%, and 6% by weight, combined with either 10% fly ash or 3% and 6% cement by weight, and 0% and 1% fiber. The experimental program comprised a multi-tiered approach: characterization of physical properties through geotechnical tests (e.g., particle size distribution, Atterberg limits, and standard Proctor tests), preparation of composite specimens for unconfined compressive strength (UCS) and direct shear testing, and evaluation of environmental resistance through freeze-thaw cycles (7 cycles after 14 days of curing and 12 cycles after 28 days of curing). Additionally, large-scale testing was conducted using the Large-Scale Track Wheel test to simulate field conditions. Results showed that lime and fly ash significantly reduced the plasticity index of gray shale, with less pronounced effects on clay soil. The UCS values for gray shale ranged from 61.2 to 300.7 psi for lime stabilization, 137 to 272 psi for lime and fly ash stabilization, and 129 to 490.8 psi for lime-cement stabilization. For clay soil, UCS values ranged from 68 to 149 psi for lime stabilization, 119 to 146 psi for lime and fly ash stabilization, and 204 to 379.2 psi for lime-cement stabilization. The inclusion of fiber further enhanced the shear strength parameters of the soils, particularly increasing cohesion. Cement-lime stabilization demonstrated superior UCS retention and resistance to freeze-thaw cycles for both soil types, outperforming lime alone and lime-fly ash treatments. These findings highlight the importance of incorporating cementitious materials to enhance the durability and performance of lime-stabilized soils under harsh environmental conditions.				
17. Key Words Enhance lime stabilization, fiber stabilization, freezing-thawing cycles, large-scale trucking wheel test, dynamic cone penetrometer		18. Distribution Statement No restrictions. This document is available through the National Technical Information Service. 5285 Port Royal Road Springfield, VA 22161		
19. Security Classification (of this report) Unclassified	20. Security Classification (of this page) Unclassified	21. No. of Pages 151	22. Price	

Disclaimer

The contents of this report reflect the views of the authors, who are responsible for the facts and the accuracy of the information presented herein. The contents do not necessarily reflect the official views or policies neither of the Nebraska Department of Transportations nor the University of Nebraska-Lincoln. This report does not constitute a standard, specification, or regulation. Trade or manufacturers' names, which may appear in this report, are cited only because they are considered essential to the objectives of the report.

The United States (U.S.) government and the State of Nebraska do not endorse products or manufacturers. This material is based upon work supported by the Federal Highway Administration under SPR-FY23(015). Any opinions, findings and conclusions or recommendations expressed in this publication are those of the author(s) and do not necessarily reflect the views of the Federal Highway Administration.

This report has been reviewed by the Nebraska Transportation Center for grammar and context, formatting, and compliance with Section 508 of the Rehabilitation Act of 1973.

Table of Contents

TECHNICAL REPORT DOCUMENTATION PAGE	ii
Disclaimer	iii
Table of Contents	iv
List of Figures	v
List of Tables	ix
Chapter 1 Introduction	1
1.1 Problem Statement	3
1.2 Objective of the study	4
Chapter 2 Literature Review	6
2.1 Mechanisms of Lime Stabilization	6
2.2 Combined Lime and Cement Stabilization for Soil Improvement	9
2.3 Fiber Reinforcement in Soil Stabilization.....	10
2.4 Environmental Resistance.....	13
2.5 Specifications and Guidelines of Other States' Department of Transportation.....	16
Chapter 3 Materials.....	30
3.1 Subgrade Soil Types	30
3.2 Stabilizers and Additives	34
Chapter 4 Methodology	38
4.1 Soil Preparation.....	39
4.2 Testing Matrix for Admixture Combinations	41
4.3 Basic Geotechnical Tests	42
4.4 Unconfined Compressive Strength Test	45
4.5 Direct Shear Test.....	51
4.6 Assessment of Environmental Resistance	52
4.7 Large-Scale Tracking Wheel (LSTW) Test.....	55
4.8 Dynamic Cone Penetrometer Test	66
Chapter 5 Results and Discussion.....	68
5.1 UCS Results.....	68
5.2 Direct Shear Results.....	74
5.3 Assessment of Environmental Resistance	81
5.4 Empirical Model for Estimating the UCS of Cementitious-Stabilized Soil	93
5.5 Analysis of LSTW test results	96
Chapter 6 Conclusion.....	118
Chapter 7 Recommendations	124
References.....	126

List of Figures

Figure 2.1 Comparison of soil state before and after lime application (adapted from Sargent, 2015).	7
Figure 2.2 Flocculation/agglomeration of clay sheets after lime application.	7
Figure 2.3 Formation of cementitious bonding products from hydration and pozzolanic reactions (adapted from Sargent, 2015).	9
Figure 2.4 Straw blower used to distribute the fiber in the Iowa Expo project (White et al., 2013).	12
Figure 2.5 UCS of lime-stabilized soil vs FT cycles (Tebaldi et al., 2016).	14
Figure 2.6 Lime-treated high-plasticity clay soil specimen with 7% dosage a) after the second drying cycle and b) after the fourth wetting cycle (Kumar et al., 2024).	15
Figure 2.7 Selected and surveyed states for DOT stabilization specifications.	17
Figure 2.8 Selecting stabilizer types for Texas (TxDOT, 2019).	20
Figure 2.9 Decision flowchart for selecting stabilizers based on soil properties and PI for CA DOT (Adapted from Jones et al, 2010).	26
Figure 3.1 Location of Grey Shale – Lynch and Location of Clay – Plattsmouth Soil Characteristics.	30
Figure 3.2 a) Grey shale from Lynch site and b) clay soil at Plattsmouth site.	31
Figure 3.3 Compaction curve for grey shale and clay soil.	33
Figure 3.4 Hydrometer analysis for grey shale and clay soil.	33
Figure 3.5 Additives used in the research: (a) Lime, (b) Cement, (c) Fly Ash, and (d) Fiber.	34
Figure 4.1 Overview of the methodology tasks for enhancing lime stabilization using cementitious materials and fiber.	39
Figure 4.2 Air drying clay soil.	40
Figure 4.3 Grinding of soil lumps.	40
Figure 4.4 Comparison of the impact of different lime contents with 0% and 10% fly ash on: a) liquid limit, b) plastic limit, and c) plasticity index of grey shale soil, and d) liquid limit, e) plastic limit, and f) plasticity index of clay soil.	45
Figure 4.5 GeoJac equipment for UCS testing.	47
Figure 4.6 UCS sample after testing.	47
Figure 4.7 (a) UCS mold and plugs (b) Sample Preparation (c) Sample extraction (d) UCS sample.	47
Figure 4.8 Curing Technique.	48
Figure 4.9 Instron testing device for fiber reinforced UCS.	49
Figure 4.10 UCS fiber reinforced preparation.	50
Figure 4.11 Grey shale fiber reinforced sample after testing.	50
Figure 4.12 Soil mixing, specimen molding, and final compacted sample prepared for direct shear testing.	52
Figure 4.13 Direct shear testing setup and failed samples after testing.	52
Figure 4.14 UCS samples stored in the Freezer.	55
Figure 4.15 Tire used for LSTW test.	57
Figure 4.16 LSTW test setup	57
Figure 4.17 Heavy duty plate compactor.	59
Figure 4.18 Placement of clay soil in steel box.	59
Figure 4.19 Compacted clay-fiber layer.	59
Figure 4.20 Schematic showing LVDTs and pressure cells positions in steel box.	60
Figure 4.21 String Potentiometer position.	61
Figure 4.22 Pressure cell on compacted sand layer.	63
Figure 4.23 Pressure cell on compacted clay layer.	63

Figure 4.24 Schematic of load cell position.....	64
Figure 4.25 Load cell positioned beneath actuator.	65
Figure 4.26 LSTW complete test setup.....	66
Figure 4.27 Schematic of DCP device.....	67
Figure 4.28 DCP test on compacted fiber reinforced clay layer.....	67
Figure 5.1 Comparison of UCS for grey shale and clay with 0%, 3%, and 6% lime (L), 0% and 10% fly ash (FA), and their combinations.	69
Figure 5.2 UCS results for grey shale soil: (a) stress-strain curves for lime-stabilized soil, (b) stress-strain curves for lime-fly ash stabilized soil, and (c) average UCS versus lime content.	70
Figure 5.3 UCS results for clay soil: (a) stress-strain curves for lime-stabilized soil, (b) stress-strain curves for lime-fly ash stabilized soil, and (c) average UCS versus lime content.....	71
Figure 5.4 Comparison of UCS for grey shale and clay with 0%, 3%, and 6% lime (L), 3%, and 6% cement (C), and their combinations.....	73
Figure 5.5 UCS values for grey shale and clay stabilized with lime and fiber.....	74
Figure 5.6 Shear stress versus normal stress for GL0F0.	76
Figure 5.7 Shear stress versus normal stress for GL0F1.	77
Figure 5.8 Shear stress versus normal stress for GL6F0.	77
Figure 5.9 Shear stress versus normal stress for BL0F0.....	79
Figure 5.10 Shear stress versus normal stress for BL0F1.....	80
Figure 5.11 Shear stress versus normal stress for BL3F0.....	80
Figure 5.12 Comparison of UCS for grey shale soil stabilized with lime and lime-fly ash after 28 days of curing and after 14 days of curing followed by 7 FT cycles.....	82
Figure 5.13 Comparison of UCS for clay soil stabilized with lime and lime-fly ash after 28 days of curing and 14 days of curing, followed by 7 FT cycles.	83
Figure 5.14 Comparison of UCS for grey shale soil stabilized lime-Cement after 28 days of curing and 14 days of curing, followed by 7 FT cycles.....	84
Figure 5.15 Comparison of UCS for clay soil stabilized lime-Cement after 28 days of curing and 14 days of curing, followed by 7 FT cycles.....	85
Figure 5.16 Comparison of UCS for grey shale and clay soil stabilized with Fiber and lime-fiber after 28 days of curing and 14 days of curing, followed by 7 FT cycles.	86
Figure 5.17 Comparison of UCS for grey shale soil stabilized with lime and lime-fly ash after 28 days of curing and 28 days of curing, followed by 12 FT cycles.	87
Figure 5.18 Comparison of UCS for clay soil stabilized with lime and lime-fly ash after 28 days of curing and 28 days of curing, followed by 12 FT cycles.	88
Figure 5.19 Comparison of UCS for grey shale soil stabilized with lime-cement after 28 days of curing and 28 days of curing, followed by 12 FT cycles.	90
Figure 5.20 Comparison of UCS for clay soil stabilized with lime-cement after 28 days of curing and 28 days of curing, followed by 12 FT cycles.....	91
Figure 5.21 Comparison of UCS for grey shale and clay soil stabilized with Fiber and lime-fiber after 28 days of curing and 28 days of curing, followed by 12 FT cycles.	92
Figure 5.22 Comparison of measured and predicted UCS.	95
Figure 5.24 Comparison of DPI versus depth for unreinforced and fiber-reinforced clay layers.	98
Figure 5.25 DPI comparison for unreinforced and fiber reinforced cases before and after rolling wheel loading.	98
Figure 5.26 Comparison of resilient modulus for clay soil pre- and post-rolling wheel loads in unreinforced and fiber-reinforced cases.....	100
Figure 5.27 Rutting measurement using a measuring tape for the fiber-reinforced case.	101

Figure 5.28 Comparison of rutting recorded from string potentiometer for unreinforced and fiber-reinforced cases.....	101
Figure 5.29 Comparison of total rutting in fiber-reinforced and unreinforced cases under applied wheel loads.....	102
Figure 5.30 LVDT deformation readings for fiber-reinforced and control cases: (a) LVDT 1 deformation readings, (b) LVDT 2 deformation readings.....	103
Figure 5.31 LVDT deformation readings for fiber-reinforced and control cases: (a) LVDT 3 deformation readings, and (b) LVDT 4 deformation readings.	103
Figure 5.32 Pressure cell readings over a 30-second period for both unreinforced and fiber-reinforced cases: (a) top pressure cell, (b) middle pressure cell, and (c) bottom pressure cell.	106
Figure 5.33 Comparison of pressure distribution across the clay layer for unreinforced and fiber-reinforced cases.....	107
Figure 5.34 Cumulative blows vs depth for grey shale and lime stabilized cases.....	109
Figure 5.35 DPI vs depth for grey shale and lime stabilized cases.....	109
Figure 5.36 DPI comparison for control (grey shale) and stabilized lime cases before and after rolling wheel loading.	110
Figure 5.37 Resilient Modulus for control and lime stabilized cases.....	111
Figure 5.38 Comparison of rutting recorded from string potentiometer for grey shale and lime stabilized case.	113
Figure 5.39 Comparison of LVDT deformation readings for control and lime-stabilized cases: (a) LVDT 1 deformation readings, (b) LVDT 2 deformation readings, (c) LVDT 3 deformation readings, and (d) LVDT 4 deformation readings.....	114
Figure 5.40 Pressure cell readings over a 30-second period for both control and lime-stabilized cases: (a) top pressure cell, (b) middle pressure cell, and (c) bottom pressure cell.....	117
Figure 5.41 Comparison of pressure distribution across the grey shale layer for control and lime stabilized case.	117
Figure A.1 Air drying the wet soil.....	131
Figure A.2 Grinding clay soil.....	131
Figure A.3 Clay soil after grinding.....	132
Figure A.4 Breaking down clay soil clumps using a rubber mallet to achieve finer particles for testing.....	132
Figure A.5 Grey shale divided into three equal layers for consistent compaction and testing.....	133
Figure A.6 Pouring Grey shale soil into the UCS mold for sample preparation and compaction.....	133
Figure A.7 Extracting UCS samples from the mold using a hydraulic jack.....	134
Figure A.8 Prepared UCS sample of grey shale soil, ready for UCS testing.	134
Figure A.9 UCS sample after testing.....	135
Figure A.10 Mixing clay soil with fiber reinforcement.....	135
Figure A.11 Fiber-reinforced clay sample under the testing machine.....	136
Figure A.12 Fiber-reinforced grey shale sample under the testing machine.	136
Figure A.13 Fiber-reinforced clay sample after testing.....	137
Figure A.14 Fiber-reinforced grey shale sample after testing.	137
Figure A.15 Pouring grey shale soil to prepare the first lift of the grey shale base layer for testing.....	138
Figure A.16 Installing the middle pressure cell after compacting the first lift of the grey shale base layer to measure stress distribution.....	138
Figure A.17 Leveling the surface after compacting the second lift of the grey shale.	139

Figure A.18 This picture was taken during the test, capturing the deformation during the test.	139
Figure A.19 Measuring permanent rutting depth using a tape measure after terminating the test on the grey shale base layer.	140
Figure A.20 Pour 0000the mixed fiber and clay soil to prepare the first lift of the fiber-reinforced clay base layer.	140
Figure A.21 Installing pressure sensors within the fiber-reinforced clay layer.	141
Figure A.22 Performing a sand cone test to measure the density of the compacted fiber-reinforced clay layer.	141
Figure B.1 Stress vs. strain curves for two samples of grey shale stabilized with 3% lime.	142
Figure B.2 Stress vs. strain curves for two samples of grey shale stabilized with 6% lime.	142
Figure B.3 Stress vs. strain curves for two samples of grey shale stabilized with 10% fly ash.	143
Figure B.4 Stress vs. strain curves for two samples of grey shale stabilized with 3% lime and 10% fly ash.	143
Figure B.5 Stress vs. strain curves for two samples of grey shale stabilized with 6% lime and 10% fly ash.	144
Figure B.6 Stress vs. strain curves for two samples of grey shale stabilized with 3% cement.	144
Figure B.7 Stress vs. strain curves for two samples of grey shale stabilized with 3% lime and 3% cement.	145
Figure B.8 Stress vs. strain curves for two samples of grey shale stabilized with 6% lime and 3% cement.	145
Figure B.9 Stress vs. strain curves for two samples of grey shale stabilized with 6% cement.	146
Figure B.10 Stress vs. strain curves for two samples of grey shale stabilized with 3% lime and 6% cement.	146
Figure B.11 Stress vs. strain curves for two samples of grey shale stabilized with 6% lime and 6% cement.	147
Figure B.12 Stress vs. strain curves for two samples of grey shale stabilized with 3% lime .	147
Figure B.13 Stress vs. strain curves for two samples of grey shale stabilized with 6% lime.	148
Figure B.14 Stress vs. strain curves for two samples of grey shale stabilized with 0% lime and 10 fly ash.	148
Figure B.15 Stress vs. strain curves for two samples of grey shale stabilized with 3% lime and 10 fly ash.	149
Figure B.16 Stress vs. strain curves for two samples of grey shale stabilized with 6% lime and 10 fly ash.	150
Figure B.17 Stress vs. strain curves for two samples of grey shale stabilized with 3% cement.	150
Figure B.18 Stress vs. strain curves for two samples of grey shale stabilized with 3% lime and 3% cement.	151
Figure B.19 Stress vs. strain curves for two samples of grey shale stabilized with 6% lime and 3% cement.	151

List of Tables

Table 2.1 Criteria for PI, LL, and PI for lime application (Adapted from by Elseifi et al., 2017).	27
Table 2.2 Recommended layer coefficients for lime-stabilized soil (Adapted from by Elseifi et al., 2017).	28
Table 2.3 Criteria for Accepting Lime-Modified and Lime-Stabilized Layers (Adapted from Elseifi et al., 2017).	29
Table 3.1 Properties of the subgrade types.	32
Table 3.2 Properties of lime.	35
Table 3.3 Properties of cement.	35
Table 3.4 Properties of Fly ash.	36
Table 3.5 Properties of fiber.	37
Table 4.1 Testing matrix for admixture combinations with grey shale and clay.	42
Table 4.2 Maximum dry density and optimum moisture content.	43
Table 4.3 Freeze – Thaw sets.	54
Table 4.4 LSTW testing matrix.	58
Table 4.5 LVDT R2 summary.	61
Table 4.6 Pressure Cell R2 Summary.	62
Table 5.1 Peak Residual shear strength parameters for grey shale and its stabilized cases.	75
Table 5.2 Residual shear strength parameters for grey shale and its stabilized cases.	76
Table 5.3 Peak shear strength parameters of the clay soil combinations its stabilized cases.	79
Table 5.4 Residual shear strength parameters of the clay soil combination its stabilized cases.	79
Table 5.5 Regression coefficient for empirical model of UCS cementitious-stabilized soil.	94
Table 5.7 Correlation between Resilient Modulus (Mr) with Dynamic Penetration Index.	99
Table 5.8 Changes in Mr for unreinforced and fiber-reinforced cases in pre- and post-rolling wheel load conditions.	99
Table 5.9 Average peak pressure for top, middle, and bottom pressure cells in both unreinforced and fiber-reinforced cases.	105
Table 5.10 Summary of DPI for untreated and soil + 6% lime cases.	108
Table 5.11 Resilient modulus of the control and lime stabilized cases.	111
Table 5.12 Average peak pressure for top, middle, and bottom pressure cells for both control and lime-stabilized cases.	115
Table 7.1 Summary of soil stabilization recommendations for lime, fly ash, cement, and their combination applications.	125

Chapter 1 Introduction

Soil stabilization is the process of enhancing the engineering properties of weak soil significantly using stabilizers such as lime or cement. When materials, design, and construction are properly considered, stabilized soils can outperform non-stabilized soils. Furthermore, incorporating a stabilized soil layer into pavement structural design can reduce the thickness of subsequent layers, resulting in considerable cost savings. Stabilized soils not only exhibit improved strength and stiffness but also form a solid monolith that reduces permeability. This, in turn, mitigates shrink/swell potential and the adverse effects of freezing and thawing cycles (McDowell, 1959; Sharma et al., 2012; Kumar et al., 2007).

Lime stabilization has been widely recognized as a traditional chemical stabilizer for weak subgrade soils in highway projects since its initial testing in Nebraska in 1956 (Ramsey et al., 1959). Commonly used in road construction as a modification agent or stabilizer, lime is frequently considered a cost-effective method for enhancing the strength and stiffness of weak or problematic subgrades, similar to cement and fly ash stabilization (Basna & Runcer, 1991; Bell, 1996; Negi & Faizan, 2013; Rabab'ah et al., 2021).

Frost action, which involves repeated cycles of freezing and thawing, often occurs in cold regions and results in damage to transportation infrastructure such as pavements (Sadiq et al., 2023; Solanki et al., 2013). The formation of ice lenses between soil particles during freezing and the excess water during thawing severely impact the mechanical properties of soil mechanical properties of weak subgrade and cause significant deterioration after freeze-thaw cycles that affect its dynamic response under load (Cui et al., 2023; Kakroudi et al., 2024). These changes can significantly diminish the strength and bearing capacity of foundation soils (Li et al., 2014). For highway agencies, it is crucial to evaluate the durability of lime-stabilized soils during the mix design, as this assessment determines the long-term effectiveness and permanency of the

treatments (National Lime Association, 2004; Akula et al., 2020). Environmental conditions, particularly freezing-thawing and drying-wetting cycles, can negatively affect the durability of lime stabilization (Padmaraj & Arnepalli, 2023).

Hotineanu et al. (2015) studied the effect of freeze-thaw cycles on the mechanical properties of lime-stabilized soil and found that the formation of ice lenses in the pores of lime-stabilized soil caused significant damage (crack formation), leading to a degradation of soil strength. Kumar et al. (2024) conducted durability tests on soils stabilized with different stabilizers and observed a reduction in strength after the soils were subjected to multiple cycles. Tebald et al. (2013) examined the mechanical performance of lime-stabilized soil under freeze-thaw conditions and found that the unconfined compressive strength of the soil decreased with an increasing number of cycles, reaching an asymptotic value after five cycles. There is a limited number of studies on enhancing lime stabilization with cementitious materials to improve environmental resistance against the impacts of freezing and thawing in cold regions.

However, lime cannot be active when there is less alumina in the soil. Therefore, some concerns exist about the performance and durability of lime stabilization associated with fewer silica and alumina soils (or high sulfur compounds) and other conditions such as poor drainage, freezing, and thawing. In this case, cement as a stabilizing method can be used to increase the strength of weak soils by mixing it with cement and water. The water hydrates the cement, generating reactions that create a matrix between the soil particles and give the soil strength. The cost of cement is more expensive than lime, thus the appropriate amount of mixing should be known depending on site-specific conditions. Also, the mixing ratio between lime and cement can be uncertain depending on the soil properties and environmental factors such as pH or moisture contents.

As an alternative, previous studies on discrete fiber-reinforced natural and chemically stabilized soils have generally shown improvements in soil shear strength, bearing capacity, ductility, toughness, and resistance to rutting (Gray & Ohashi, 1983; Santoni & Webster, 2001; Kaniraj & Havanagi, 2001; Consoli et al., 2003; Newman & White, 2008). Accordingly, microfiber reinforcement could be promising for enhancing the performance of the subgrade as an alternative to lime stabilization.

Gray and Ohashi (1983) reported that the failure mechanism of a fiber-reinforced soil depends on the acting average effective stress. Failure occurs through slippage of fibers up to critical stress and, as the stresses increase, failure is governed by the tensile strength of the fiber element (Consoli et al., 2011). Santoni and Webster (2001) reported that in unconfined compressive strength tests, the fiber-reinforced soil yielded higher shear strengths due to the development of tension in the fibers with increasing strains. Consoli et al. (2003) indicated that the fiber content, the orientation of fibers concerning the shear surface, and the elastic modulus of the fibers influence the contribution of the reinforcement to the shear strength. In Iowa loess, Hoover et al. (1982) found that the inclusion of fibers decreased freeze-thaw volumetric changes by 40% compared to soils with no fibers.

1.1 Problem Statement

Lime and cement have been shown to work synergistically in soil stabilization, offering enhanced strength and durability when used in combination. In Nebraska, lime stabilization was found to be less effective for certain problematic soils, particularly the shale soils prevalent in the northeastern region. Previous research has demonstrated that the addition of supplementary materials—such as fly ash, cement, or fiber reinforcement—can mitigate shrinkage and swelling

while significantly improving soil strength and stiffness. This combined stabilization approach effectively addresses the limitations associated with lime treatment alone.

NDOT has yet to investigate the optimal proportions of additives combined with lime to establish practical guidelines and construction practices for field applications. A systematic study is needed to support NDOT in advancing the use of these combinations for subgrade stabilization. Such research would assess the effectiveness of incorporating cementitious materials and fiber reinforcement with lime, ultimately contributing to a more reliable and region-specific design approach for Nebraska's soils.

1.2 Objective of the study

The objectives of this research are to 1) Identify the effectiveness of mixing cementitious materials and fiber reinforcement to enhance lime stabilization and 2) evaluate the design properties of cementitious materials and fiber reinforcement to enhance lime stabilization for weak subgrade in Nebraska. Based on the expertise of the team, the scope of work includes:

- 1) Performing extensive literature review from other DOT's cases and practices that applied to mix cementitious materials and fiber reinforcement to subgrade stabilization,
- 2) Evaluating geotechnical properties of weak subgrade soils (e.g., Pierre Shale) treated and non-treated with cementitious materials and fiber reinforcement,
- 3) Assessing environmental resistance of treated soils with freezing-thawing cycles,
- 4) Analyzing the performance of treated and non-treated subgrades through the Large-Scale Track Wheel.
- 5) Suggesting a design guideline of lime, cementitious materials, and fiber mixture. The site-specific applicability and cost-effectiveness of treated and non-treated subgrades will be identified.

Chapter 2 Literature Review

2.1 Mechanisms of Lime Stabilization

2.1.1 Cation Exchange and Flocculation-Agglomeration

The initial phase of lime stabilization, known as cation exchange, is crucial for modifying the soil's physical properties. When hydrated lime is introduced into the soil, calcium ions (Ca^{2+}) from the lime replace monovalent ions such as sodium (Na^+) and potassium (K^+) that are attached to the clay particles. This ion exchange modifies the electrical charges on the surface of the clay particles. Consequently, it leads to a reduction in the space between clay sheets (Figure 2.1). This process facilitates the formation of larger aggregates, known as flocculation. Flocculation increases the effective grain size and reduces the soil's plasticity, which improves workability and load-bearing capacity. Agglomeration further compacts these particles, enhancing the strength and stability of the soil matrix by forming a more cohesive and less plastic structure (Figure 2.2). These immediate changes significantly improve the soil's mechanical properties, making it more manageable for subsequent construction applications (Little, 1999).

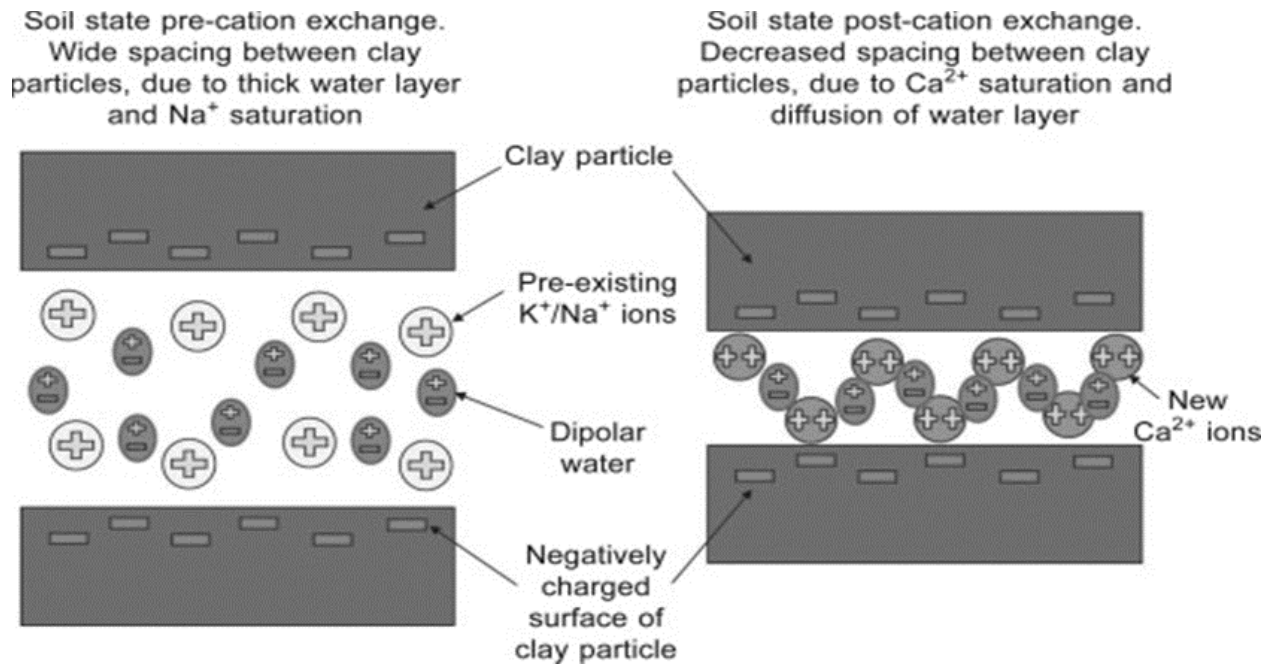


Figure 2.1 Comparison of soil state before and after lime application (adapted from Sargent, 2015).

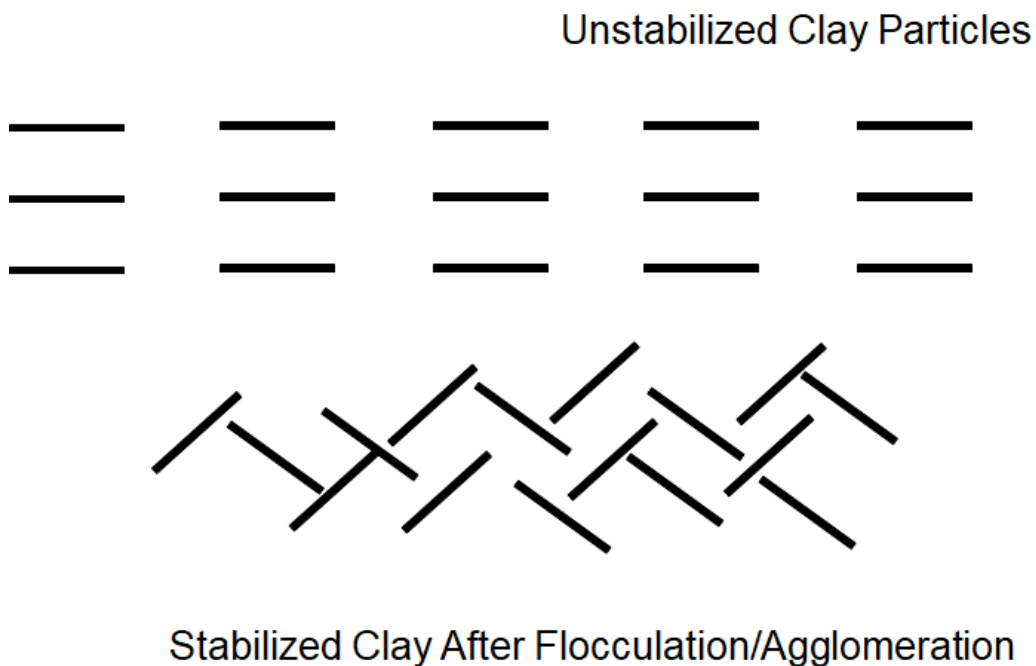


Figure 2.2 Flocculation/agglomeration of clay sheets after lime application.

2.1.2 Pozzolanic Reaction and Carbonate Cementation

After the initial structural changes caused by cation exchange and agglomeration, the pozzolanic reaction becomes the main long-term stabilization mechanism. This reaction is initiated by the high pH environment produced by calcium hydroxide, leading to the solubilization of silicate and aluminate compounds on the clay surface. These compounds bond chemically with calcium ions, forming calcium silicate hydrates (C-S-H) and calcium aluminate hydrates (C-A-H) (Figure 2.3).

These hydrates enhance the soil's durability and strength over time, serving as cementitious compounds that bind the soil particles into a cohesive, dense matrix. This process increases load-bearing capacity and reduces vulnerability to environmental factors like moisture and frost. Additionally, carbonate cementation occurs when calcium oxide reacts with atmospheric carbon dioxide, forming calcium carbonate. This secondary binder further strengthens the soil structure. Together, these processes create a durable, impermeable layer ideal for infrastructure foundations and road bases (Little, 1999).

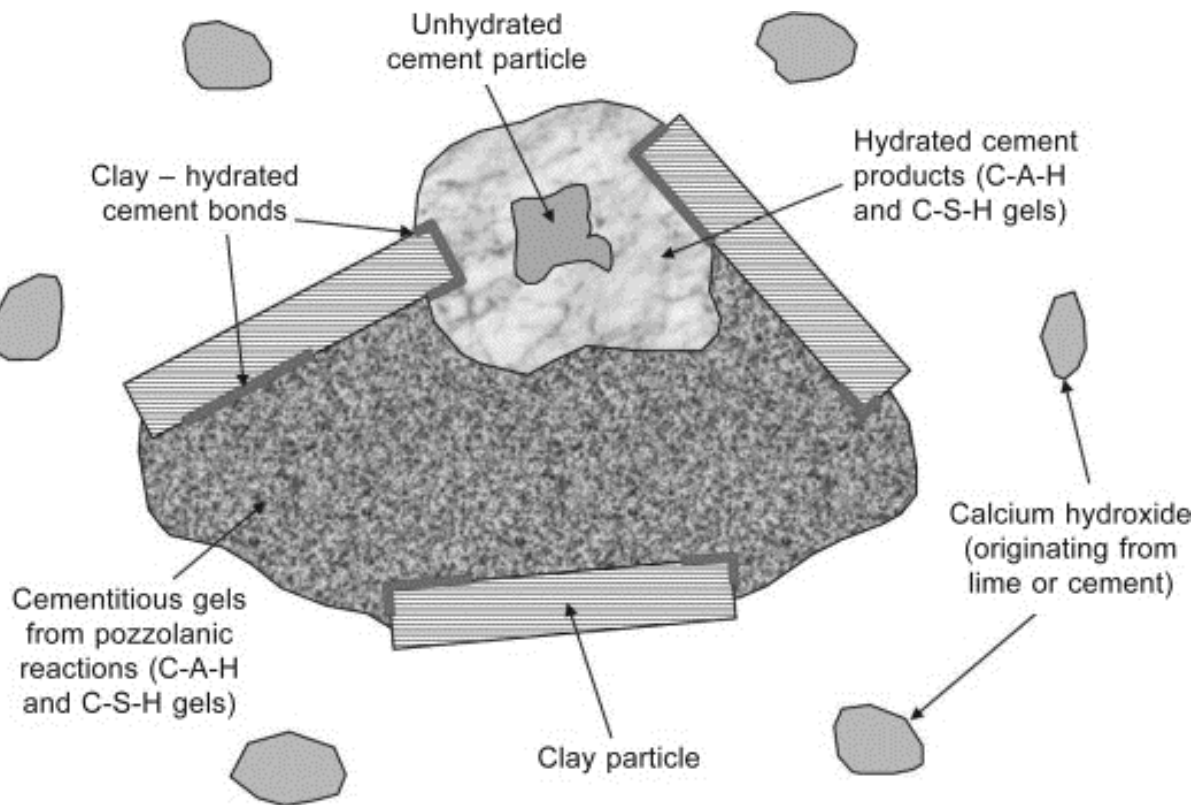


Figure 2.3 Formation of cementitious bonding products from hydration and pozzolanic reactions (adapted from Sargent, 2015).

2.2 Combined Lime and Cement Stabilization for Soil Improvement

The research on combined lime and cement stabilization techniques for soil modification and pavement foundations has significantly advanced our understanding of how to enhance the mechanical properties of soils for more durable and sustainable road infrastructures. Studies conducted across different geographical regions, including Texas and Southern Italy, have focused on the effective use of these combined treatments to address specific challenges posed by expansive and problematic soils.

Texas Experience with Low-Volume Roads: The study conducted in Texas focused on the application of combined lime and cement stabilization for low-volume roads, demonstrating its capacity to significantly enhance the strength and durability of subgrades composed predominantly

of expansive clays. The research, illustrated by Sirivitmaitrie et al. (2008), detailed that treatment combinations of 4% lime followed by 4% cement resulted in improved unconfined compressive strength and reduced plasticity indexes, leading to more stable and less susceptible pavement structures under environmental changes.

Southern Italy's Freight Terminals: In Southern Italy, Praticò and Puppala (2012) explored the stabilization of subgrades within intermodal freight terminals, addressing specific challenges like low-frequency, high-pressure loads from container movements. Their findings highlighted that combined lime and cement stabilization not only improved the mechanical properties of the soils but also efficiently managed the moisture dynamics that often compromise pavement integrity in such freight-intensive environments.

Arlington, Texas – Expansive Soils with Low to Medium Soluble Sulfate Levels: Further research by Sirivitmaitrie et al. (2011) on expansive soils in Arlington, Texas, emphasized the potential of combined stabilization to enhance soil workability and strength. By adjusting lime and cement ratios (6% each by dry weight), significant improvements were noted in unconfined compressive strength, with field applications showing effective control over heave-related movements and cracking in the pavement structures.

2.3 Fiber Reinforcement in Soil Stabilization

In recent years, soil stabilization using fiber has gained significant interest from researchers worldwide. The inclusion of synthetic or natural fibers in soils aims to enhance both mechanical and physical properties. The random distribution of fibers within the soil contributes to increased peak strength by intersecting potential shear planes, while also enhancing the ductility of the soil (Maher et al, 1994). These improvements in strength and ductility are accompanied by reductions in swell potential and compressibility, further enhancing the overall stability and performance of the soil.

The study at the Central Iowa Expo Pavement Test Sections investigated the combined use of Portland cement and fiber reinforcement to stabilize subbase materials in roadways. Researchers used two types of polypropylene fibers: black fibrillated fibers and white monofilament fibers, together with 5% cement to improve recycled subbase materials. They aimed to enhance long-term performance, particularly during freeze-thaw cycles. The construction team mixed 0.4% fiber and 5% cement by dry weight of the soil, added moisture, and compacted the material, as illustrated in Figure 2.4, which shows the construction procedure for fiber reinforcement.

The combined stabilization approach significantly improved the mechanical properties of the subbase, increasing compressive strength, stiffness, and durability. Dynamic Cone Penetrometer and Falling Weight Deflectometer (FWD) tests showed higher California Bearing Ratio (CBR) values and FWD modulus measurements compared to untreated or single material stabilized subbases. The results confirmed that cement with fiber reinforcement substantially increased strength, stiffness, and resilience to environmental challenges, such as freeze-thaw conditions, making it a promising strategy for sustainable roadway foundation design (White et al., 2013).



Figure 2.4 Straw blower used to distribute the fiber in the Iowa Expo project (White et al., 2013).

Eun et al., (2024) explored the potential of microfiber reinforcement as an alternative technique for weak subgrade soils in roadway construction. The study provides a comprehensive examination of the benefits of incorporating microfibers into Nebraska soils, focusing on improving mechanical properties such as strength, stiffness, and resistance to deformation. The experimental procedures included UCS tests and large-scale experimental tests to evaluate the performance of soils with varying microfiber content. The UCS tests demonstrated improvements in the strength of weak soils. The results showed that the application of fibers increased the ductility of the specimens stabilized with fiber. The large-scale tests confirmed enhanced resistance to deformation under repeated loads. These results indicate that microfiber reinforcement effectively reduces the susceptibility of treated soils to rutting, which is a critical factor in maintaining road durability and performance. The practical application of microfiber reinforcement, as demonstrated in this study, highlights its ability to provide a cost-effective and

environmentally friendly technique, offering a promising solution for enhancing road infrastructure resilience.

Li, (2003) investigated the stabilization of unsaturated subgrade soils through the combined use of lime and fiber reinforcement. The main objective was to develop new constitutive models to predict the behavior of these treated soils under static and dynamic loading conditions. The experimental program included direct shear tests and triaxial tests to evaluate the mechanical properties of soils reinforced with lime and polypropylene geofiber. The results indicated that the newly developed models effectively represented the mechanical response of the soil. The findings highlighted significant improvements in shear strength and stiffness due to lime and fiber reinforcement. The study concluded that the combination of lime and fiber offers substantial benefits for subgrade stabilization in highway construction, providing enhanced stability and resilience.

2.4 Environmental Resistance

The effectiveness of soil stabilization methods in mitigating damage due to freeze-thaw cycles is crucial, particularly for infrastructure in regions with significant seasonal temperature variations. Various studies have focused on the environmental resistance of stabilized soils when subjected to durability tests such as freeze-thaw cycles and wet-dry cycles, with an emphasis on assessing long-term performance under such challenging conditions. The environmental resistance of stabilized soils can be significantly influenced by factors like the type of stabilizer used, type of soil, moisture control, and compaction.

Tebaldi et al., (2016) investigated the effect of repeated freeze-thaw cycles on lime-stabilized clay soil. The study found that lime stabilization effectively improves the mechanical strength of clay soils, but the performance deteriorates significantly after several freeze-thaw

cycles. Unconfined compressive strength and direct shear strength tests indicated a reduction of up to 35% and 20%, respectively, after multiple freeze-thaw cycles. It was observed that the UCS reduction tended to stabilize after a certain number of FT cycles, indicating a stabilization in the degradation process (Figure 2.5).

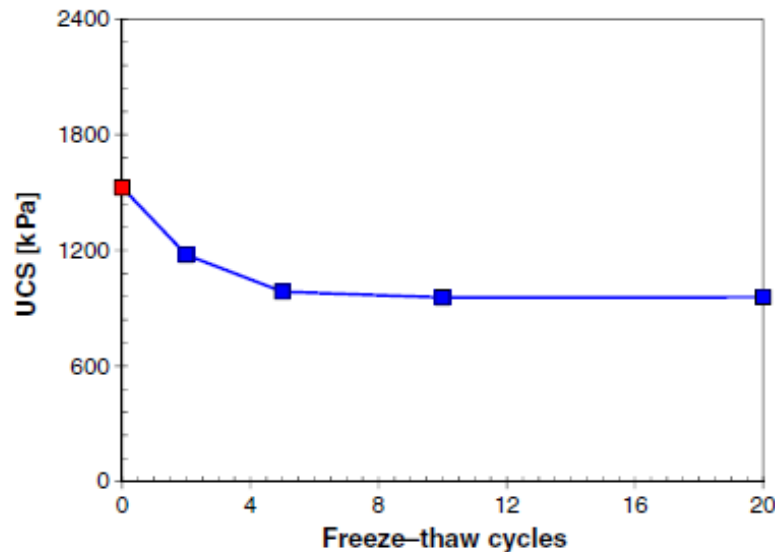


Figure 2.5 UCS of lime-stabilized soil vs FT cycles (Tebaldi et al., 2016).

Kumar et al. (2024) conducted a comprehensive study on the durability of chemically stabilized clayey soils from Texas using moisture-susceptible methods such as tube suction tests, wet-dry tests, and ERDC wet tests. The research aimed to evaluate the moisture susceptibility and long-term performance of different stabilization techniques under wetting-drying cycles, highlighting the permanency of stabilizer effectiveness. The study found that cement-stabilized soils showed higher resistance to moisture fluctuations, while lime-stabilized soils exhibited moisture susceptibility, particularly under ASTM wet-dry conditions (Figure 2.6). These findings suggest that lime stabilization methods need to be enhanced to improve their performance under moisture fluctuations and wet-dry conditions.

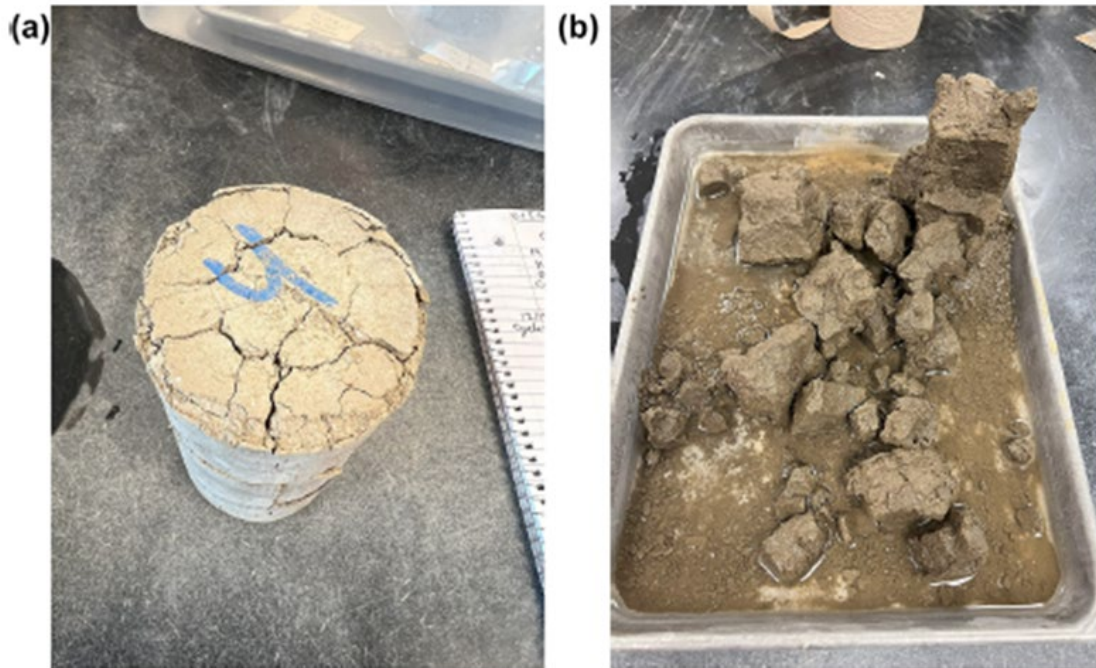


Figure 2.6 Lime-treated high-plasticity clay soil specimen with 7% dosage a) after the second drying cycle and b) after the fourth wetting cycle (Kumar et al., 2024).

Solanki et al. (2013) focused on evaluating the effect of freeze-thaw cycles on the durability of subgrade soils stabilized with different additives, including hydrated lime, fly ash, and cement kiln dust. Specimens were subjected to several freeze-thaw cycles, and unconfined compressive strength and resilient modulus tests were performed to evaluate the performance of the stabilized soils. The results showed that cementitious additives generally improved the durability of soils against freeze-thaw cycles, although the extent of improvement varied with the type of additive used and the soil characteristics. It was also found that the unconfined compressive strength and resilient modulus values tended to decrease significantly after the first freeze-thaw cycle when the rate of reduction stabilized. Among the tested additives, cement kiln dust provided the highest resistance to freeze-thaw cycles in Port series soil, while lime-stabilized specimens exhibited lower

percentage reductions in unconfined compressive strength values for clayey soils, indicating their effectiveness for such soil types.

One important study on the durability of low-cost rural surfaces in Iowa investigated different stabilization methods to mitigate freeze-thaw damage on granular surfaced roads. The main goal of the study was to evaluate the effectiveness of various stabilization techniques in improving the durability of road surfaces subjected to freeze-thaw cycles. The study implemented a variety of stabilization techniques, including chemical stabilizers, macadam stone bases, geotextiles, and geocomposites, and assessed their effectiveness over two freeze-thaw cycles. Chemical stabilization methods involving fly ash and cement exhibited notable improvements in durability. These chemical treatments enhanced the strength and reduced the frost susceptibility of the soils. For instance, fly ash stabilization led to a considerable reduction in surface damage during thawing by improving the soil's resistance to freezing-induced expansion. Cement further contributed to the stabilization by enhancing cohesion and reducing permeability, which helped in maintaining soil integrity during freeze-thaw cycles (Li et al, 2015).

Previous research has shown that traditional lime stabilization methods need improvement to better withstand environmental conditions, especially in high plasticity soils. Bhattacharja and Bhatta (2003) conducted a comparative study of Portland cement and lime stabilization in moderate to high plasticity clay soils under various durability tests, including vacuum saturation and wet-dry cycles. The results demonstrated that cement stabilization offered superior durability compared to lime.

2.5 Specifications and Guidelines of Other States' Department of Transportation

The specifications and guidelines for lime and cement stabilization vary significantly across the United States. This section reviews the specifications from seven selected states, including Virginia, Texas, North Carolina, Georgia, Louisiana, California, and Indiana, which

were chosen from a total of fifteen surveyed states (Figure 2.7). The primary focus of this review is to analyze and summarize the best practices and criteria for lime and cement application as outlined by the DOTs of these states. By understanding the similarities and differences in stabilization techniques, this review aims to provide insights into effective methods for enhancing soil properties and supporting pavement infrastructure. The selected states represent a wide geographical spread, offering valuable perspectives on how regional factors influence stabilization guidelines, including the use of combined lime-cement and lime-fly ash. The main criteria for selecting the type of stabilization, pavement design considerations, and acceptance criteria are also examined in this review.

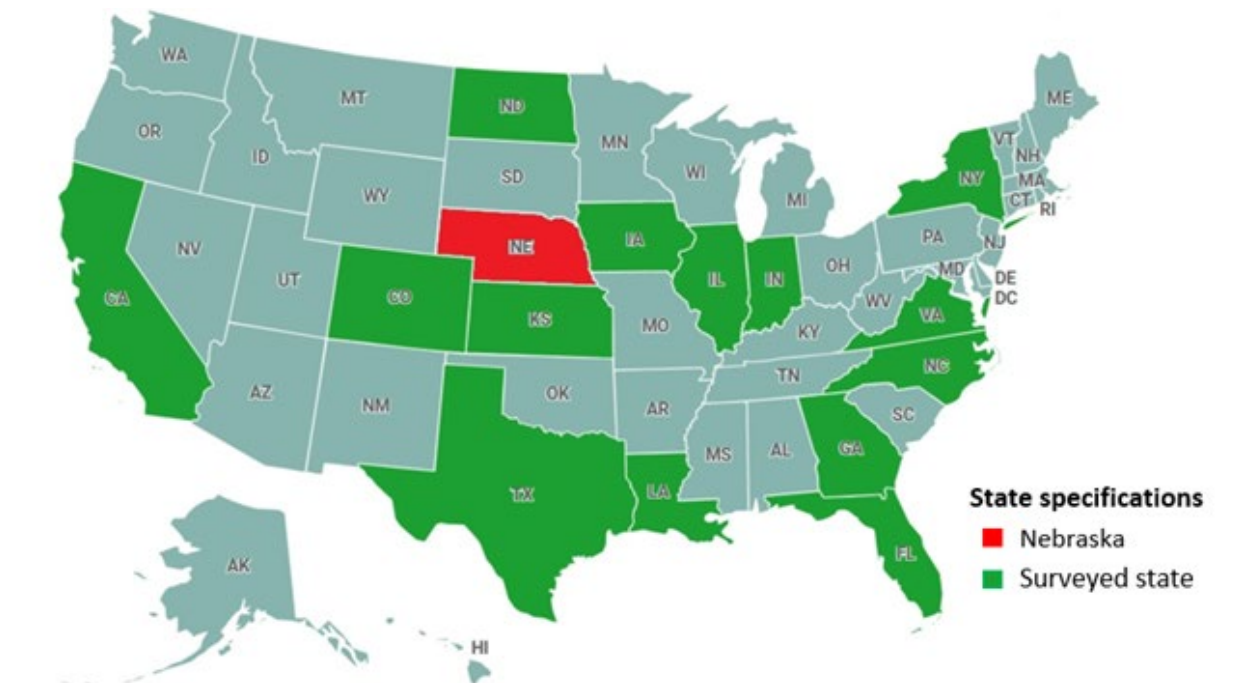


Figure 2.7 Selected and surveyed states for DOT stabilization specifications.

2.5.1 Virginia Specifications for Lime, Cement, and Lime-Cement Stabilization

Lime stabilization in Virginia is primarily applied to fine-grained soils, such as silt and clay, especially under wet conditions with a high plasticity index (PI). Lime should not be mixed with frozen soil or when air temperatures are below 40 °F. The moisture content for lime-stabilized soil should be maintained between the optimum moisture content (OMC) and 120% of OMC. The stabilized soil must achieve 95% of the maximum dry density (MDD) within 24 hours after compaction. After compaction, a mellowing period of 24 to 48 hours is required before final compaction to ensure an effective reaction between lime and soil (Virginia Department of Transportation [VDOT], 2020, p. 141).

Cement stabilization is generally used for sandy and gravelly soils, but it can also be suitable for fine-grained soils with low plasticity. Typically, the cement content ranges from 5% to 10% by volume of soil. During stabilization, the moisture content should be maintained between OMC and 120% of OMC. The stabilized soil must achieve 98% of the MDD within four hours of mixing. To ensure proper curing and protection, the stabilized layer should be covered with the next pavement or an asphalt layer within seven days (VDOT, 2020, p. 141).

Lime-cement stabilization is used when wet conditions make cement alone ineffective. Initially, lime is applied to dry the saturated soil before cement is added to improve its strength. The amount of lime and cement used depends on the soil's saturation level, its properties, and specific project requirements. Similar to lime stabilization, lime-cement stabilization should not be performed if the soil is frozen or if air temperatures are below 40 °F. The moisture content should be maintained between OMC and 120% of OMC, and a curing period of seven days is necessary to allow for proper hydration and strength development (VDOT, 2020, p. 141).

2.5.2 Texas Specifications for Lime, Cement, and Lime-Cement Stabilization

For lime stabilization in Texas, lime is typically used to stabilize the soil as base or subgrade layers, especially for soils with moderate to high PI values. Lime is added to enhance the workability of the soil, reduce its moisture susceptibility, and increase the layer structural number. For soils with sulfate content that does not exceed 3000 ppm, a normal mixture design process is recommended, and a mellowing period of at least 24 hours should be allowed to ensure adequate reaction between the lime and soil (TxDOT, 2019, p. 12). It is important to maintain the moisture content within the optimum range, and a mellowing period is crucial for allowing adequate reaction before any further treatment (Texas Department of Transportation [TxDOT], 2019, p. 12).

Cement stabilization in Texas is applied to low-to-moderate plasticity index (PI) soils. The cement content is determined according to Tex-120-E (TxDOT, 2019, p. 8). The construction criteria for cement-stabilized subgrade include maintaining the moisture content within a recommended range, from the OMC to 2% above OMC. The stabilized soil must achieve 100% of the MDD within two hours after mixing. To ensure proper curing, the treated layer should be cured for at least three days using sprinkling or an asphalt membrane (TxDOT, 2019, p. 8).

Lime-cement stabilization is often used when soils have high moisture content or poor workability. Initially, lime is used to dry the saturated soil, and then cement is added to further enhance the soil's strength. This combination is suitable for subgrades with plasticity indices ranging from 15 to over 35, where lime first modifies the soil properties, and cement provides additional stabilization. It is crucial to allow a mellowing period after lime treatment to ensure proper reactions before adding cement (TxDOT, 2019, p. 12).

For combined lime-fly ash stabilization, lime is used to modify the soil first, especially for soils with moderate to high PI values. Lime is added to improve workability, followed by the addition of fly ash to achieve increased strength and reduced moisture sensitivity. For Class F fly

ash, compaction must be completed within six hours, while for Class C fly ash, compaction must be completed within two hours (TxDOT, 2019, p. 12). To manage these time constraints effectively in field applications, particularly under adverse weather conditions, it is recommended to have proper planning and sufficient equipment on-site to ensure timely compaction. Additionally, contingency measures such as covering the area to protect against moisture or scheduling compaction during favorable weather should be considered.

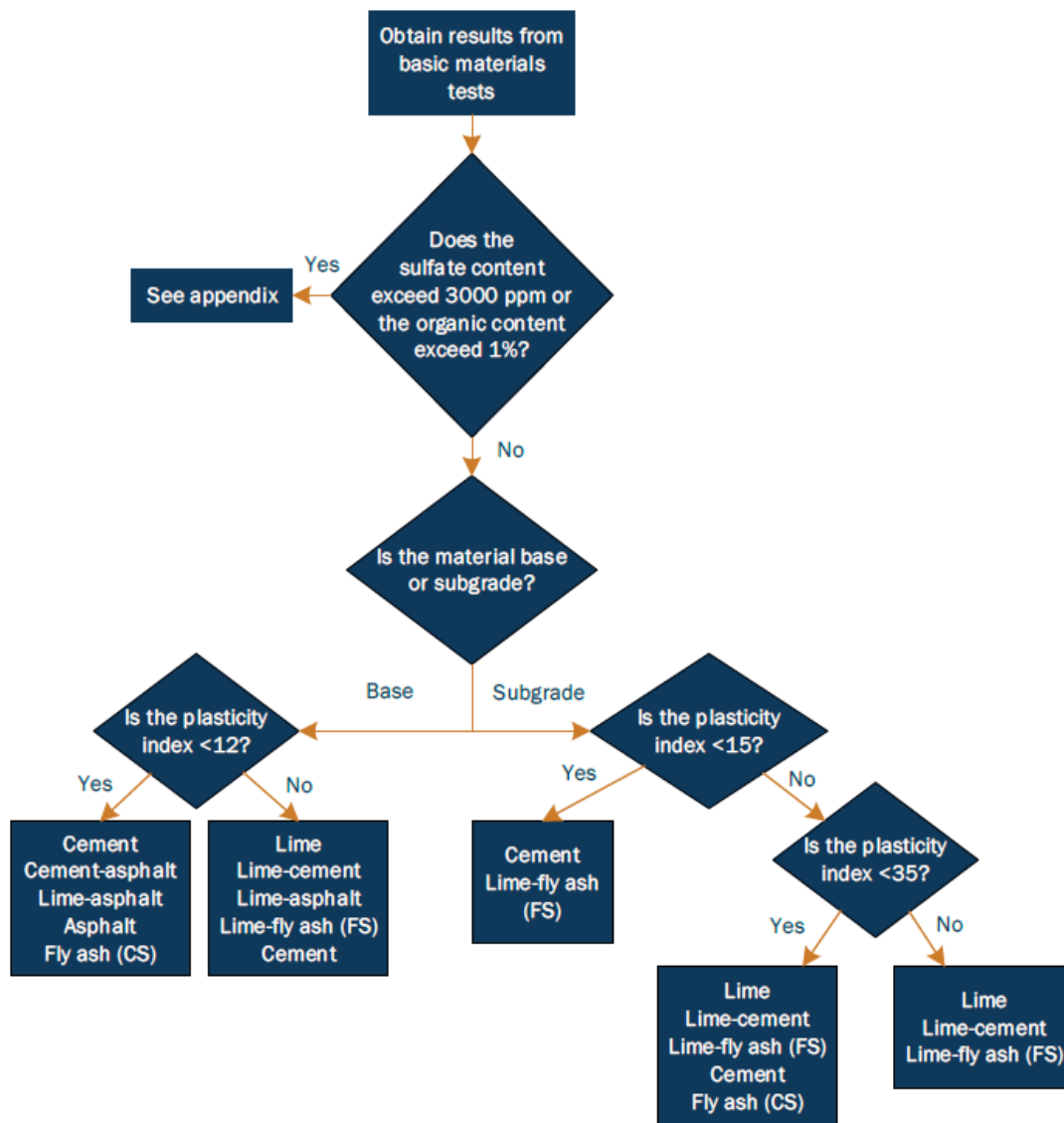


Figure 2.8 Selecting stabilizer types for Texas (TxDOT, 2019).

2.5.3 North Carolina Specifications for Lime Stabilization and Cement Stabilization

For lime stabilization in North Carolina, subgrade, embankment, natural ground, or existing pavement structures are treated by adding water and lime, mixing, shaping, compacting, and finishing the mixture to achieve the required density. Lime content is typically 27 lbs per yard or adjusted to achieve a UCS of 60 psi. The construction criteria for lime-stabilized subgrade include maintaining the moisture content between the OMC and 3% above OMC. A mellowing period of one to four days is required to allow adequate reaction between the lime and soil. The stabilized soil must achieve 95% of the MDD. The curing period involves covering the treated soil with a bituminous curing coat for a minimum of seven days. Quality assurance testing includes UCS testing with a minimum value of 60 psi or dynamic cone penetrometer testing with a minimum of 0.5 in/blow. Additional guidelines specify that lime stabilization should not be performed when the air temperature is below 45 °F or on soils that are frozen or contain frost. Lime-treated soil must be cured properly if not covered with a pavement or base layer before December 1 of the same year. The contractor must ensure that the lime-treated soil is maintains acceptable condition, and any failure to apply the required sand seal within 72 hours may lead to corrective measures directed by the Engineer (North Carolina Department of Transportation (NC DOT, Section 501).

Cement stabilization in North Carolina involves using 5 to 8% cement by weight, with the requirement that the UCS must exceed 200 psi. Cement-stabilized subgrade can be used as a base or subbase layer. The construction criteria for cement-stabilized subgrade include maintaining the moisture content within a range from OMC to 3% above OMC, and the stabilized layer must achieve at least 95% of the MDD. A curing period of seven days is required, during which the treated soil is covered with a bituminous curing coat. Quality assurance testing includes a UCS range of 200 psi to 400 psi (NC DOT, Section 542).

2.5.4 Georgia Specifications for Lime, Cement, and Lime-Cement Stabilization

In Georgia, lime stabilization is commonly employed to modify high plasticity soils, such as clay, to enhance their engineering properties, which include increased stability and improved workability. Lime stabilization involves adding lime to the soil, which subsequently undergoes a mellowing period, usually lasting 24 to 48 hours, allowing chemical reactions to occur between the lime and the clay particles. This process significantly reduces soil plasticity and enhances its strength. The treated soil must be compacted to achieve at least 95% of its MDD to ensure adequate performance under load. Furthermore, lime-treated soils are cured with a sealing coat or membrane to maintain adequate moisture, which is crucial for completing chemical reactions and achieving the desired strength. Lime stabilization is performed at temperatures above 40 °F, as chemical reactions are more efficient at these temperatures (GDOT, 2021, Section 225).

Cement stabilization, on the other hand, is suitable for low-to-moderate plasticity index soils in Georgia. The typical cement content used ranges from 4% to 8% by dry weight of the soil. Cement stabilization enhances soil strength by bonding soil particles together, thereby reducing permeability and increasing stiffness. The construction process involves spreading the cement, mixing it with soil, and adding sufficient water to achieve the optimum moisture content. After mixing, the soil is compacted to at least 98% of the MDD to ensure durability under traffic loads. After compaction, a curing period of seven days is required, during which the stabilized layer is either sprinkled with water or covered with a curing membrane to maintain moisture levels. The UCS for cement-stabilized layers is required to be a minimum of 450 psi, depending on the project requirements and soil type (GDOT, 2021, Section 301).

2.5.5 Virginia Specifications for Lime, Cement, and Lime-Cement Stabilization

In Georgia, lime stabilization is commonly employed to modify high plasticity soils, such as clay, to enhance their engineering properties, which include increased stability and improved

workability. Lime stabilization involves adding lime to the soil, which subsequently undergoes a mellowing period, usually lasting 24 to 48 hours, allowing chemical reactions to occur between the lime and the clay particles. This process significantly reduces soil plasticity and enhances its strength. The treated soil must be compacted to achieve at least 95% of its maximum dry density (MDD) to ensure adequate performance under load. Furthermore, lime-treated soils are cured with a sealing coat or membrane to maintain adequate moisture, which is crucial for completing chemical reactions and achieving the desired strength. Lime stabilization is performed at temperatures above 40 °F, as chemical reactions are more efficient at these temperatures (VA DOT Road and Bridge Specifications, Section 307). Additionally, lime can be combined with fly ash to improve certain soil properties, though specific details for lime-fly ash stabilization are not comprehensively outlined in the GDOT specifications.

Cement stabilization, on the other hand, is suitable for low-to-moderate plasticity index (PI) soils in Georgia. The typical cement content used ranges from 4% to 8% by dry weight of the soil. Cement stabilization enhances soil strength by bonding soil particles together, thereby reducing permeability and increasing stiffness. The construction process involves spreading the cement, mixing it with soil, and adding sufficient water to achieve the optimum moisture content. After mixing, the soil is compacted to at least 98% of the MDD to ensure durability under traffic loads. After compaction, a curing period of seven days is required, during which the stabilized layer is either sprinkled with water or covered with a curing membrane to maintain moisture levels. The unconfined compressive strength (UCS) for cement-stabilized layers is required to be a minimum of 450 psi, depending on the project requirements and soil type (VA DOT Road and Bridge Specifications).

2.5.6 Louisiana Specifications for Lime, Cement, and Lime-Cement Stabilization

Lime stabilization in Louisiana involves adding lime to the soil, which undergoes a mellowing period, usually lasting 24 to 48 hours, allowing chemical reactions to occur between the lime and the clay particles (LA DOTD, 2016, Section 304.02). This process significantly reduces soil plasticity and enhances its strength. Lime-treated soils are compacted to at least 95% of the MDD and are cured with a sealing coat or membrane to maintain adequate moisture, which is crucial for completing chemical reactions and achieving the desired strength. Lime stabilization is performed at temperatures above 40 °F to ensure the efficiency of chemical reactions.

Cement stabilization in Louisiana involves incorporating Portland cement into soils to enhance structural strength. Cement stabilization is suitable for low-to-moderate plasticity index soils and is used to construct base and subbase layers. The cement content is determined based on design requirements or as specified by the engineer. Cement stabilization enhances soil strength by bonding soil particles together, thereby reducing permeability and increasing stiffness. The construction process involves spreading the cement, mixing it thoroughly with the soil, and adding sufficient water to achieve the optimum moisture content. After mixing, the soil is compacted to at least 93% of the MDD to ensure durability under traffic loads. A curing period of seven days is required, during which the stabilized layer must be kept moist either by sprinkling with water or using a curing membrane. The UCS for cement-stabilized layers must be at least 300 psi (LA DOTD, 2016, Section 303).

For lime-cement stabilization, lime is commonly employed to modify the subgrade prior to cement stabilization, particularly for soils with a plasticity index ranging from 16 to 35. Lime is typically used to improve the engineering properties of high plasticity soils, such as clay, enhancing stability and workability. The treated soil must be compacted to at least 95% of the MDD, with moisture content maintained at optimum or within $\pm 2\%$, and cured properly to ensure

the desired strength improvements. For soils with a PI between 16-25, a combination of 6% (by volume) lime and 6% cement by volume is recommended, while for soils with a PI between 26-35, both 9% lime and 6% cement by volume are required. This combined approach is intended to ensure effective modification of soil properties, including reduced plasticity and improved strength (LA DOTD, 2016, Section 305.04).

2.5.7 California Specifications for Lime Stabilization and Other Cementitious Materials

The primary criteria used to select the type of stabilizer in California include sulfate content, the percentage of soil passing through sieve No. 200, and the PI. As illustrated in Figure 2.9, lime is often used with cement to reduce the PI of soils, enhancing workability and stability. Additionally, lime can be combined with Class F fly ash to increase the strength of stabilized soils.

Lime applications in California is typically used for soils with a high plasticity index, including CL (lean clay), MH (silty clay), CH (high plasticity clay), and OH (organic clay) soils. The minimum lime or lime-cement content for soils with low strength must be determined to maintain the pH of the soil at 12.4, referred to as the initial consumption of stabilizer (ICS) as per ASTM D 6276. Following this, unconfined compressive strength (UCS) tests are conducted on three soil samples: one with ICS, one with ICS + 1%, and one with ICS + 2%, to achieve a UCS between 30 psi and 60 psi.

For soils with high PI, according to California Test 204, the soil is tested with lime content levels of 1.0%, 2.0%, 3.0%, and 4.0% by weight. The lime content that reduces the PI to below the design requirement is then selected (CADOT, 2021).

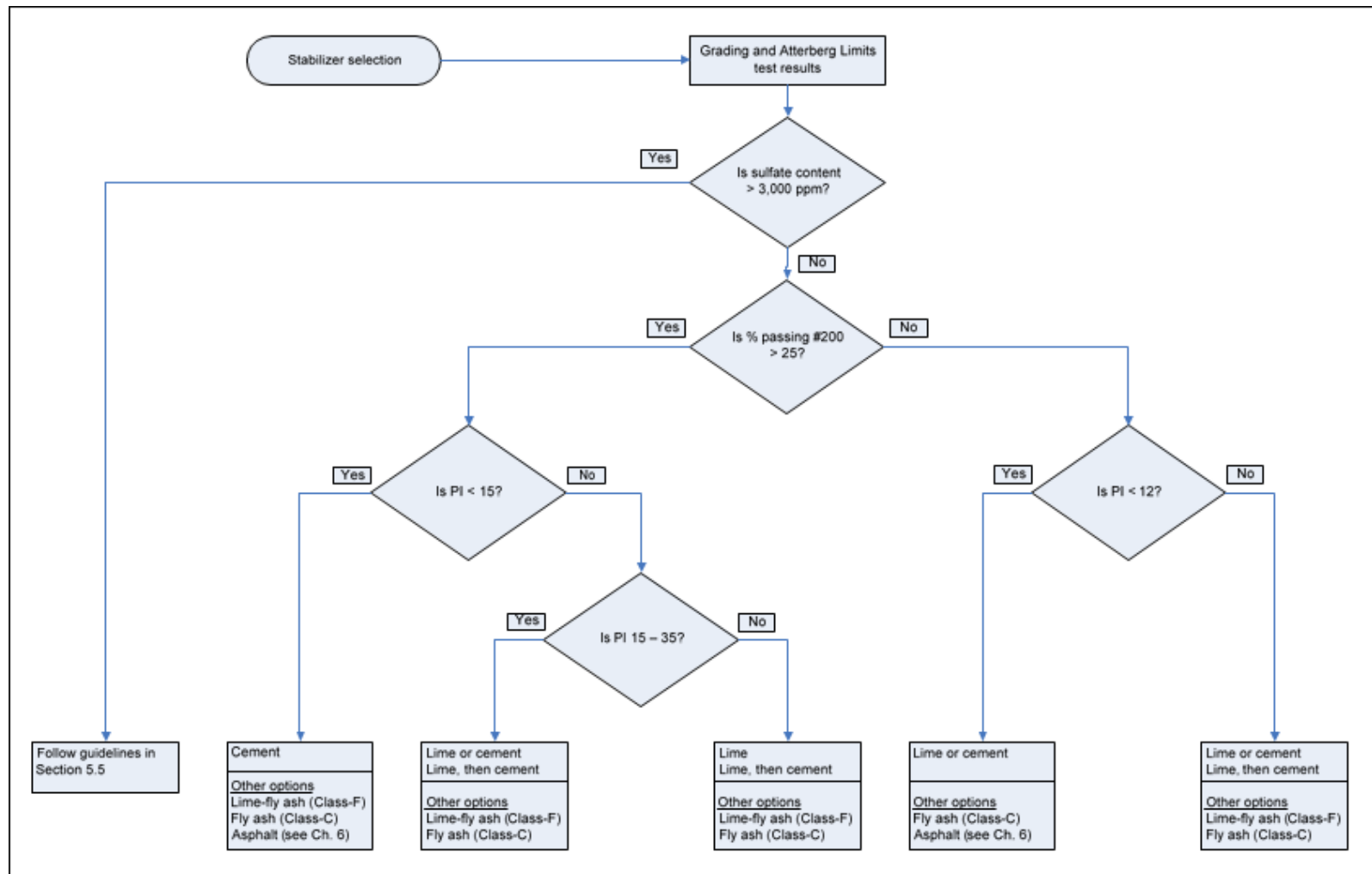


Figure 2.9 Decision flowchart for selecting stabilizers based on soil properties and PI for CA DOT (Adapted from Jones et al, 2010).

2.5.8 Summary of surveyed DOT specification

Lime stabilization is generally more effective with high-plasticity soils containing more than 25% clay. The minimum lime content needed to stabilize the subgrade should maintain the soil's pH at 12.4 and achieve a UCS of at least 60 psi. In cement-lime stabilization, lime reduces the water content to the OMC or achieves the PI required by design, while cement enhances strength development. Lime-fly ash stabilized subgrade is recommended for soils with high PI or for soils with low silica dioxide and alumina oxide concentrations.

A technical report by Elseifi et al. (2017), prepared for the Louisiana Transportation Research Center, reviewed the utilization of lime in pavement applications. The primary objective of this research was to document best practices for using lime to dry soils, as working platforms, and in pavement applications. The report also explored the incorporation of lime into pavement design across the United States, detailing test methods, field applications, and evaluation techniques used to assess the quality of field construction. The literature review and survey of multiple state Departments of Transportation (DOTs) found that for states using lime-stabilized subgrades in design, a structural layer coefficient of approximately 0.11 is commonly adopted.

Elseifi et al. (2017) also analyzed the types of soils suitable for lime applications, focusing on their PL, LL, and PI, as shown in Table 2.1. Based on the survey, this summary reflects specifications from various DOTs regarding soil suitability for lime application. Louisiana, Indiana, and Oklahoma use lime for A-6 and A-7 soil types, while Alabama specifically applies lime to A-6 soils. Lime is predominantly used for CL and CH soils in Missouri, Saskatchewan, Arizona, and California. Kansas applies lime to ML, MH, CL, and CH soils. In Arkansas, New York, and Michigan, lime is used for clays and silty clays, whereas in Virginia, it is used for wet fine soils. The incorporation of lime-modified and lime-stabilized soils in pavement design is presented in Table 2.1. Also, the acceptance criteria for these stabilized layers are summarized in

Table 2.2 and Table 2.3.

Table 2.1 Criteria for PI, LL, and PI for lime application (Adapted from by Elseifi et al., 2017).

State	PL	LL	PI
Oklahoma	Practically ≥ 10	Practically ≥ 21	≥ 11
Virginia	20-30	30-90	30-40
Georgia	N/A	> 25	> 15
Kansas	> 17	> 25 (roughly)	> 8
North Carolina	N/A	N/A	> 25
Louisiana	N/A	N/A	> 15
Indiana	N/A	N/A	> 10
Arkansas	N/A	N/A	> 18
Mississippi	N/A	N/A	> 15
Alabama	N/A	N/A	> 12
California	N/A	N/A	> 12

Table 2.2 Recommended layer coefficients for lime-stabilized soil (Adapted from by Elseifi et al., 2017).

States	Structural Layer Coefficient	Comments
North Carolina	0.125	—
Indiana	—	Lime increases MR by 25% over the natural soils.
Arkansas	0.07 (Lime Treated Subgrade)	SN is only used for LTS in roadway typical section. SN value is not assigned for stabilization.
Oklahoma	0.05	Stabilized layers may be considered as a structural layer in areas that do not have a high water table.
Virginia	0.18	Virginia typically do not count modified subgrade in pavement design.
Mississippi	0.2	Only account lime treated subbase/base in pavement design.
Alabama	0.1	ALDOT generally performs soil modification than soil stabilization.
California	Gravel Factor = $0.9 + \text{ucs} / 1000$ (only for flexible pavement)	—
Kansas	0.14	—
Nebraska	0.22	Lime or Fly Ash Stabilized Subgrade

Table 2.3 Criteria for Accepting Lime-Modified and Lime-Stabilized Layers (Adapted from Elseifi et al., 2017).

States	Acceptance Criteria	
	Lime-Modified Layer	Lime-Stabilized layer
North Carolina	N/A	Lime purity of at least 84%
Louisiana	Density	N/A
Indiana	DCP or LWD	
Arkansas	Sounding with indicator solution to determine treated depth	Stability for working platform, sounding with indicator solution to determine treated depth
Oklahoma	Application rate, depth and uniformity of application, compacted density and moisture	
Saskatchewan	QA tests are done during construction. These tests can include Atterberg limits, water content and density etc.	
Michigan	N/A	Acceptance is based on layer thickness, lime content (%) and density. Testing for acceptance is conducted for each 4000 square yards of stabilized subgrade but at least once per day
Virginia	Spec 306; density, moisture, cure.	
Mississippi	Lime application rate and density.	
Alabama	Check of soil pulverization by gradation testing; moisture/density testing by AASHTO T 99 both before and after lime incorporation; In- place density testing by AASHTO T 310; lime application rate checks; and layer thickness checks	
California	UCS	Relative compaction
Georgia	Compaction testing only	
New York	Follows approved method	
Oregon		Nuclear density testing and proof rolling.
Kansas	Performance and phenolphthalein	
Missouri	Proof rolling	

Chapter 3 Materials

3.1 Subgrade Soil Types

Two types of subgrade soils were selected for this study from different sites in Nebraska: grey shale and clay. The grey shale was sourced from Lynch, while the clay was collected from Plattsmouth. Figure 3.1 and Figure 3.2 show the locations where the grey shale and clay were obtained, respectively.

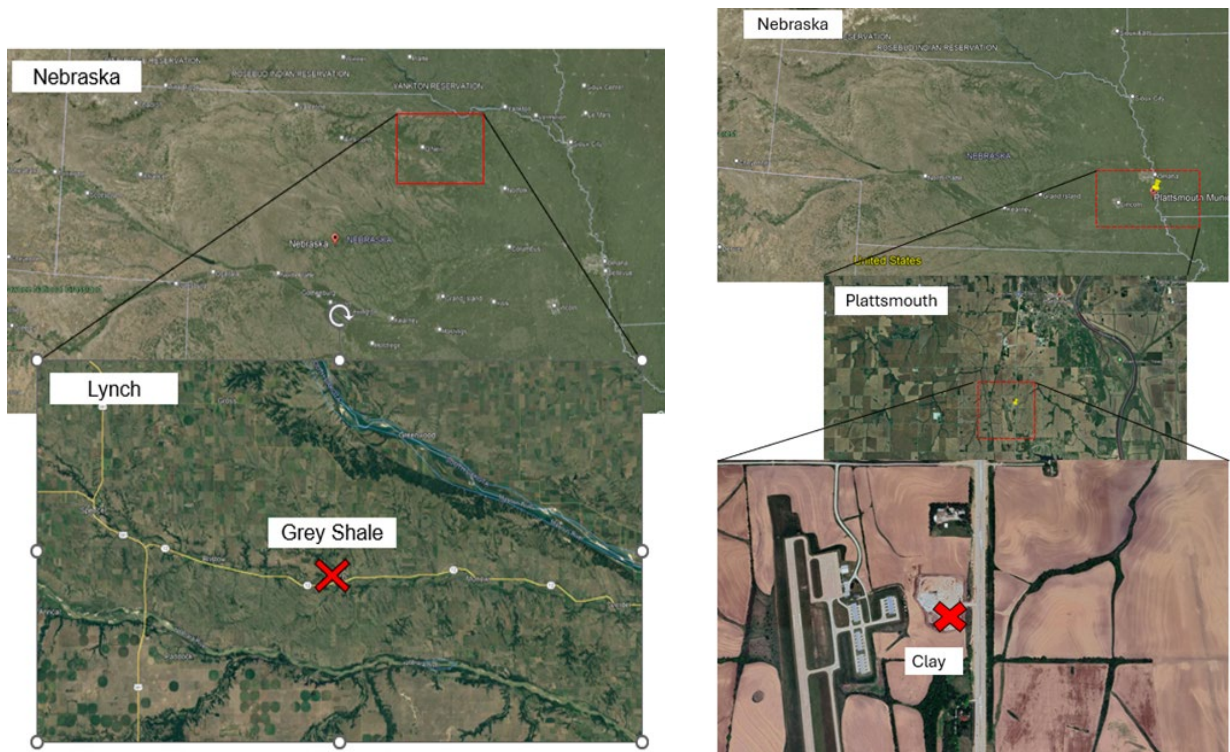


Figure 3.1 Location of Grey Shale – Lynch and Location of Clay – Plattsmouth Soil Characteristics.



Figure 3.2 a) Grey shale from Lynch site and b) clay soil at Plattsmouth site.

Preliminary tests, including Proctor tests, hydrometer tests, and Atterberg limits were conducted on the two types of subgrade soils according to ASTM procedures. The soil classification of the grey shale was determined to be MH, while the clay was classified as CL based on the Soil Classification System (USCS). The Grey Shale soil was classified as a high-plasticity silt soil with a Plasticity Index (PI) of 37.8, while the Clay was classified as a moderate-plasticity

clay with a PI of 19.0 (Table 3.1). The results of the hydrometer tests, which give detailed particle size distribution data, are presented in Figure 3.4. Additionally, the compaction curves, illustrating the relationship between moisture content and dry density for the tested soils, are shown in Figure 3.3. All tests followed the USCS and ASTM procedures.

Table 3.1 Properties of the subgrade types.

Soil Type	Grey Shale	Clay
Property	Value	Value
Liquid Limit (LL) (%)	67.5	43
Plastic Limit (PL) (%)	29.7	24
PI (%)	37.8	19
OMC (%)	28.5	18
MDD (lbs/ft ³)	92	105
USCS Classification	MH	CL
AASHTO Classification	A-7-6	A-7-5
Specific Gravity (G _s)	2.69	2.75

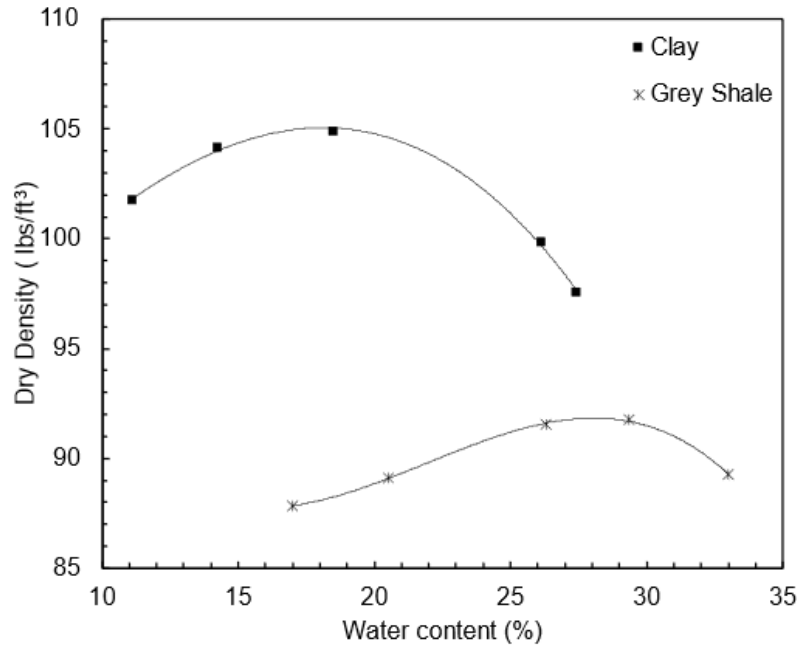


Figure 3.3 Compaction curve for grey shale and clay soil.

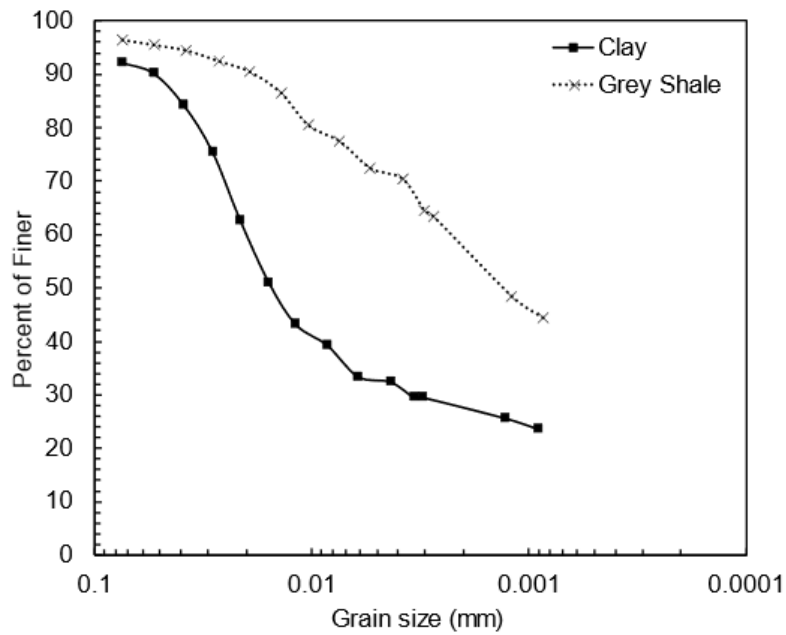


Figure 3.4 Hydrometer analysis for grey shale and clay soil.

3.2 Stabilizers and Additives

This research utilized three different calcium-based chemical stabilizers (lime, cement, fly ash) and one type of fiber, with various combinations of these materials applied to enhance lime stabilization (

Figure 3.5). The lime used in this study was hydrated lime, with a calcium hydroxide content greater than 96% (Table 3.2), and the cement was Type IL Portland cement with a calcium oxide content greater than 65% (Table 3.3). The fly ash was classified as Class C according to ASTM C618-19 (Table 3.4). The fiber used was a polypropylene monofilament fiber with a length of 19 mm, and its additional mechanical and physical properties are presented in Table 3.5.

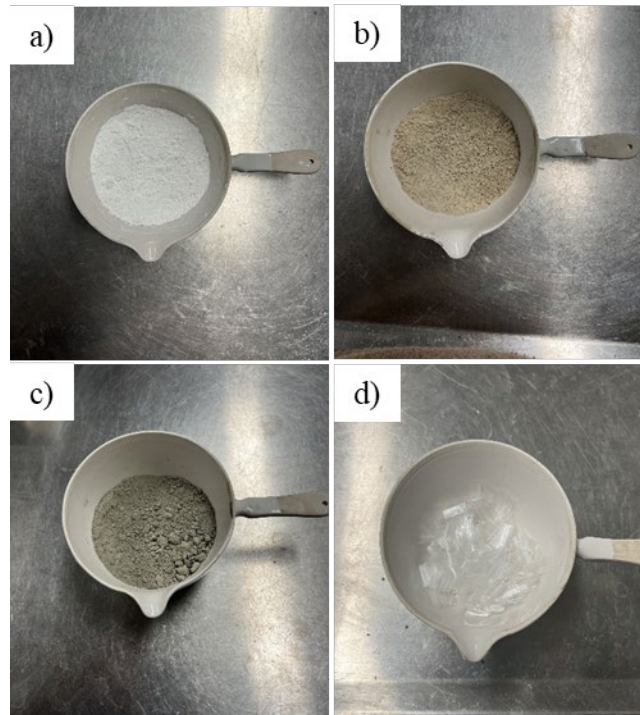


Figure 3.5 Additives used in the research: (a) Lime, (b) Cement, (c) Fly Ash, and (d) Fiber.

Table 3.2 Properties of lime.

Hydrated Lime*	
Chemical Composition (%)	
Calcium Hydroxide Ca(OH)_2	96.0 to 97.2 %
Calcium Carbonate	0.65 to 1.75 %
Magnesium Oxide	0.05 to 0.10 %
Calcium Sulfate	< 0.1 % to 0.5 %
Crystalline Silica SiO_2	0.1

*Properties of Lime were obtained from Manufacturer

Table 3.3 Properties of cement.

Cement Type 1L*	
Calcium oxide	65%
Silicon dioxide	21%
Aluminum Oxide	5%
Other	<9%

*Properties of Cement were obtained from Manufacturer.

Table 3.4 Properties of Fly ash.

Fly Ash		
Standard	ASTM C618-19, Class C	
Chemical Composition (%)		
Total Silica, Aluminum, Iron Oxides:	60.2	≥50.0%
Sulfur Trioxide:	1.6	≤5%
Calcium Oxide:	26.2	>18.0%
Volatile Composition (Mass%)		
Moisture Content	0.1	<3%
Loss on Ignition:	6	≤6%
Physical Test Results		
Fineness, Retained on #325 Sive (%):	15	≤34%
Strength Activity Index		
Percent of Control @ 7 Days:	96	≥75%
Percent of Control @ 28 Days:	107	≥75%
Water Requirement, % of Control:	95	≤105%
Soundness, Autoclave Expansion (%):	0	≤.08%
Density (g/cm3)	2.68	N/A

Table 3.5 Properties of fiber.

Fiber	
Property Raw Material	Polypropylene Fiber type monofilament
Cross-Section shape	Trefoil
Length (mm)	19
Moisture (%)	3 Max
Elastic Modulus (Mpa)	>3500
Elongation (%)	5-10
Tensile strength (Mpa)	≥ 500
Elongation at breaking (%)	≥ 15
Melting point (°C)	160-180
Acid-base resistance property (%)	≥ 94.4

Note: Properties were obtained from Manufacturer.

Chapter 4 Methodology

The methodology for this research is designed to evaluate the effectiveness of enhancing lime stabilization using cementitious materials and fiber, focusing on improving the performance of Nebraska soils. A multi-tiered experimental approach was employed, consisting of various geotechnical tests (e.g., particle size distribution, Atterberg limits, standard Proctor, UCS, and direct shear tests), environmental resistance assessments through freeze-thaw cycles, and large-scale testing using the Large-Scale Track Wheel test.

These tasks provided insights into the mechanical behavior, durability, and long-term performance of treated soils under simulated field conditions. Therefore, a comprehensive experimental program consisting of multi-scale studies was undertaken to evaluate the geotechnical properties, environmental resistance, and overall performance of stabilized soils (Figure 4.1). Based on the results from geotechnical testing, environmental assessment, and large-scale testing, design recommendations were developed to optimize the performance of stabilized subgrade soils in Nebraska. This chapter provided details for each task and experiment in the following sections.

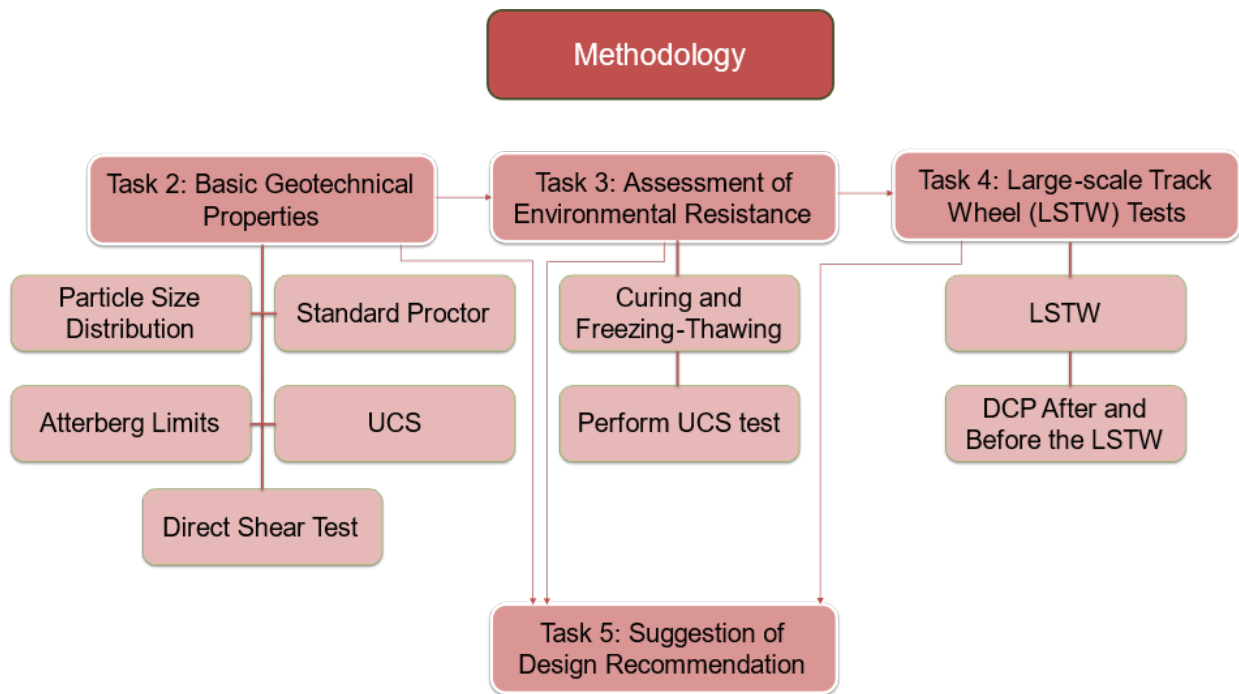


Figure 4.1 Overview of the methodology tasks for enhancing lime stabilization using cementitious materials and fiber.

4.1 Soil Preparation

The two types of subgrade soil obtained from the field were air-dried before use (Figure 4.2). The soil lumps were sieved through sieve No. 4. The portion retained on sieve No. 4 (4.75mm) was then ground using a soil grinder (Figure 4.3). The grounded soil (portion passing sieve No. 60) was used to perform laboratory scale tests such as UCS, Procter test, Atterberg limits test etc. For the Large-Scale Tracking Wheel test, the portion of soils that passed through sieve No. 4 was used.



Figure 4.2 Air drying clay soil.



Figure 4.3 Grinding of soil lumps.

4.2 Testing Matrix for Admixture Combinations

The state of Nebraska provides specific recommendations for the application of lime, cement, and fly ash for soil stabilization. According to the NDOT manual guidelines for pavement design (2018), the typical application rates for these stabilizers are as follows: lime at 4% to 6%, cement at 3% to 7%, and fly ash at 10% to 15%. Lime is primarily used to improve the plasticity and workability of cohesive soils, while cement is used to enhance the strength and stiffness of subgrade materials. Fly ash is applied to enhance both workability and long-term pozzolanic reactions.

It is important to note that there are no specific guidelines regarding the combined use of these additives, nor are there established standards for the use of fiber alone in soil stabilization. In this research, the combined effects of these additives, specifically evaluating lime contents of 0%, 3%, and 6%, cement contents of 0%, 3%, and 6%, and 10% fly ash by weight was studied. Additionally, 1% fiber was incorporated to investigate its effects, despite the lack of a standardized guideline for fiber usage in soil stabilization.

This testing matrix provides a systematic approach to assess the impact of each combination on soil properties, ultimately identifying the optimal stabilization method for improving soil performance. The testing matrix involves various admixture combinations of lime, Portland cement, fly ash, and fiber with grey shale and clay soils, as shown in

Table 4.1 Testing matrix for admixture combinations with grey shale and clay.

Soil Type	Grey Shale					Clay				
Lime Content	Control	C 3%	C 6%	FA 10%	F 1%	Control	C 3%	C 6%	FA 10%	F 1%
0%	GL0	GL0C3	GL0C6	GL0FA10	GL0F1	BL0	BL0C3	BL0C6	BL0FA10	BL0F1
3%	GL3	GL3C3	GL3C6	GL3FA10	-	BL3	BL3C3	BL3C6	BL3FA10	BL3F1
6%	GL6	GL6C3	GL6C6	GL6FA10	GL6F1	BL6	BL6C3	BL6C6	BL6FA10	-

Note: G: Grey shale B: Clay L: Lime, C: Portland cement, FA: Fly ash, and F: Fiber.

4.3 Basic Geotechnical Tests

4.3.1 Moisture-Density Relationships

Each soil/additive combination was tested to determine the optimum moisture content (OMC) and maximum dry density (MDD) according to ASTM D698-12 (ASTM. 2021). The OMC and MDD values for the untreated soils and each of the treated combinations are presented in Table 4.2.

Table 4.2 Maximum dry density and optimum moisture content.

Soil Type	Grey Shale		Clay	
Combination	MDD (lbs/ft ³)	OMC (%)	MDD (lbs/ft ³)	OMC (%)
L0	91.9	28.0	104.3	18.0
L3	91.3	32.0	98.7	22.0
L6	91.0	32.0	98.1	22.0
L0FA10	94.4	30.0	104.3	20.0
L3FA10	90.4	31.0	97.5	21.0
L6FA10	88.3	31.0	96.8	21.0
L0C3	90.9	30.0	106.8	20.0
L3C3	90.7	31.0	100.3	21.0
L6C3	89.5	31.0	95.9	21.0
L0C6	92.6	30.0	106.8	20.0
L3C6	91.5	31.0	99.1	21.0
L6C6	90.0	31.0	97.5	21.0
L0F1	88.7	28.0	103.1	18.0
L3F1	-	-	91.8	21.0
L6F1	86.3	31.0	-	-

4.3.2 Atterberg Limits

The liquid limit (LL), plastic limit (PL), and plasticity index (PI) of the two types of subgrades and the lime-treated, fly ash-treated soil, and combined lime and fly ash-treated soil mixtures were determined according to ASTM D4318. For treated soil with chemical admixture, the dry mixtures were mixed with water at optimum moisture content, then covered and mellowed for 24 hours. Atterberg limits were then determined in accordance with ASTM D4318-17e1 (ASTM. 2018). Cement-treated soils were excluded from this test because the mellowing period was sufficient to initiate the initial set of the cement-soil mixture. The initial set of cement-treated soils can begin within a short period after mixing with water (Halsted, Adaska, & McConnell, 2008).

The results of tests for Atterberg limits with the various soil/additive combinations are presented in Figure 4.4. For grey shale, the LL decreased with increasing lime content, with a more pronounced reduction observed upon the incorporation of 10% fly ash. The PL exhibited a consistent increase with lime content for both 0% and 10% fly ash treatments. Consequently, the PI demonstrated a substantial decrease. The untreated grey shale had a PI of 37.8. Following the addition of 3% lime, the PI decreased to 18.5, and with 6% lime, it further reduced to 11.4, reflecting reductions of 51% and 70%, respectively. The inclusion of 10% fly ash amplified this reduction, with the PI decreasing to 6.8 for 3% lime and 6.5 for 6% lime, corresponding to reductions of 82% and 83%, respectively. These findings highlight the effectiveness of the combined lime and fly ash technique in reducing the plasticity of grey shale soil.

Similarly, for clay soil, the LL, PL, and PI values exhibited notable changes with the application of lime and fly ash. The untreated clay soil had a PI of 19. With the addition of 3% lime, the PI decreased to 9.7, and with 6% lime, it further reduced to 7.9, reflecting reductions of 49% and 58%, respectively. When 10% fly ash was added, the PI values were 12.5 for untreated soil, 9.2 for soil treated with 3% lime, and 8.5 for soil treated with 6% lime, corresponding to reductions of 52% and 55%, respectively. These results indicate that the application of lime alone achieves similar PI reductions as lime combined with 10% fly ash.

The addition of fly ash and lime reduced the liquid limit of the soil by decreasing the thickness of the diffuse double layer. This reduction occurred due to cation exchange and flocculation processes triggered by calcium ions in fly ash and lime (Sivapullaiah et al., 1996). Moreover, combining lime and fly ash increased the soil's plastic limit. The presence of free lime in these stabilizers further diminished the diffuse double layer's thickness and enhanced flocculation of soil particles, ultimately reducing the plastic limit (Bell, 1996).

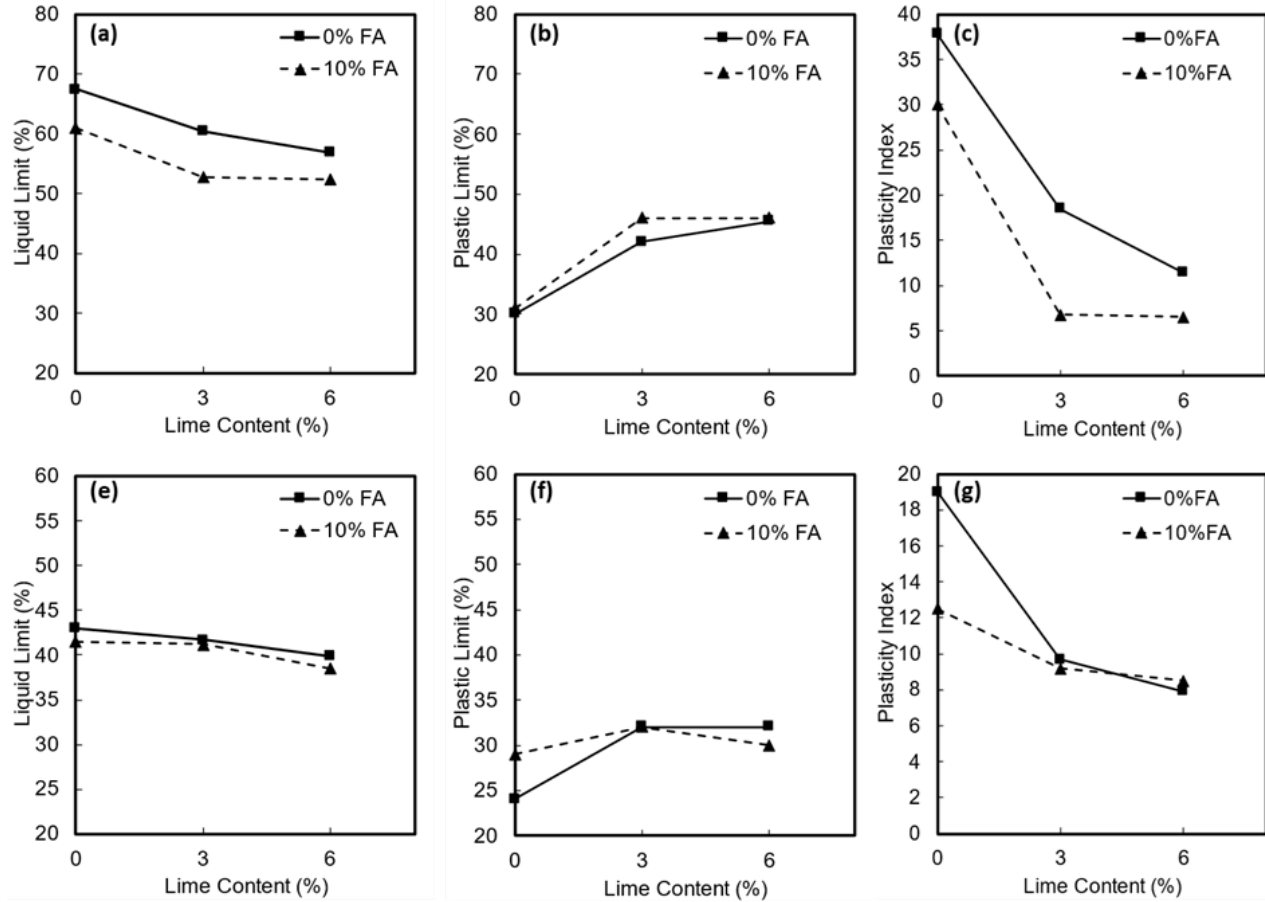


Figure 4.4 Comparison of the impact of different lime contents with 0% and 10% fly ash on: a) liquid limit, b) plastic limit, and c) plasticity index of grey shale soil, and d) liquid limit, e) plastic limit, and f) plasticity index of clay soil.

4.4 Unconfined Compressive Strength Test

The unconfined compression strength (UCS) test, performed in accordance with ASTM D D2166/D2166M (ASTM, 2016) and ASTM D5102 (ASTM, 2022), is crucial for assessing soil stabilization techniques. The UCS test involves axially loading cylindrical samples at a constant rate to obtain a continuous measurement of the load and deformation until failure, determined by the sudden fracture of samples. The load-deformation profile is evaluated to identify the peak load sustained by the samples before failure. The maximum compressive stress is obtained by dividing the peak load by the cross-sectional area of the sample.

4.4.1 UCS for Chemical Stabilized Samples

A compact and lightweight GeoJac actuator was used in conducting the UCS test (Figure 4.5). This test setup has a load capacity of 2000 pounds and a 1.5-inch stroke. It offers high precision and accuracy in applying and measuring compressive loads. This device allows for a constant rate of loading as specified in the ASTM Standards. The loading rate was set at a fixed rate of 1%/min for all tests.

For chemical stabilized soil, the UCS of the different admixture types were assessed as shown in Table 4.1.

The UCS samples were cylindrical in shape with a 1.3-inch diameter and a 2.7-inch height. Lime, fly ash, and lime-fly ash stabilized samples were prepared at MDD by mixing soil at OMC. Samples were sealed and stored in plastic bags for 24 hours, allowing the moisture to distribute evenly throughout the sample. After the 24-hour period, the samples were prepared in the mold in three layers by applying static loading using four different plugs (Figure 4.7).

For cement treated soil, cement was added to the wet mixture before the UCS samples preparation and without any mellowing to avoid cement hydration reaction. After extruding the UCS samples, the samples were wrapped by plastic film sheet and stored in a curing room for 28 days to ensure that the moisture content of the samples were preserved. Then the UCS test was performed on the samples. After testing, failure occurred along a shear plan are shown in Figure 4.6. Two samples were prepared and tested for repeatability. This approach allows for the assessment of consistency and accuracy in the testing process, providing confidence in the validity of the obtained data.

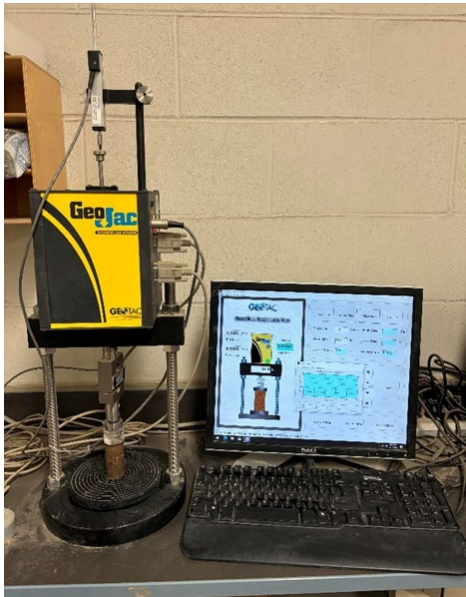


Figure 4.5 GeoJac equipment for UCS testing.



Figure 4.6 UCS sample after testing.

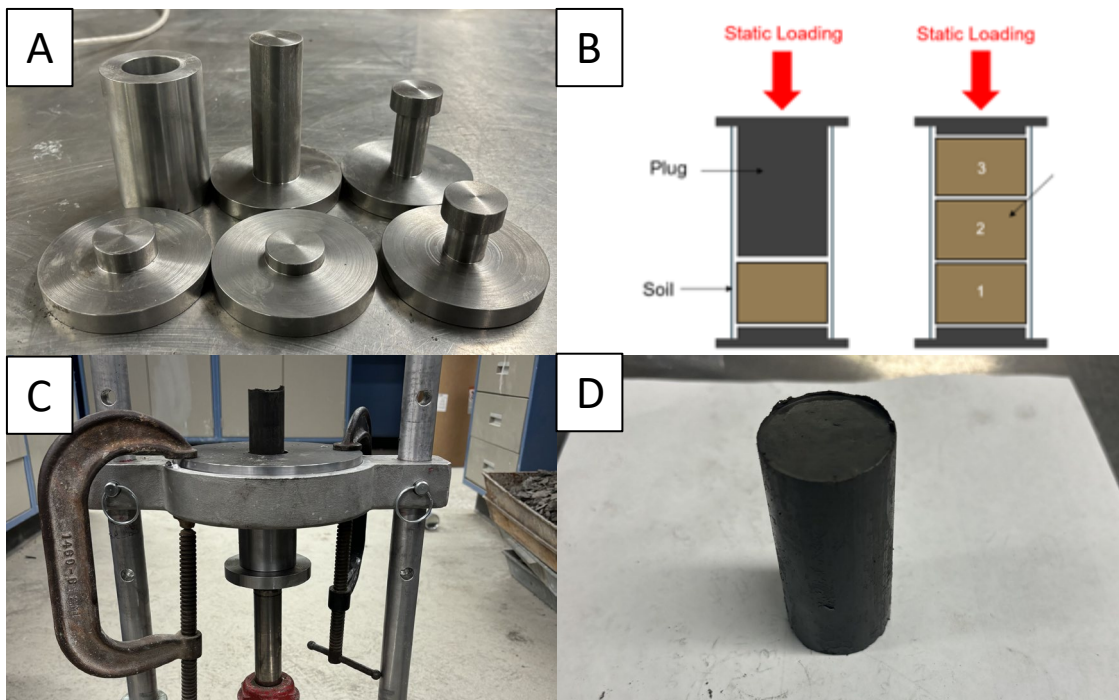


Figure 4.7 (a) UCS mold and plugs (b) Sample Preparation (c) Sample extraction (d) UCS sample.



Figure 4.8 Curing Technique.

4.4.2 UCS for Fiber Reinforced Samples

For fiber reinforced soil, the Instron 68TM-50 was used for UCS testing (Figure 4.9). This is a compact and versatile device, designed for a wide range of mechanical testing applications. It has a 11250 lbf (50 kN) force capacity. The load application and measurement are highly precise, with an accuracy of $\pm 0.5\%$. The system supports a constant loading rate as specified in ASTM and is powered by Bluehill Universal software. The system also features a data acquisition rate of up to 5 kHz and various safety and ergonomic enhancements, ensuring reliability and user-friendliness.

UCS tests were conducted at a constant strain rate of 1% per minute as specified in ASTM. The UCS of fiber with different admixture types were assessed as shown in Table 4.1. UCS samples with fiber had a 4 in. diameter and 8 in. height to avoid the scale effect of fiber. The research team conducted UCS tests with different percentages of fiber and found 1% to be the optimum fiber content which provided a higher peak and residual compressive strength (Eun et

al., 2024). Static loading was applied on the soil sample in the mold to obtain the MDD (Figure 4.10). Two samples were tested for each soil-fiber combination and the average strength reported. The fiber admixture stabilized by lime cured for 28 days, the same amount of time as the chemical stabilized UCS samples mentioned previously.



Figure 4.9 Instron testing device for fiber reinforced UCS.

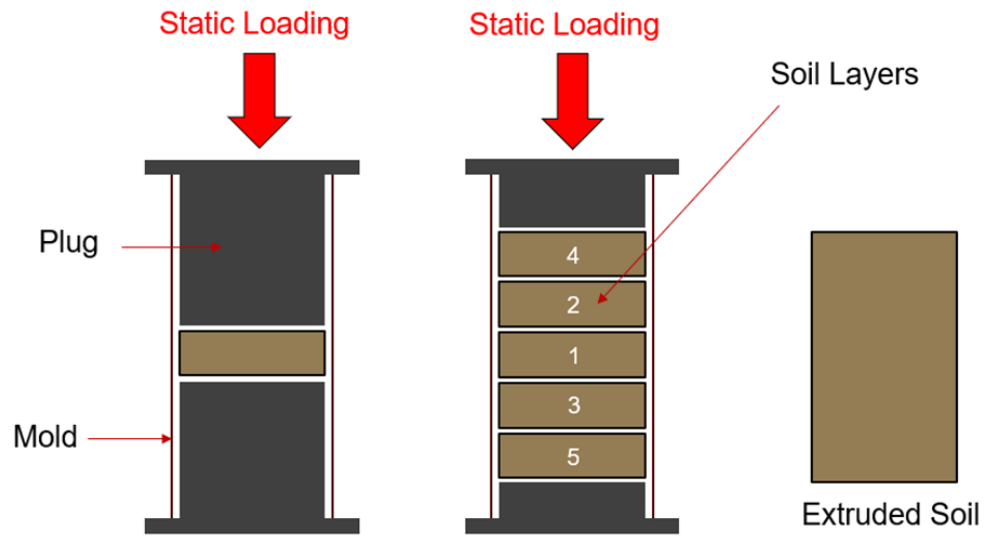


Figure 4.10 UCS fiber reinforced preparation.

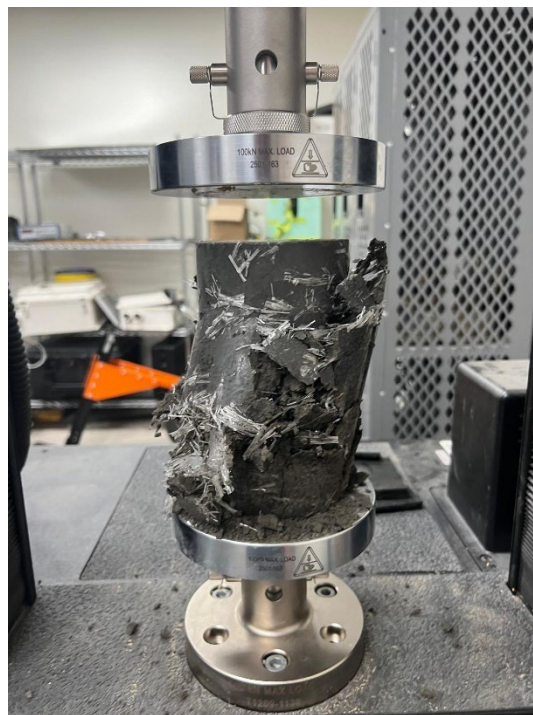


Figure 4.11 Grey shale fiber reinforced sample after testing.

4.5 Direct Shear Test

The direct shear tests were conducted using the DigiShear™ Automated Direct Shear Testing System, a computer-controlled device that automates the direct shear testing process. Equipped with GeoJacs (automated load actuators), the system applies both vertical and horizontal loads and includes four channels of 22-bit data acquisition for precise data collection. The system has a vertical and horizontal load capacity of 2000 pounds each, with a speed range from 0.000002 to 0.2 inches per minute, and horizontal travel of ± 0.5 inches. The tests were performed using specimen rings with a diameter of 2.5 inches in accordance with ASTM D3080/D3080M-23 (ASTM. 2023) for direct shear testing of soils.

The tests were conducted on a series of soil samples labeled GL0, GL0F1, BL0, and BL0F1 as presented in Table 4.1. The research team conducted a UCS test with different percentages of fiber using Nebraska soil and found that 1% was optimal (Eun et al., 2024). The samples were prepared using a mold and two plugs to achieve MDD of the soil mixture at OMC, as illustrated in Figure 4.12. For lime-stabilized samples, the lime was mixed with soil at OMC and allowed to mellow for 24 hours before sample preparation. The samples were then cured for seven days. This preparation method ensured consistent compaction and moisture conditions for accurate comparison of shear behavior across different admixture combinations. The samples were placed into the direct shear ring, and normal stresses of 60 kPa, 120 kPa, and 180 kPa were applied sequentially. Subsequently, the shear load was applied at a displacement rate of 0.06 mm/min (Figure 4.13).



Figure 4.12 Soil mixing, specimen molding, and final compacted sample prepared for direct shear testing.

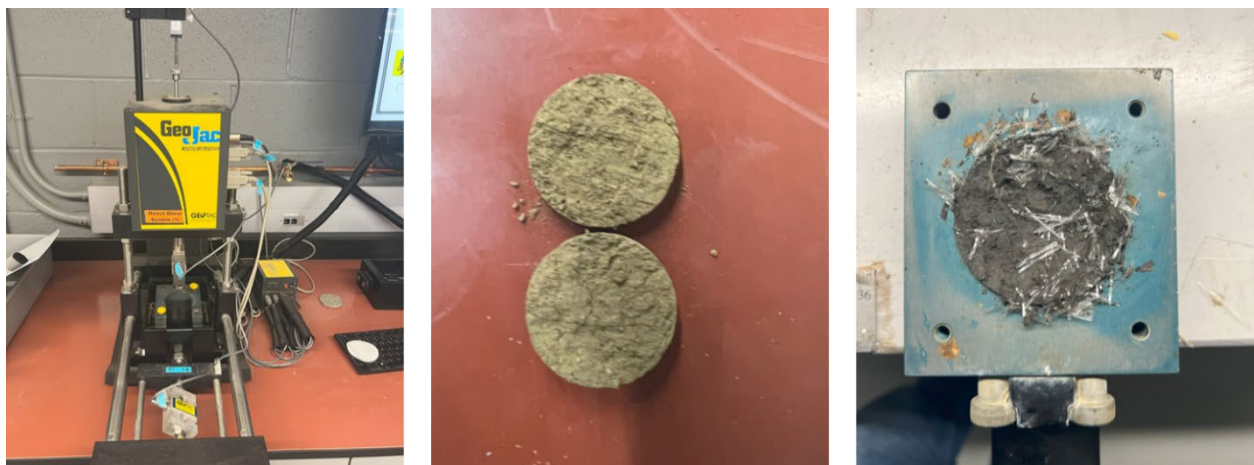


Figure 4.13 Direct shear testing setup and failed samples after testing.

4.6 Assessment of Environmental Resistance

The UCS is a key input for stabilized subgrade design in the Mechanistic-Empirical Pavement Design Guide (MEPDG) (AASHTO 2020), which is implemented in the AASHTOWare Pavement Mechanistic-Empirical Design (PMED) software. UCS indicates subgrade strength, but freezing-thawing cycles weaken it, causing failures and increasing costs. Accounting for strength

loss helps mitigate these issues, making stabilization and drainage crucial. With 113 annual freezing-thawing cycles in Omaha, Nebraska, it is essential to consider these cycles in subgrade design to ensure long-term performance and durability (National Weather Service, 2022). Therefore, a comprehensive methodology was adopted to assess the environmental resistance of stabilized soil treated with lime, cement, fly ash, and their combinations

A freezing-thawing (FT) test was used in this study to assess the environmental resistance of stabilized soil samples to simulate the harsh climatic conditions of Nebraska. An FT cycle consists of storing the stabilized soil sample at $-35^{\circ}\text{C} \pm 3^{\circ}\text{C}$ in the freezer for 24 hours, then thawing the sample at $23^{\circ}\text{C} \pm 1.5^{\circ}\text{C}$ for 24 hours (Figure 4.14). The degradation in UCS due to FT cycles was used as an indicator to assess the environmental resistance of the stabilized samples.

Two sets of FT cycles have been designed to estimate how the strength of the samples degrades with increasing cycles. The first set, developed by the research team, aimed to examine the impact of FT cycles during the early stage of stabilization. This set involved 7 FT cycles conducted after 14 days of curing to ensure the total duration of curing and FT cycles equaled 28 days. This approach allowed a direct comparison with samples cured for 28 days without being subjected to freeze-thaw cycles. The second set evaluated the environmental effect on soil strength during the later phase of stabilization with 12 FT cycles (ASTM D560/D560M) after 28 days of curing. Table 4.3 provides a summary of the curing period and FT cycles. Two UCS samples were prepared for each combination in each set of FT cycles. The UCS test was conducted after completing the FT cycles in accordance with ASTM D5102.

The reduction factor was calculated to examine the influence of FT cycles on stabilized soil using Eq.(1). The reduction factor was calculated for both stabilized and untreated soils to

evaluate the performance of each mixing combination against two sets of environmental tests.

Further discussion on these findings will be provided in subsequent sections.

$$RDF = \frac{UCS_0 - UCS_{FT}}{UCS_0} \quad (1)$$

where UCS_0 represents the unconfined compressive strength of the soil samples without FT cycles, and UCS_{FT} represents the unconfined compressive strength of the soil samples subjected to FT cycles.

Table 4.3 Freeze – Thaw sets

Set #	Curing		Freezing - Thawing	
1	Days	14	# of Cycles	7
2	Days	28	# of Cycles	12

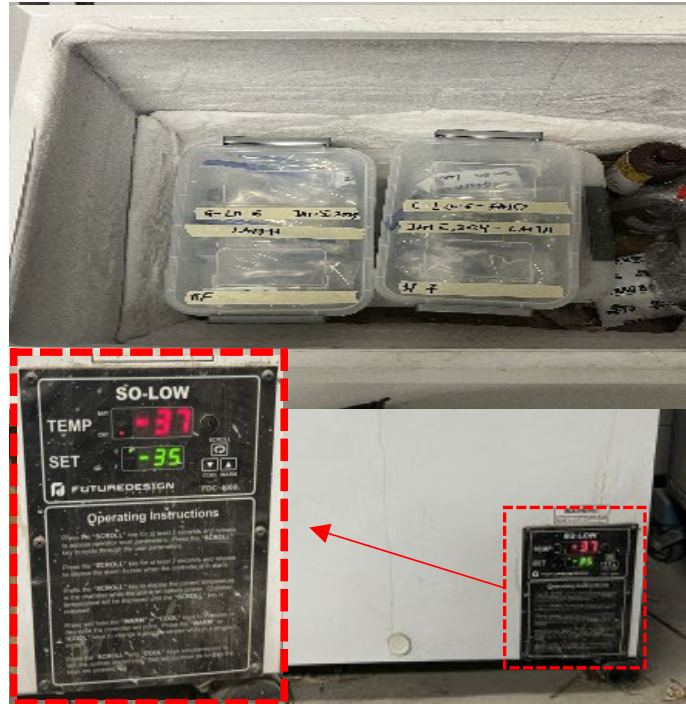


Figure 4.14 UCS samples stored in the Freezer.

4.7 Large-Scale Tracking Wheel (LSTW) Test

4.7.1 LSTW Apparatus Set-up

The research team at the University of Nebraska-Lincoln designed and constructed the LSTW testing apparatus. The mechanical performance of unreinforced, fiber reinforced and lime stabilized subgrade was evaluated using the LSTW. The test conditions closely mirrors real-world field load rolling wheel load application. To assess the long-term rutting performance of the subgrade, the team performed rolling wheel loading tests on the pavement layers, monitoring the progression of rutting over time. Additionally, the impact of cementitious and fiber materials on the strength of pavement layers, as well as the changes in pressure across the untreated soil and treated soil were evaluated.

The design of the box was taken in part from research performed by Bagshaw et al. (2015) and Kim et al. (2019) in conjunction with the Georgia Department of Transportation. Our research team fabricated the LSWT and conducted several tests on it as part of an NDOT project examining the performance of geosynthetic materials in reinforcing pavement layers (Eun et al., 2024). The box was one steel piece with additional ribs on the sides to help provide reactionary stiffness. The interior of the box was spray-painted with a black gloss to minimize friction and to prevent rust.

The large-scale box was constructed with 5.5-foot wide, 5.5-ft long, and 2.0-ft tall (1.67 meter \times 1.67 meter \times 0.61 meter) internal dimensions. The layout and the entire assembly are shown in the Appendix. The box was placed atop a track that was doweled into the floor. The track was made from c-channel steel with four outer plate extensions with holes in them for the dowels to pass through. These extensions were bolted to the inner track at one end and doweled into place on the other, stabilizing the track. The box was attached to a pulley frame which was in turn connected to a motor and a crank arm to push and pull the box in a unidirectional motion.

Ten wheels were attached to the bottom of the box to aid with unidirectional movement. The tire used during testing to apply rolling wheel loading on the soil layer surface had a 30-inch diameter with a 7.5-inch (Figure 4.15). A mounted ball bearing with two-bolt flange was placed in the wheel and connected to the setup frame by a 6-ft high strength carbon steel rod. This enabled the tire to rotate freely in place. A hydraulic actuator was used to apply a load of approximately 10 kN through the rectangular steel frame, through the steel rod and then to the wheel. The test was run at an approximate speed of 1 mph (0.447 m/s) which is similar to works by Bagshaw et al. (2015) and Wright et al. (2020) as way to standardize the testing procedure. The test set-up is shown in Figure 4.16.



Figure 4.15 Tire used for LSTW test.

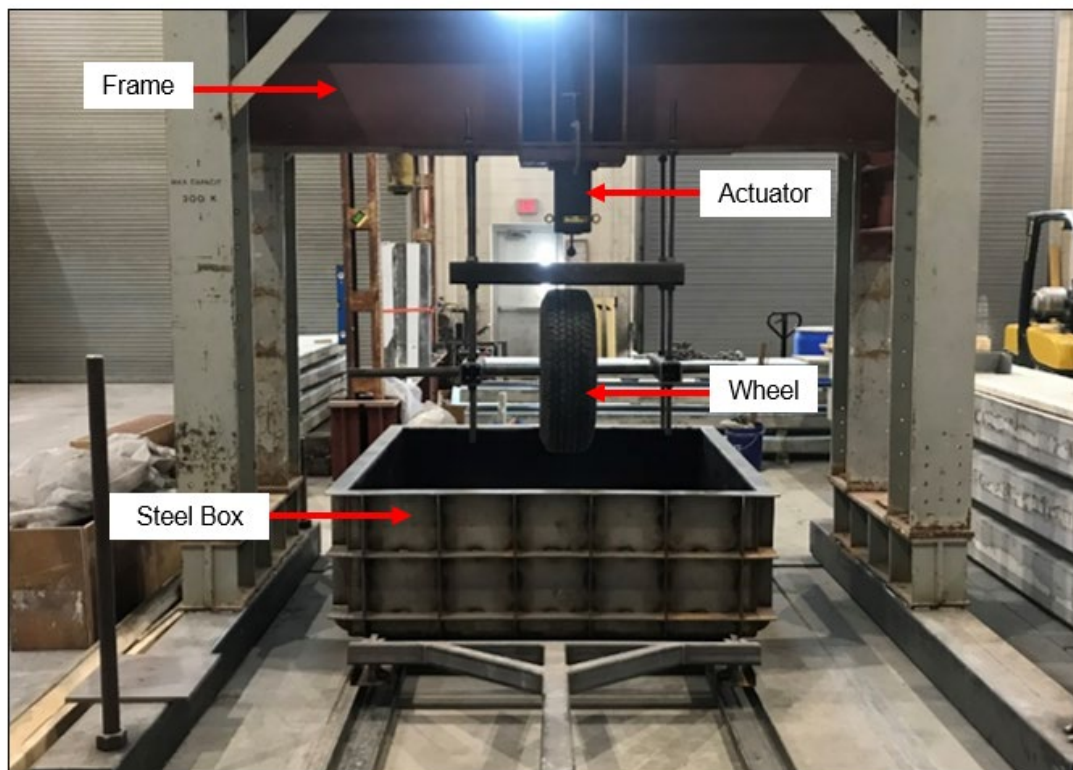


Figure 4.16 LSTW test setup.

4.7.2 Testing Matrix

For the Large-Scale Tracking Wheel test, four distinct scenarios were examined to determine the extent of permanent deformation the soil layer sustains, pressure distribution, and

the change in strength and stiffness of the pavement layers due to the use of additives. Details of these evaluations are presented in Table 4.4.

Table 4.4 LSTW testing matrix.

Case	Condition	Base thickness (in)	Sand thickness (in)
1	Control 1 (Clay)	8 in	12 in
2	Clay + 1% Fiber		
3	Control 2 (Grey Shale)		
4	Grey Shale + 6% Lime		

The steel box was filled with 12 in. of sand soil to reduce the boundary condition effect at the base of the steel box. The sand was compacted using a heavy-duty plate compactor as shown in Figure 4.17 to a relative density of approximately 80%. The sand layer compaction was performed in two lifts approximately 6 in. thick each.

The Clay and Grey Shale soils obtained from the field were first air-dried and sieved through sieve No. 4 as discussed in Section 4.1. The soil that passed through sieve No. 4 (4.75 mm) was mixed at OMC using a concrete mixer and was placed in the steel box (Figure 4.19). Cases 2 and 4, which were the fiber reinforced, and lime stabilized cases were prepared in the same way by mixing the soil and fiber/lime mixture with water in the concrete mixer. The fiber reinforced and lime stabilized soils were mixed at OMC and compacted with a heavy-duty plate compactor to a relative density of approximately 90%. Figure 4.19 shows the compacted Clay and fiber mixture in the steel box. The compaction was performed in two lifts approximately 4 in. thick each. The total height of the Clay and Grey Shale layers were 8 in each. For the lime-stabilized case, the soil was allowed to cure for seven days before the test was conducted.



Figure 4.17 Heavy duty plate compactor.



Figure 4.18 Placement of clay soil in steel box.



Figure 4.19 Compacted clay-fiber layer.

4.7.3 LSTW Test Instrumentation

4.7.3.1 Linear Variable Displacement Transducer

Four linear variable displacement transducers (LVDTs) from Harold G. Schaevits Industries with a measuring range of 2 in. were used to record the vertical deformation of the surface layer. These were made from industrial duty material for resistance to dust, temperature, shock, and variable. The vertical deformation recorded showed how rutting progressed during the test. These were fixed along a wooden beam that was held in place by a threaded rod on the sides of the steel box with bolts at the top and bottom to prevent movement during testing. The position of the LVDTs along the center of the steel box are shown in Figure 4.20. All LVDTs were calibrated before usage. The R^2 for LVDTs, representing the relationship between the voltage and calibrated readings, ranged between 0.9979 to 0.9996, as highlighted in Table 4.5. This range signifies the accuracy and precision of the LVDTs readings. The LVDTs were connected to a Keysight DAQ970A 20-channel data logger using the Benchvue software.

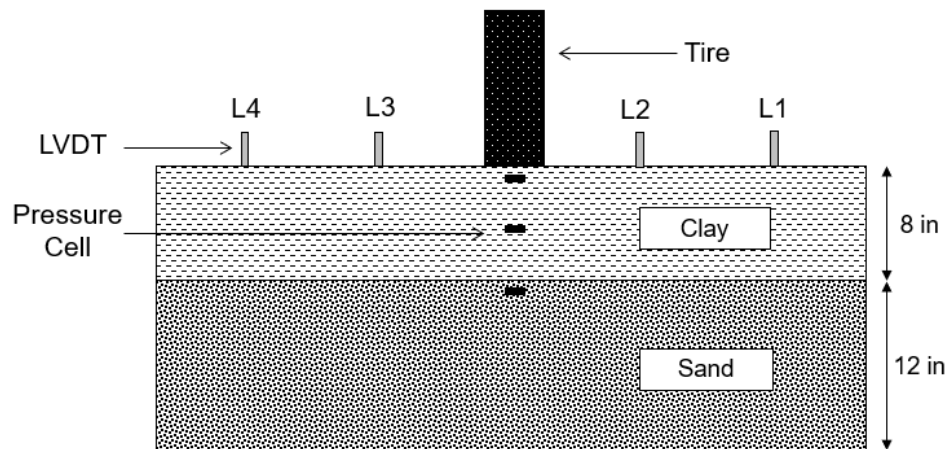


Figure 4.20 Schematic showing LVDTs and pressure cells positions in steel box.

Table 4.5 LVDT R2 summary.

LDVT	R ²
1	0.9996
2	0.9996
3	0.9979
4	0.9982

4.7.3.2 Spring Potentiometer

The UniMeasure LX-PA-20 Series linear position transducer is a low cost, compact transducer with a measuring range of 500 mm. This transducer was connected to the frame and wheel shaft to measure the deformation that occurred at the surface layer (Figure 4.21). The string potentiometer was calibrated before use. The R² for the transducer was obtained as 0.99.

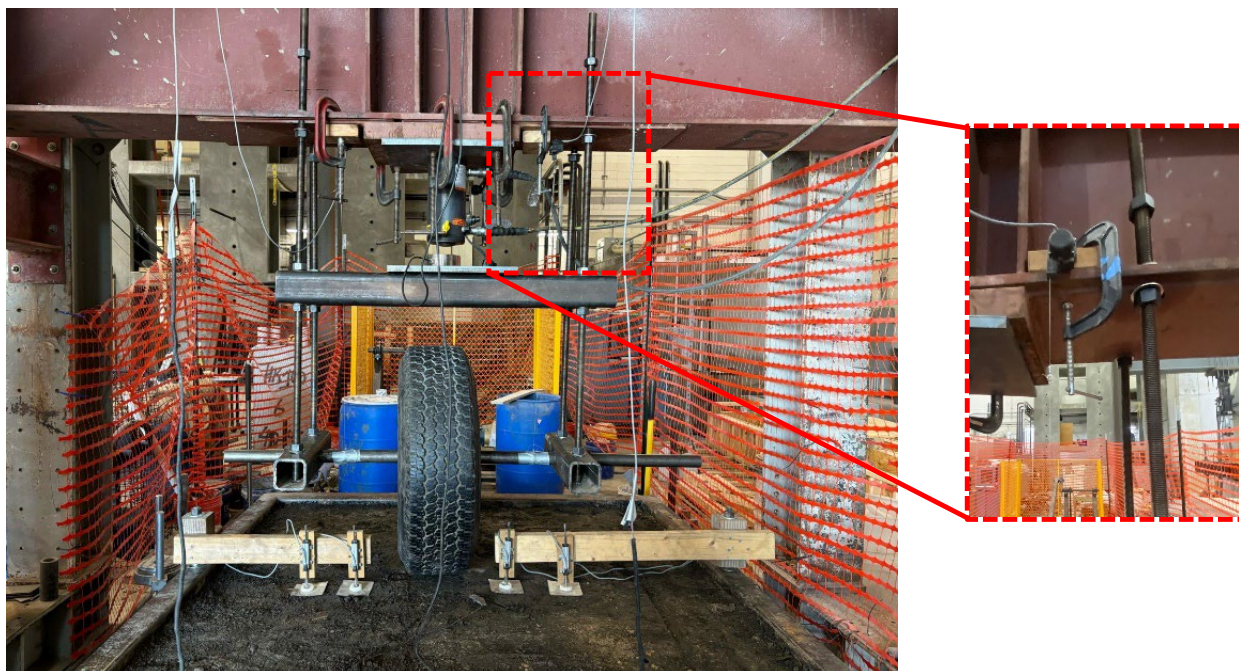


Figure 4.21 String Potentiometer position.

4.7.3.3 Pressure Cells

Three stainless steel pressure cells with excellent corrosion resistance from Tokyo Measure Instrument Lab were used to measure the pressure exerted across the soil layers. They had a 50 mm outer diameter and a dual diaphragm structure. The pressure cells were calibrated by applying different loads with the help of a calibrated actuator. A linear trend was established from which an equation was obtained for the relationship between the pressure and output voltage. The R^2 for the three pressure cells used are found in Table 4.6. The pressure sensors were also connected to a Keysight DAQ970A 20-channel data logger using the Benchvue software.

One pressure cell was installed on the compacted sand layer which is also the interface of the sand and clay/grey shale layer (Figure 4.22). A second pressure cell was installed mid-height in the clay/grey shale layer approximately 4 in. from the surface with a third pressure cell installed on top of the clay/grey shale layer (Figure 4.23). These pressure cells were used to monitor pressure distribution across the layers during testing. The schematic of the individual pressure cell positions can be seen in Figure 4.20.

Table 4.6 Pressure Cell R^2 Summary.

Pressure Cell	R^2
1	0.9999
2	0.9996
3	0.9990



Figure 4.22 Pressure cell on compacted sand layer.



Figure 4.23 Pressure cell on compacted clay layer.

4.7.3.4 Load Cell

A load cell was installed beneath the hydraulic piston to measure the load applied during the test as shown in Figure 4.24 and Figure 4.25. Assisted by an electric hydraulic pump system, an approximate load of 10 kN was applied through the actuator. The applied load was continuously monitored using a load cell and adjusted throughout testing.

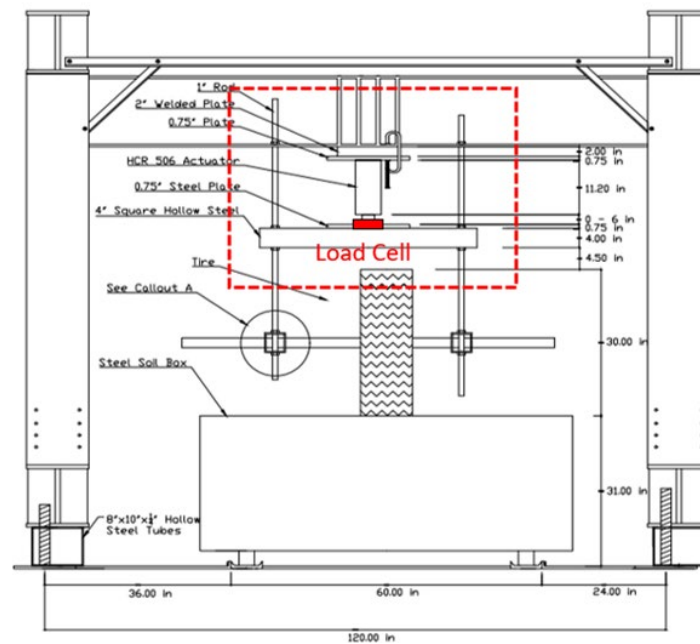


Figure 4.24 Schematic of load cell position.



Figure 4.25 Load cell positioned beneath actuator.

4.7.3.5 Test Run

The load cell, LVDTs, string potentiometer and pressure cells were connected to their respective power supply units and the data acquisition system. The data acquisition box was connected to a laptop to record the data during testing. The wheel was gently lowered onto the surface of the soil in the steel box. A 10 kN load was applied on the surface of the layers. The test setup was then turned on from the control unit initiating the unidirectional motion of the box at a speed of approximately 1 mph. The testing setup showing the LVDTs and pressure cell positions is shown in Figure 4.26.

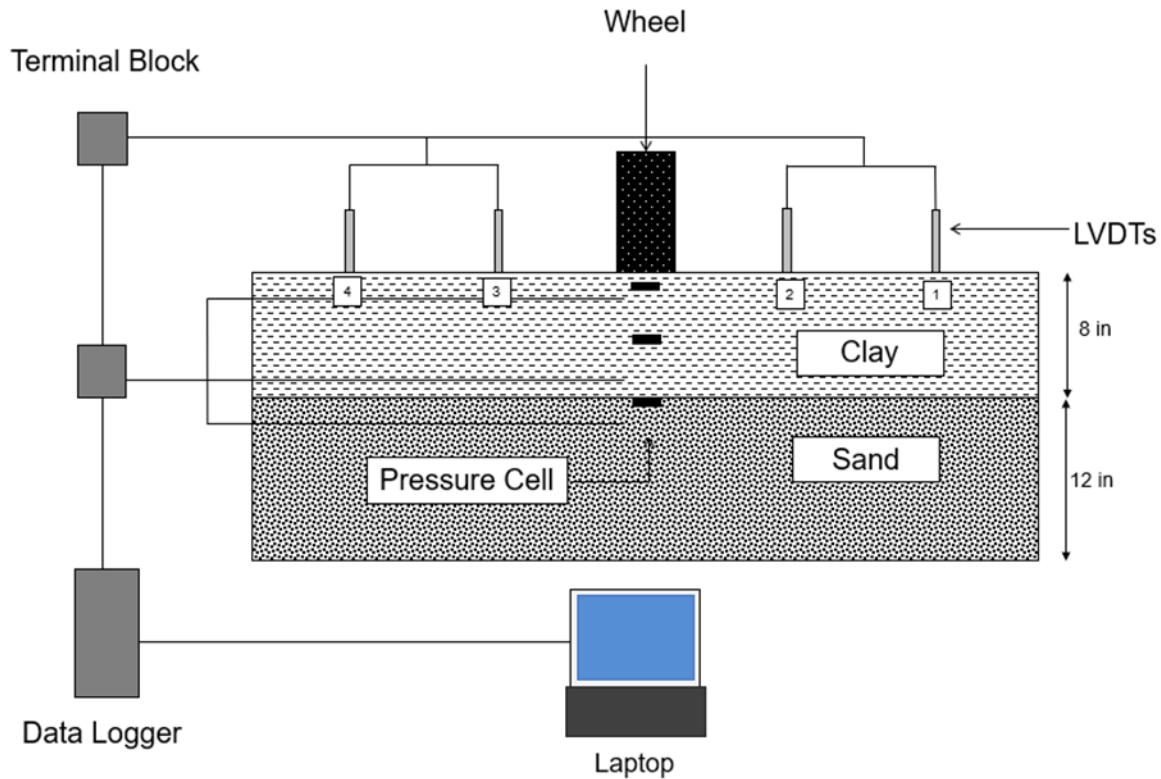


Figure 4.26 LSTW complete test setup.

4.8 Dynamic Cone Penetrometer Test

The Dynamic Cone Penetration (DCP) Test provides a measure of a material's in-situ resistance to penetration. The DCP device is shown in Figure 4.27. The number of blows required for the cone to penetrate a specific depth (usually measured in mm/blow) gives an indication of the soil's strength and is called Dynamic Penetration Index (DPI). This test was conducted before and after applying rolling wheel loads to the surface of the prepared layers (Figure 4.28). The DPI was correlated with resilient modulus using Herath et al. (2005) (Eq. 1) to provide an indication of how the stiffness within the pavement layer changes for both stabilized and untreated cases.

$$Mr \text{ (MPa)} = 16.28 + \frac{928.24}{DPI} \quad (1)$$

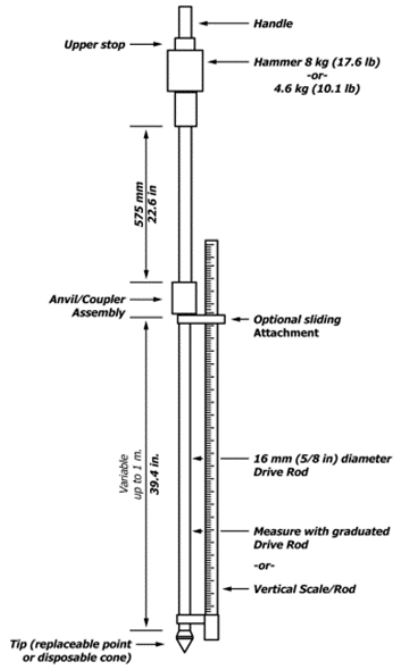


Figure 4.27 Schematic of DCP device.



Figure 4.28 DCP test on compacted fiber reinforced clay layer.

Chapter 5 Results and Discussion

5.1 UCS Results

The UCS results for grey shale and clay soils stabilized with lime and lime-fly ash are presented in Figure 5.1. Figure 5.2 shows result specifically for grey shale while Figure 5.3 presents result for clay soil. The samples were prepared and cured for 28 days.

The UCS increased from 61.2 psi (GL0) to 130.3 psi (GL3), representing an increase of approximately 113%. The UCS further increased to 300.7 psi for GL6, which is around 391% higher than GL0. The inclusion of 10% fly ash with 3% lime (GL3FA10) resulted in a UCS of 238.0 psi, resulting in an 82% improvement compared to adding only 3% lime (GL3). The UCS values for GL6 and GL6FA10 were approximately equal, which means that adding fly ash at higher lime content had a limited effect.

The stress-strain response for grey shale exhibited a significant increase in peak stress as the lime content increased from 0% to 6%, which demonstrated enhanced strength due to improved pozzolanic activity. The inclusion of fly ash (Figure 5.2b) improved the stress-strain behavior further, with higher peak stresses observed, particularly for GL3FA10. These trends align with the UCS results presented in Figure 5.2c, which indicated that adding fly ash alongside lime provided an additional strength benefit, though the effect is more pronounced at lower lime contents.

The UCS results for clay soil are illustrated in Figure 5.3. The stress-strain curves for lime-stabilized soil (Figure 5.3a) show an increase in peak stress from BL0 to BL3, with UCS increasing from 67.9 psi to 147.9 psi, which represents an improvement of approximately 118%. The UCS stabilized at 148.7 psi for BL6, and there was no significant difference compared to BL3. The average UCS versus lime content is shown in Figure 5.3c. This confirmed that the addition of fly ash had a limited effect on enhancing clay soil strength compared to lime-only stabilization.

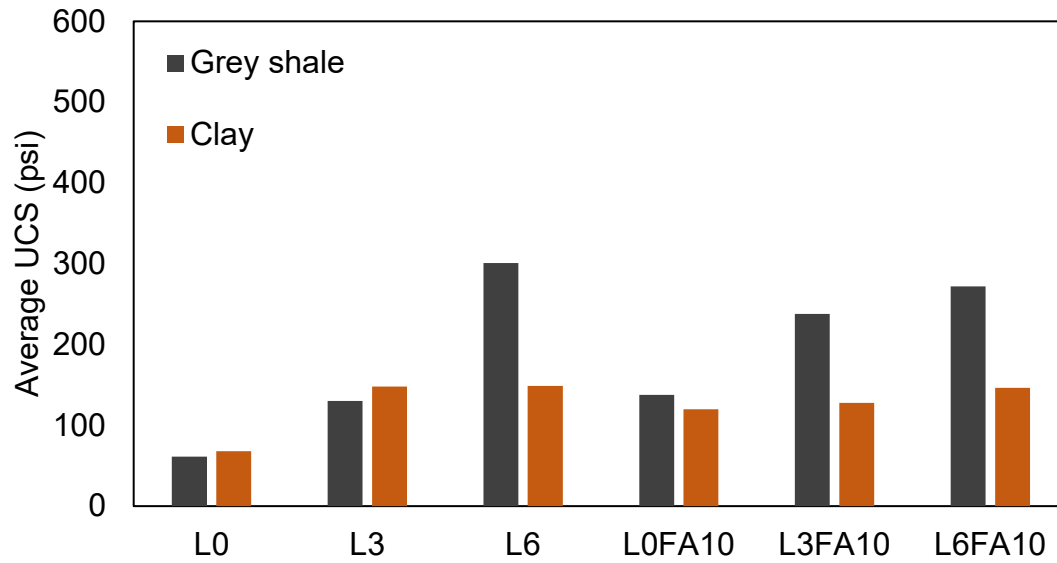


Figure 5.1 Comparison of UCS for grey shale and clay with 0%, 3%, and 6% lime (L), 0% and 10% fly ash (FA), and their combinations.

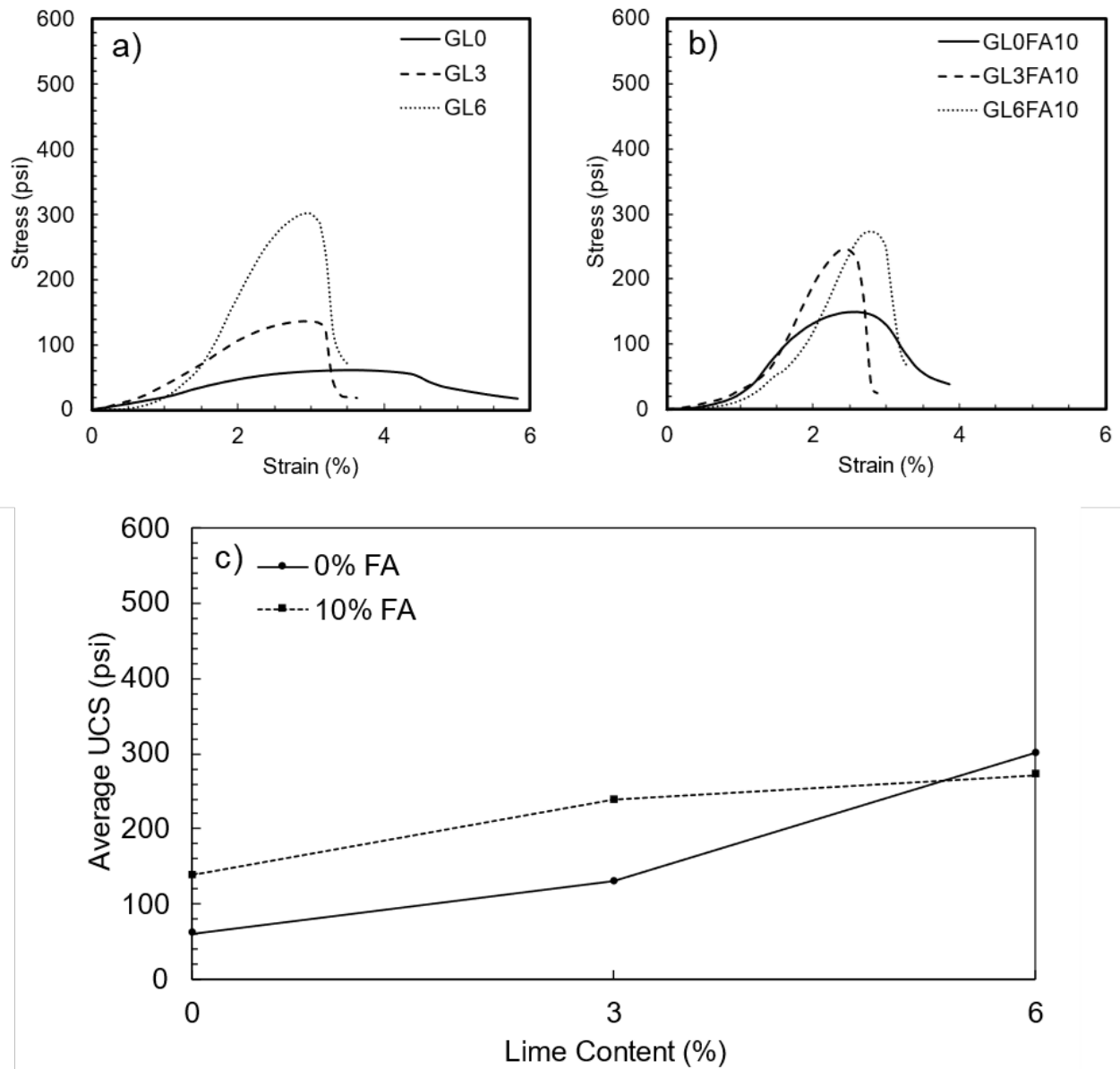


Figure 5.2 UCS results for grey shale soil: (a) stress-strain curves for lime-stabilized soil, (b) stress-strain curves for lime-fly ash stabilized soil, and (c) average UCS versus lime content.

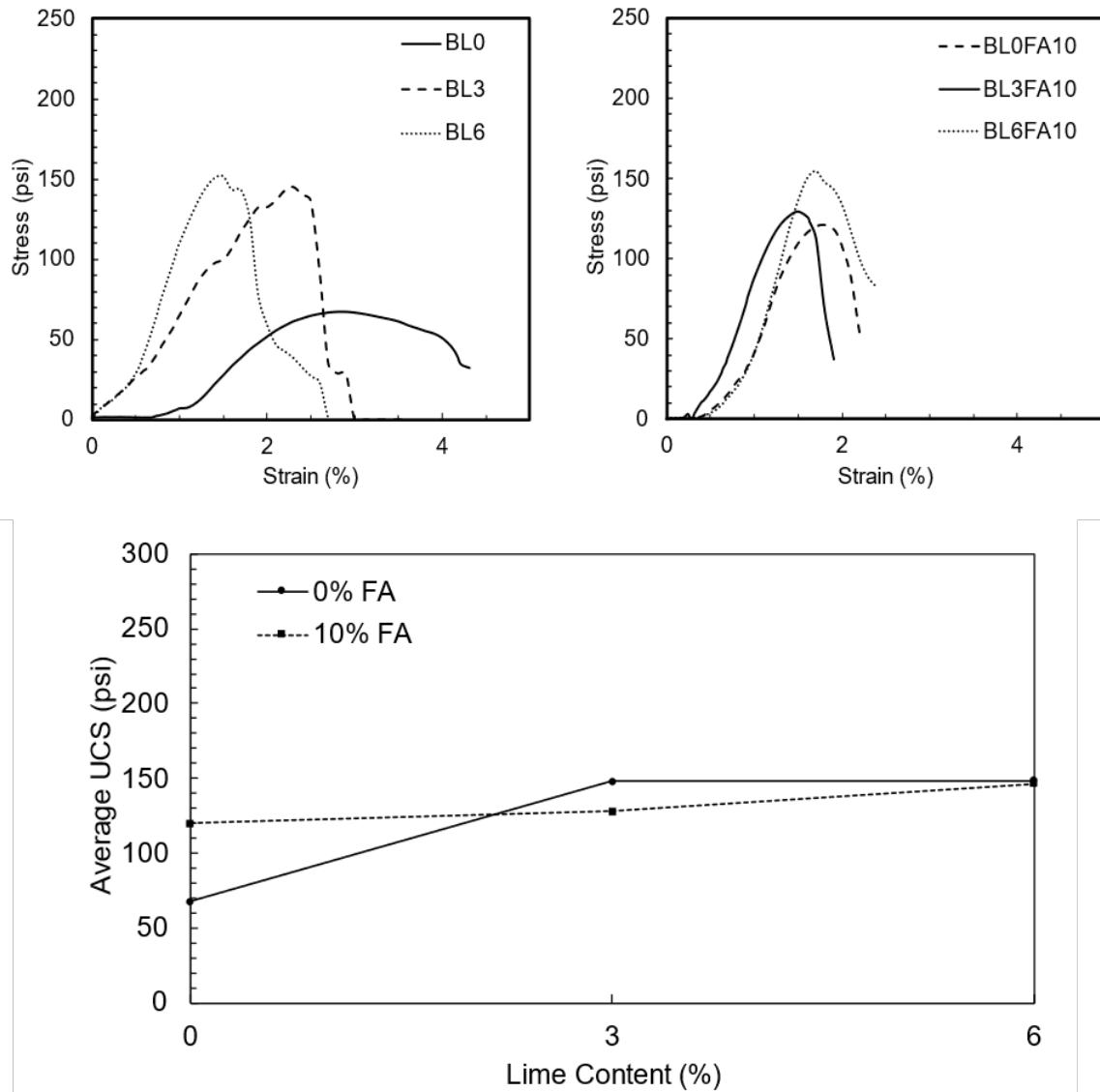


Figure 5.3 UCS results for clay soil: (a) stress-strain curves for lime-stabilized soil, (b) stress-strain curves for lime-fly ash stabilized soil, and (c) average UCS versus lime content.

The UCS results for grey shale and clay soils stabilized with lime and cement at different percentages are presented in Figure 5.4. For grey shale soil, the initial UCS was 61.2 psi, and it increased significantly with the addition of both lime and cement. The UCS values for GL0C3 (129.6 psi) and GL3C3 (287.3 psi) showed considerable strength gains compared to the unstabilized sample GL0 (61.2 psi). The improvements were approximately 112% and 369%,

respectively. The highest UCS value was observed for GL6C6 (490.8 psi), an increase of 702% compared to unstabilized grey shale (GL0). The increase in UCS can be attributed to the enhanced hydration and pozzolanic reactions between cement, lime, and the mineral components of the grey shale, which result in better binding and stronger soil matrices.

For clay soil, the initial UCS was 67.9 psi, and the values also showed an increase with higher cement content, though the overall strength gains were less pronounced compared to grey shale. The UCS for BL0C3 was 204.4 psi. This represents an improvement of approximately 201% compared to untreated clay (BL0, 67.9 psi). For BL3C3 and BL6C3, the UCS increased to 211.2 psi and 244.1 psi, representing improvements of approximately 211% and 259%, respectively, compared to BL0. The highest UCS was recorded for BL6C6 (379.2 psi), representing an improvement of approximately 458% compared to untreated clay (BL0), demonstrating that the combination of lime and cement provided a significant improvement over untreated clay soil. In comparison to grey shale, clay showed a more moderate response to stabilization. This is likely due to the mineralogy of the clay, and which may have a lower calcium content, limiting the effectiveness of reactions with cement.

The increase in UCS for two types of soil treated by lime and cementitious materials is an immediate response to adding lime and cementitious materials, caused by cation exchange, flocculation, and aggregation as calcium ions (Ca^{2+}) replace sodium ions (Na^{+}), reducing the diffuse double layer and forming a more granular structure (Bell, 1996). The improvement in soil strength when using lime, cement, fly ash, or their combinations is primarily driven by hydration and pozzolanic reactions. These reactions form cementitious compounds that coat and bind soil particles together, enhancing the soil structure (Ferguson & Levorson, 1999; Ural, 2016). Fly ash, in particular, boosts this process by increasing the availability of silica and alumina, which react

with calcium hydroxide to form additional calcium silicate hydrates, further strengthening the soil matrix and improving its durability (Rabab'ah et al., 2021; Ferguson & Levorson, 1999).

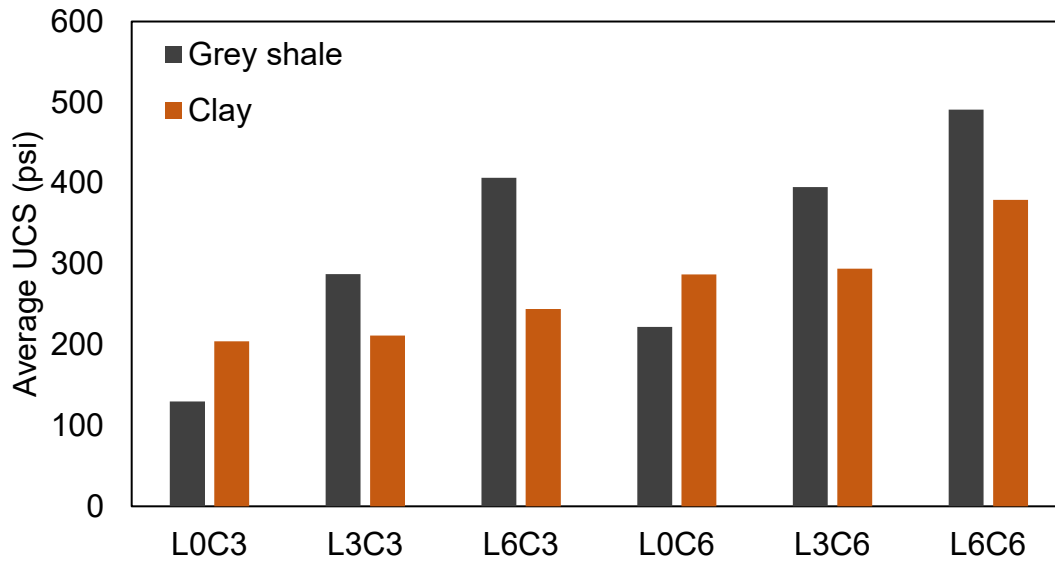


Figure 5.4 Comparison of UCS for grey shale and clay with 0%, 3%, and 6% lime (L), 3%, and 6% cement (C), and their combinations.

The UCS results for grey shale and clay soils stabilized with lime, fiber, and their combinations are presented in Figure 5.5. The GL0F1, GL6F1, BL0F1, and BL3F1 indicate the performance of the lime stabilized - fiber reinforced samples under various conditions. Based on the previous results, untreated grey shale showed significant strength improvement when lime was added, with 6% lime providing greater gains compared to 3%. In clay soil, untreated results showed similar strength improvements for both 3% and 6% lime. Therefore, 6% lime was selected for grey shale, and 3% lime for clay. Therefore, fiber was combined with 6% lime for grey shale and 3% lime for clay to optimize performance and material use.

The UCS value for GL0F1 was 57.7 psi. Compared to the untreated grey shale (GL0) with a UCS of 61.2 psi, the GL0F1 sample showed a decrease of approximately 5.7%. For the GL3 (without fiber) case, the UCS was 147.9 psi. The GL3F1 sample showed a UCS of 137.4 psi,

indicating a decrease of approximately 7.1%. The UCS values for BL0F1 and BL3F1 are 51.0 psi and 137.4 psi, respectively. Compared to the untreated clay soil (BL0) with a UCS of 67.9 psi, the BL0F1 sample showed a decrease of approximately 24.9%. For the BL3 case, the UCS was 147.9 psi. The BL3F1 sample showed a UCS of 137.4 psi, indicating a decrease of approximately 7.1%. This shows that the addition of fiber did not significantly increase the UCS compared to lime alone. This could also be related to differences in techniques when preparing the fiber-reinforced samples, apparatus testing, and the shear rate applied, which may influence these outcomes as mentioned in the previous chapter.

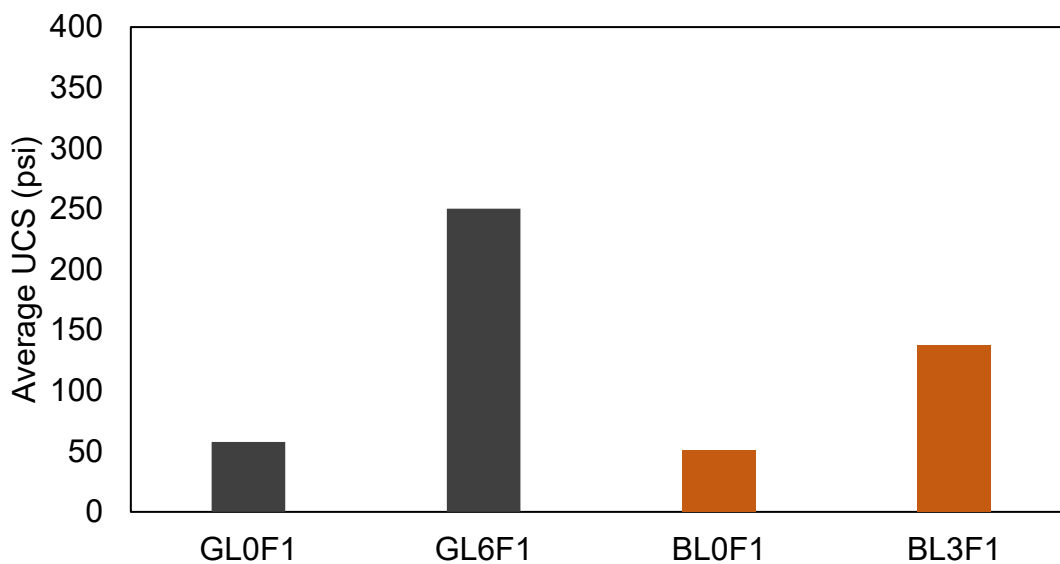


Figure 5.5 UCS values for grey shale and clay stabilized with lime and fiber.

5.2 Direct Shear Results

The direct shear test was performed to evaluate the shear strength parameters of grey shale and clay soils. Several tests were conducted with different combinations, including soil alone, fiber, lime, and lime-fiber (BL0F0, BL0F1, BL3F0, GL0F0, GL0F1, and GL6F0). The goal was to assess how the inclusion of fiber and lime affected the cohesion and internal friction angle of the soil. The results showed notable differences between the control, fiber-reinforced, and lime-

stabilized samples. These differences indicate the positive effects of both fiber reinforcement and lime stabilization on the shear strength of the soil.

The results of the direct shear test demonstrated that both fiber reinforcement and lime stabilization significantly improved the shear strength of the grey shale soil (Table 5.1). For the control sample (GL0F0), the peak cohesion value was observed to be 74.0 kPa, with an internal friction angle (ϕ) of 13.7°. For the fiber-reinforced soil (GL0F1), the peak cohesion increased to 108.4 kPa, indicating a significant improvement, while the internal friction angle showed a negligible reduction to 13.3°. For the lime-stabilized soil (GL6F0), the peak cohesion increased to 109 kPa, and the internal friction angle increased significantly to 32.7°.

The residual shear strength parameters also showed notable changes (Table 5.2). For the control sample (GL0F0), the residual cohesion was 36.6 kPa, with an internal friction angle (ϕ) of 24.3°. For the fiber-reinforced soil (GL0F1), the residual cohesion increased to 77.1 kPa, while the internal friction angle slightly decreased to 24.1°. For the lime-stabilized soil (GL6F0), the residual cohesion increased to 41.6 kPa, and the internal friction angle increased significantly to 44.0°.

Table 5.1 Peak Residual shear strength parameters for grey shale and its stabilized cases.

Combination	C (kPa)	Φ (°)
GL0F0	74	13.7
GL0F1	108.4	13.3
GL6F0	109	32.7

Table 5.2 Residual shear strength parameters for grey shale and its stabilized cases.

Combination	C (kPa)	Φ (°)
GL0F0	36.6	24.3
GL0F1	77.1	24.1
GL6F0	41.6	44.0

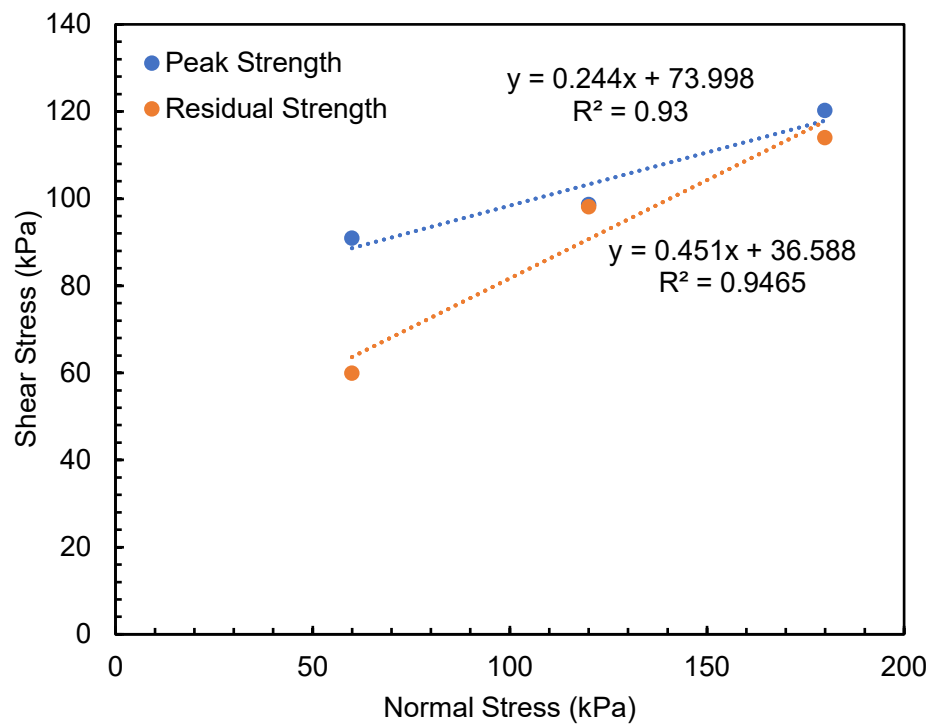


Figure 5.6 Shear stress versus normal stress for GL0F0.

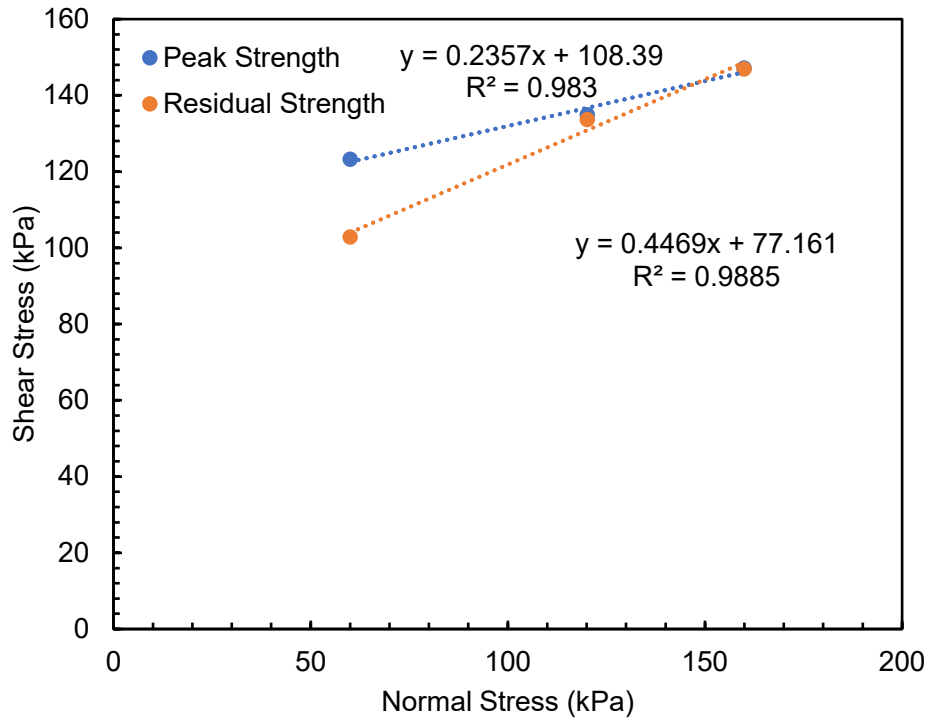


Figure 5.7 Shear stress versus normal stress for GL0F1.

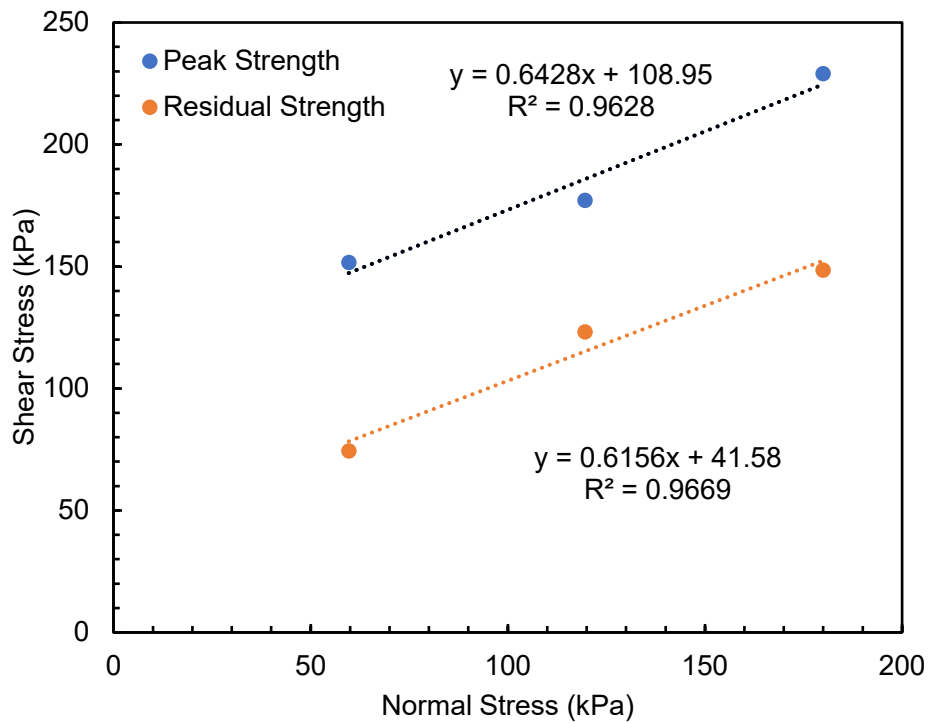


Figure 5.8 Shear stress versus normal stress for GL6F0.

The direct shear test was conducted on clay soil with different fiber contents, including BL0F0, BL0F1, and BL3F0. The peak shear strength and residual shear strength parameters obtained are shown in the Table 5.3 and Table 5.4.

The results demonstrate that adding fiber to clay soil significantly improved the peak shear strength. For the control sample (BL0F0), the cohesion was 56 kPa with an internal friction angle (ϕ) of 36.9°. When 1% fiber was added (BL0F1), the cohesion increased to 61.3 kPa, and the friction angle slightly increased to 37.1°, indicating a modest enhancement in shear strength. For the sample with 3% lime addition (BL3F0), the cohesion increased to 73 kPa, with the internal friction angle (ϕ) of 43.8°.

The residual shear strength parameters also showed significant changes. For the control sample (BL0F0), the residual cohesion was 0 kPa, with an internal friction angle (ϕ) of 45.6°. When 1% fiber was added (BL0F1), the residual cohesion increased to 40.7 kPa, while the friction angle decreased slightly to 45.0°. In the case of 3% lime addition without fiber (BL3F0), the residual cohesion was 40.7 kPa, with the internal friction angle slightly decreasing to 44.6°. These results indicate that fiber reinforcement effectively improves residual cohesion.

The increase in cohesion and internal friction angle is attributed to two factors: the interaction between fibers and soil particles, and the cementitious bonds formed by lime. Fibers interlock with soil particles, resisting shear, while lime forms bonds that improve both cohesion and friction angle. While the inclusion of fibers showed a less significant increase in the UCS of the stabilized soil, the shear strength parameters increased with fiber addition. These enhancements increase resistance to shear stress, benefiting slope and embankment stability.

Table 5.3 Peak shear strength parameters of the clay soil combinations its stabilized cases.

Combination	C (kPa)	Φ (degree °)
BL0F0	36.6	24.3
BL0F1	77.1	24.1
BL3F0	41.6	44.0

Table 5.4 Residual shear strength parameters of the clay soil combination its stabilized cases.

Combination	C (kPa)	Φ (degree °)
BL0F0	36.6	24.3
BL0F1	77.1	24.1
BL3F0	41.6	44.0

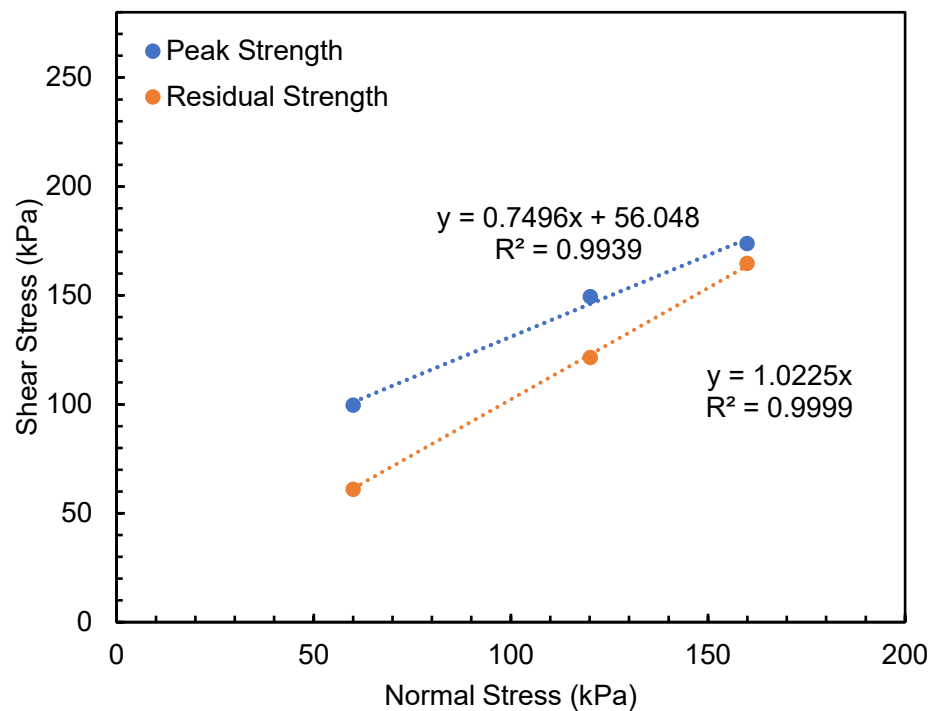


Figure 5.9 Shear stress versus normal stress for BL0F0.

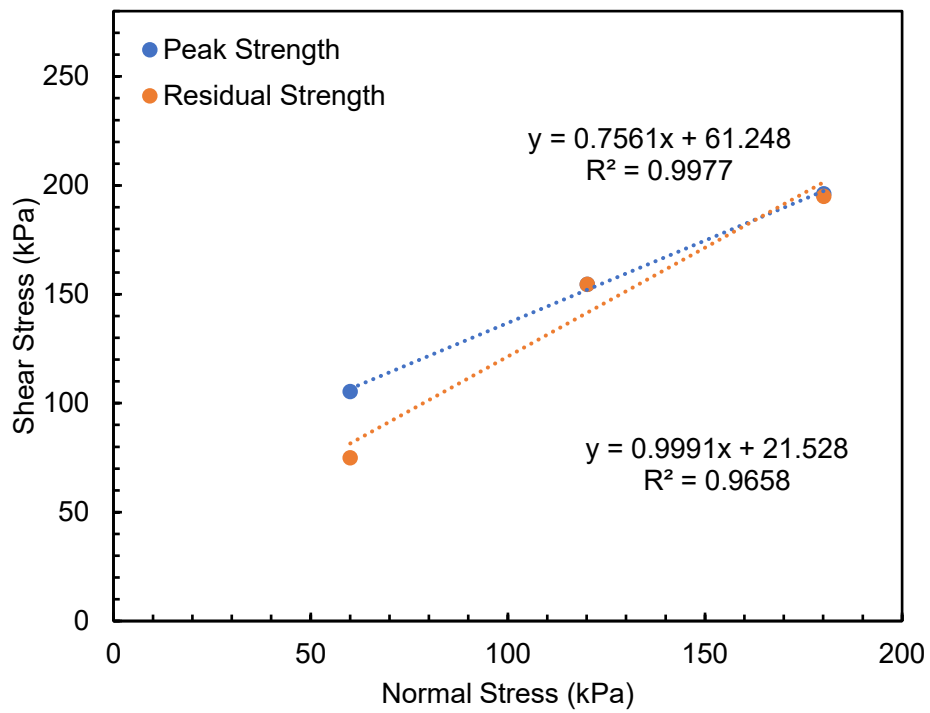


Figure 5.10 Shear stress versus normal stress for BL0F1.

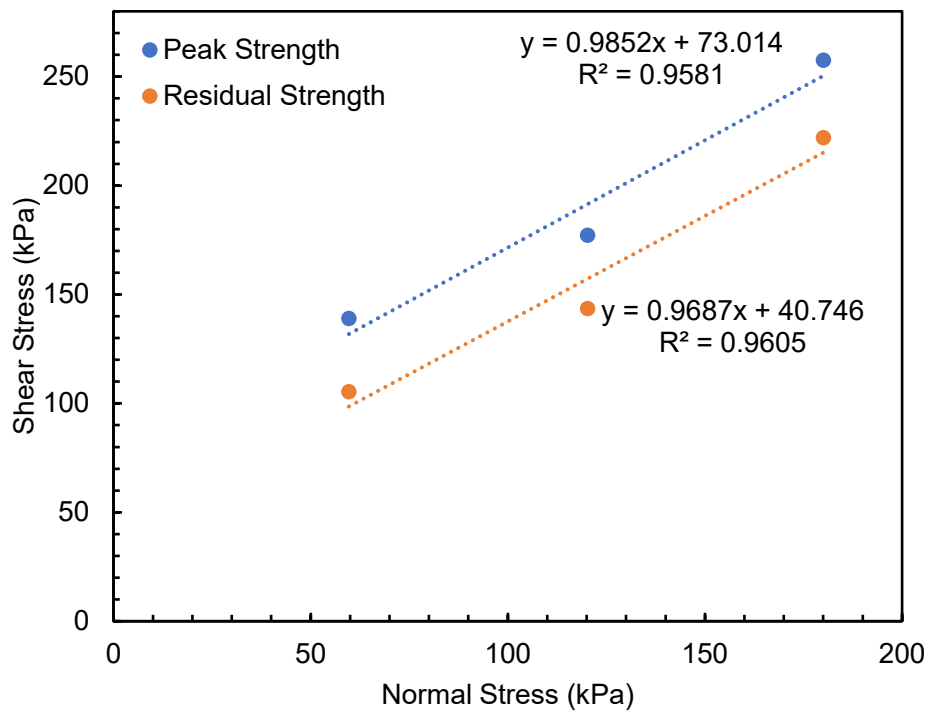


Figure 5.11 Shear stress versus normal stress for BL3F0.

5.3 Assessment of Environmental Resistance

In this section, the results of assessing the environmental resistance of stabilized soils are presented. The UCS was used as the key indicator to evaluate the mechanical integrity and durability of soils, particularly under stabilization treatments aimed at enhancing lime stabilization with cementitious materials and fiber. The focus of this section is on the performance of grey shale and clay soils under FT conditions. The assessment of environmental resistance involved evaluating the performance of stabilized samples under FT conditions, which is critical to understanding the effectiveness of the stabilization measures. Two sets of FT cycles were used to simulate different stages of exposure. The first set involved curing the samples for 14 days, followed by seven FT cycles, representing the early stage of exposure. The second set involved curing the samples for 28 days and then subjecting them to 12 FT cycles, representing the latter phase of freeze-thaw exposure.

5.3.1 Discussion of UCS Results for Grey Shale and Clay Soil Stabilized by Lime and Lime-Fly Ash After Seven FT Cycles

The UCS for grey shale soil stabilized with lime and lime-fly ash before and after seven FT cycles was compared. The UCS for unstabilized grey shale (GL0) decreased from 61.2 psi to 32.4 psi after seven FT cycles, representing a reduction of approximately 47%. Grey shale stabilized with 3% lime (GL3) experienced a reduction from 130.3 psi to 93.7 psi, resulting in a 28% decrease. For samples treated with 6% lime (GL6), UCS decreased from 300.7 psi to 202.7 psi, a reduction of 32%. The addition of fly ash to lime stabilization also showed reductions. For GL0FA10, UCS decreased by 27%, while GL3FA10 and GL6FA10 experienced reductions of 26% and 27%, respectively. Among these combinations, GL3FA10 exhibited the least reduction in strength (Figure 5.12).

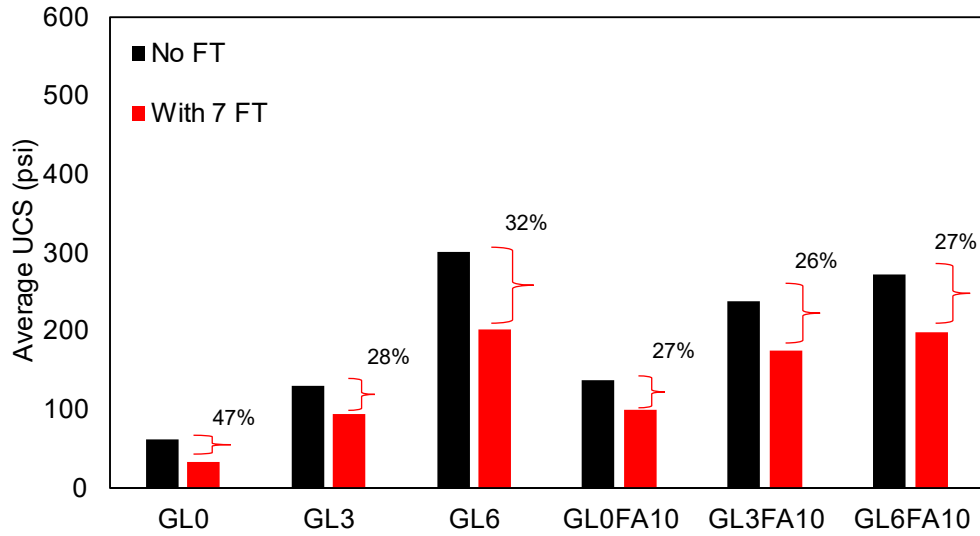


Figure 5.12 Comparison of UCS for grey shale soil stabilized with lime and lime-fly ash after 28 days of curing and after 14 days of curing followed by 7 FT cycles.

Figure 5.13 presents the UCS results for clay soil stabilized with lime and lime-fly ash. These results are presented to assess the effectiveness of different stabilization combinations in enhancing the resistance of clay soil to freeze-thaw cycles. The UCS for unstabilized clay (BL0) decreased from 67.9 psi to 48.6 psi after seven FT cycles, representing a reduction of approximately 28%. The clay soil stabilized with 3% lime (BL3) experienced a reduction in UCS from 147.9 psi to 97.1 psi, resulting in a 34% reduction. For samples treated with 6% lime (BL6), the UCS reduced from 148.7 psi to 121.8 psi, corresponding to an 18% reduction. For BL0FA10, the UCS decreased from 119.8 psi to 84.3 psi, representing a reduction of 29%. Similarly, BL3FA10 and BL6FA10 experienced reductions of 17% and 10%, respectively. Among the tested combinations, BL6FA10 exhibited the least reduction in strength, suggesting that the mix of 6% lime and 10% fly ash provided superior resistance to freeze-thaw cycles after the early stage relative to other lime-fly ash combinations.

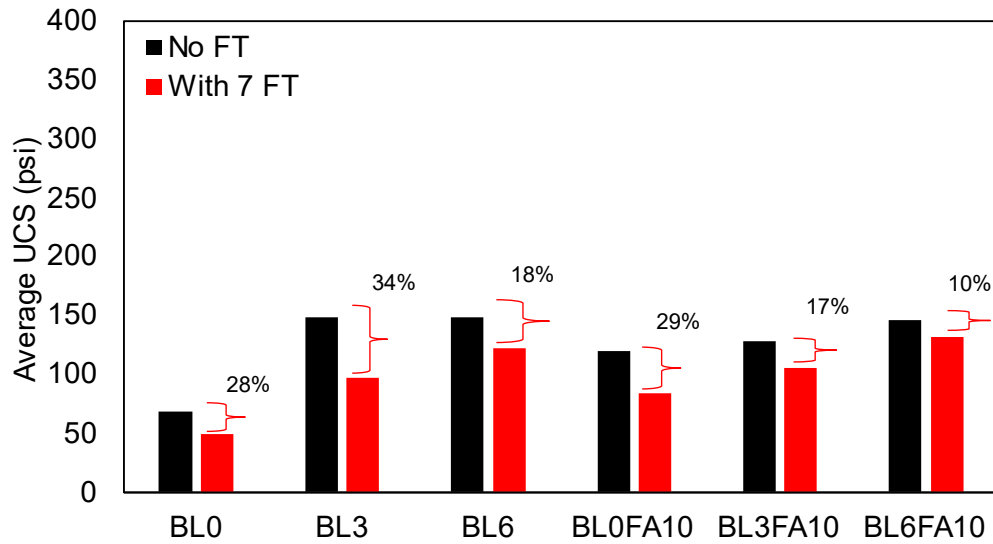


Figure 5.13 Comparison of UCS for clay soil stabilized with lime and lime-fly ash after 28 days of curing and 14 days of curing, followed by 7 FT cycles.

5.3.2 Discussion of UCS Results for Grey Shale and Clay Soil Stabilized with Lime-Cement After Seven FT Cycles

Initially, the grey shale stabilized with 3% cement (GL0C3) showed a UCS decrease from 129.6 psi to 74.9 psi after seven FT cycles, which corresponds to a 42% reduction. In comparison, grey shale stabilized with 3% lime and 3% cement (GL3C3) experienced a UCS reduction from 287.3 psi to 195.0 psi, representing a 32% decrease. When the soil was stabilized with 6% lime and 3% cement (GL6C3), UCS showed a reduction of 26%, decreasing from 406.7 psi to 300.2 psi. The UCS for grey shale stabilized with 6% cement (GL0C6) decreased from 222.2 psi to 145.2 psi, corresponding to a 34% reduction. Grey shale stabilized with 3% lime and 6% cement (GL3C6) exhibited a UCS reduction of 27%, dropping from 395.2 psi to 284.7 psi. Finally, the combination of 6% lime and 6% cement (GL6C6) demonstrated the highest UCS retention, decreasing from 490.8 psi to 406.0 psi, a reduction of only 17% (Figure 5.14).

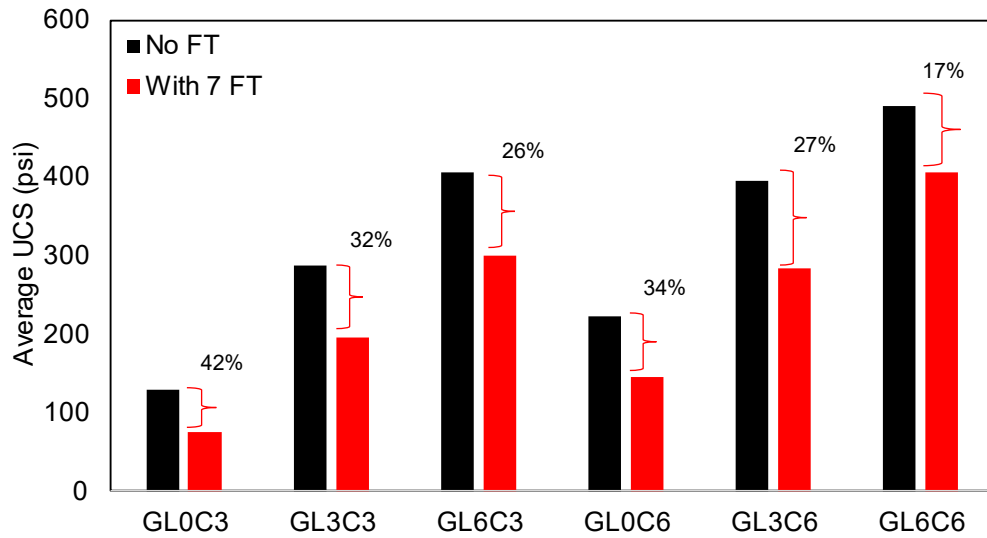


Figure 5.14 Comparison of UCS for grey shale soil stabilized lime-Cement after 28 days of curing and 14 days of curing, followed by 7 FT cycles.

For the clay soil stabilized with 3% cement (BL0C3) exhibited a UCS decrease from 204.4 psi to 137.7 psi after seven FT cycles, corresponding to a 32% reduction. In comparison, clay stabilized with 3% lime and 3% cement (BL3C3) experienced a UCS drop from 211.2 psi to 170.7 psi, representing a 19% decrease. When stabilized with 6% lime and 3% cement (BL6C3), the UCS showed a reduction of 20%, decreasing from 244.1 psi to 196.1 psi. For clay soil stabilized with 6% cement (BL0C6), the UCS decreased from 287.1 psi to 275.7 psi, corresponding to a 4% reduction. Clay stabilized with 3% lime and 6% cement (BL3C6) exhibited a UCS reduction of 10.6%, dropping from 294.2 psi to 262.8 psi. Finally, the combination of 6% cement (BL0C6) achieved the highest UCS retention, decreasing from 287.1 psi to 275.7 psi, which corresponds to a reduction of 4%.

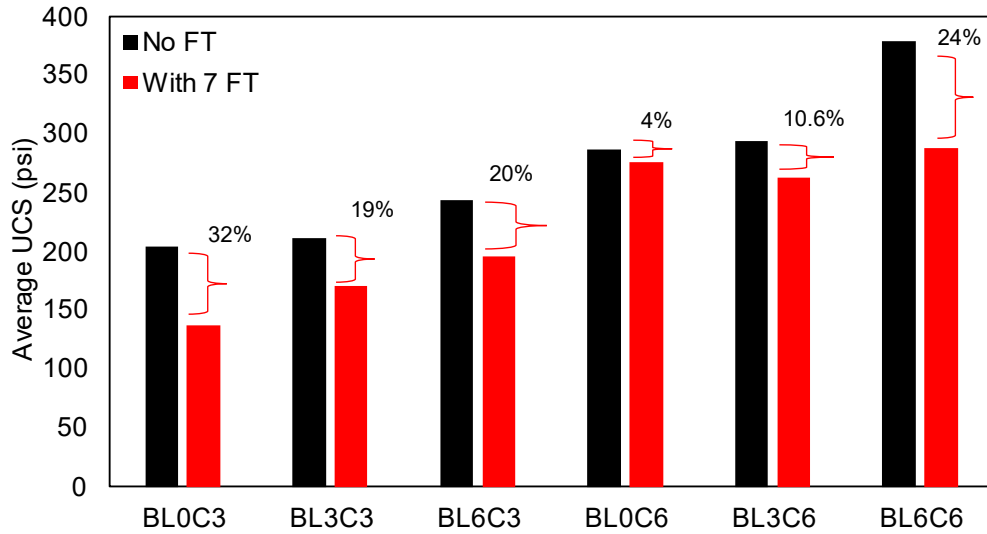


Figure 5.15 Comparison of UCS for clay soil stabilized lime-Cement after 28 days of curing and 14 days of curing, followed by 7 FT cycles.

5.3.3 Discussion of UCS Results for Grey Shale and Clay Soil Stabilized with Lime and Lime-Fiber After Seven FT Cycles

The UCS results for fiber-stabilized and lime-fiber stabilized samples (GL0F1, GL6F1, BL0F1, BL3F1) after seven FT cycles are presented in Figure 5.16. For grey shale, GL0F1 without freeze-thaw treatment initially had a UCS of 57.7 psi. After seven FT cycles, the UCS reduced to 27.0 psi, resulting in a 53.2% decrease. In GL6F1 (lime and fiber), the UCS reduced from 250.2 psi to 157.0 psi after seven freeze-thaw cycles, a reduction of 37.3%. For clay soil, the UCS of BL0F1 without FT was 51.0 psi, while after seven FT cycles it dropped to 32.4 psi, showing a reduction of 36.4%. In the case of BL3F1, the UCS decreased from 137.4 psi to 82.29 psi after seven FT cycles, which corresponds to a 40.1% reduction. The results show that fiber does not provide significant resistance against freeze-thaw cycles, as it exhibits substantial reductions in UCS, especially in grey shale.

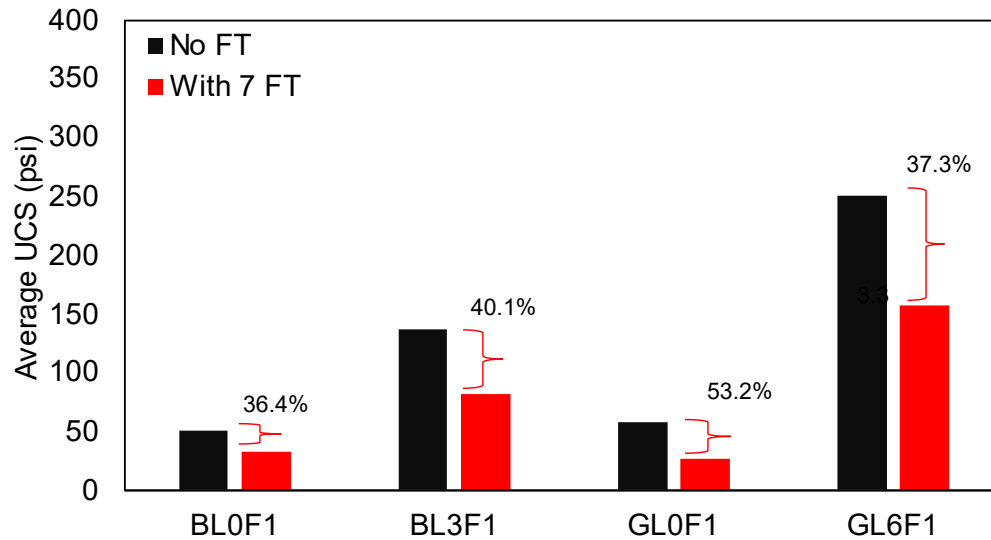


Figure 5.16 Comparison of UCS for grey shale and clay soil stabilized with Fiber and lime-fiber after 28 days of curing and 14 days of curing, followed by 7 FT cycles.

5.3.4 Discussion of UCS Results for Grey Shale and Clay Soil Stabilized with Lime and Lime-Fly Ash After 12 FT Cycles

The UCS results for grey shale soil stabilized with lime and lime-fly ash after 12 FT cycles are presented in Figure 5.17. The results illustrate the impact of 12 FT cycles on the strength of the soil, showing varying levels of strength degradation depending on the type of stabilization treatment. The UCS of the untreated soil (GL0) decreased significantly by 47%, from 61.2 psi to 32.4 psi after 12 FT cycles. This reduction is comparable to the reduction observed after seven cycles. The sample stabilized with 3% lime (GL3) experienced a 14% reduction, decreasing from 130.3 psi to 111.3 psi. The sample stabilized with 6% lime (GL6) showed a decrease from 300.7 psi to 268.9 psi, representing a reduction of only 10.5%. This indicates that increasing the lime content improved the soil's resistance to freeze-thaw degradation.

Following the discussion on lime stabilization, the effect of incorporating fly ash with lime stabilization was also evaluated. The combination of 0% lime with 10% fly ash (GL0FA10) resulted in a reduction of 25%, with UCS decreasing from 137.8 psi to 102.8 psi. The sample

treated with 3% lime and 10% fly ash (GL3FA10) exhibited a UCS reduction of 24%, from 238.0 psi to 180.8 psi. The sample stabilized with 6% lime and 10% fly ash (GL6FA10) demonstrated the least reduction of all combinations, with a 9% decrease from 272.1 psi to 247 psi. The addition of fly ash generally improved the grey shale soil's resistance to freeze-thaw degradation after the latter stage of exposure, with the best performance observed in the sample stabilized with 6% lime and 10% fly ash (GL6FA10), which had the smallest reduction in strength after 12 FT cycles.

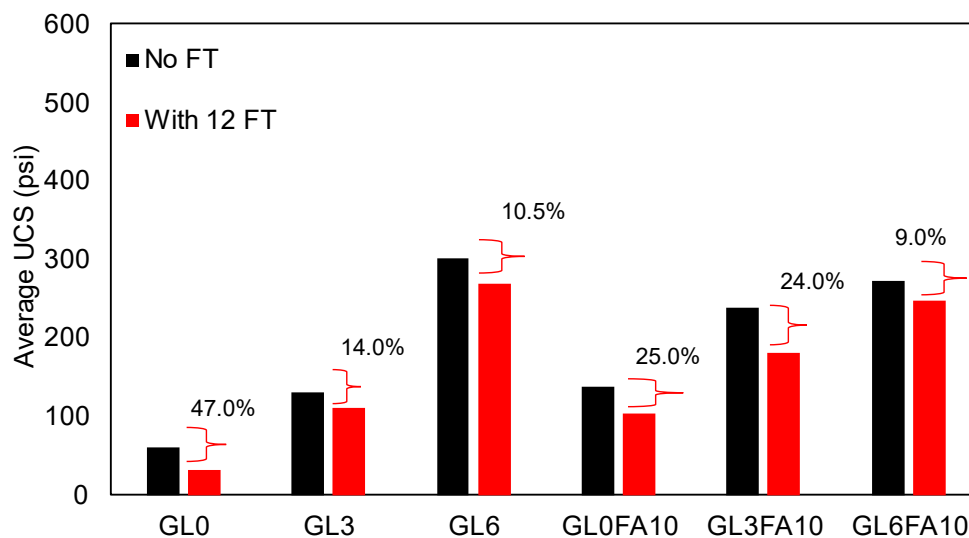


Figure 5.17 Comparison of UCS for grey shale soil stabilized with lime and lime-fly ash after 28 days of curing and 28 days of curing, followed by 12 FT cycles.

The UCS results for clay soil stabilized with lime and lime-fly ash after 12 FT cycles are presented in Figure 5.18. The UCS of the untreated clay soil (BL0) decreased by 28.3% from 67.9 psi to 48.7 psi after 12 FT cycles, which is similar to the reduction observed after 7 FT cycles. This suggests that the reduction in UCS for unstabilized soil may reach a stable level after a certain number of cycles. The sample stabilized with 3% lime (BL3) experienced a reduction of 19%, with UCS decreasing from 147.9 psi to 118.5 psi. The sample stabilized with 6% lime (BL6) showed a

decrease from 148.7 psi to 128.1 psi, representing a reduction of 13.8%. This suggests that increasing the lime content improves the clay soil's resistance to freeze-thaw degradation. The same trend was observed for grey shale soil, where higher lime content also improved resistance to freeze-thaw degradation.

Following the discussion on lime stabilization, the effect of incorporating fly ash with lime stabilization was evaluated, as fly ash is expected to improve soil stabilization by enhancing pozzolanic reactions and increasing soil strength. The combination of 0% lime with 10% fly ash (BL0FA10) showed a UCS reduction of 22%, decreasing from 119.8 psi to 92.5 psi. The sample treated with 3% lime and 10% fly ash (BL3FA10) exhibited a reduction of only 3.3%, with UCS decreasing from 127.7 psi to 123.4 psi. The sample stabilized with 6% lime and 10% fly ash (BL6FA10) had the least reduction, with a negligible 0.6% decrease from 146.5 psi to 145.6 psi.

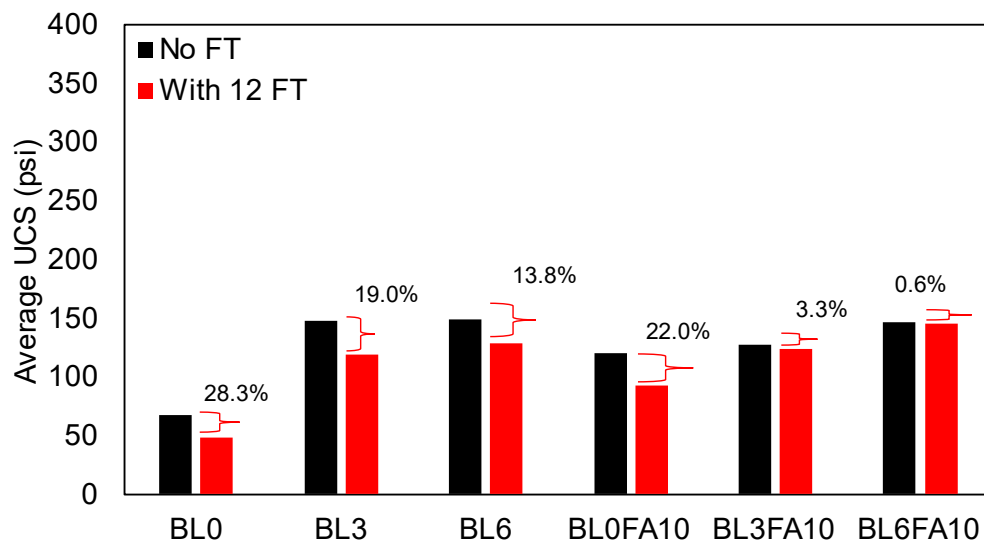


Figure 5.18 Comparison of UCS for clay soil stabilized with lime and lime-fly ash after 28 days of curing and 28 days of curing, followed by 12 FT cycles.

5.3.5 Discussion of UCS Results for Grey Shale and Clay Soil Stabilized with Lime-Cement After 12 FT Cycles

The UCS results for grey shale soil stabilized with lime and cement after 12 FT cycles are summarized in Figure 5.19. The UCS of the sample with 0% lime and 3% cement (GL0C3) decreased significantly by 39%, from 129.6 psi to 79.1 psi after 12 FT cycles. For the grey shale soil sample stabilized with 3% lime and 3% cement (GL3C3), the UCS decreased by 21%, from 287.3 psi to 225.8 psi. The sample stabilized with 6% lime and 3% cement (GL6C3) exhibited the smallest reduction of 5%, from 406.7 psi to 384.8 psi. This indicates that 6% lime and 3% cement is one of the recommended combinations for enhanced stability under FT conditions. The sample with 0% lime and 6% cement (GL0C6) experienced a reduction of 32%, from 222.2 psi to 150.3 psi, while the sample stabilized with 3% lime and 6% cement (GL3C6) showed a decrease of 19%, from 395.2 psi to 321.6 psi. The sample with 6% lime and 6% cement (GL6C6) exhibited a unique behavior, with a 7% increase in UCS, from 490.8 psi to 523.8 psi. This increase is likely due to ongoing pozzolanic reactions and cement hydration, which enhance soil strength even under freeze-thaw conditions.

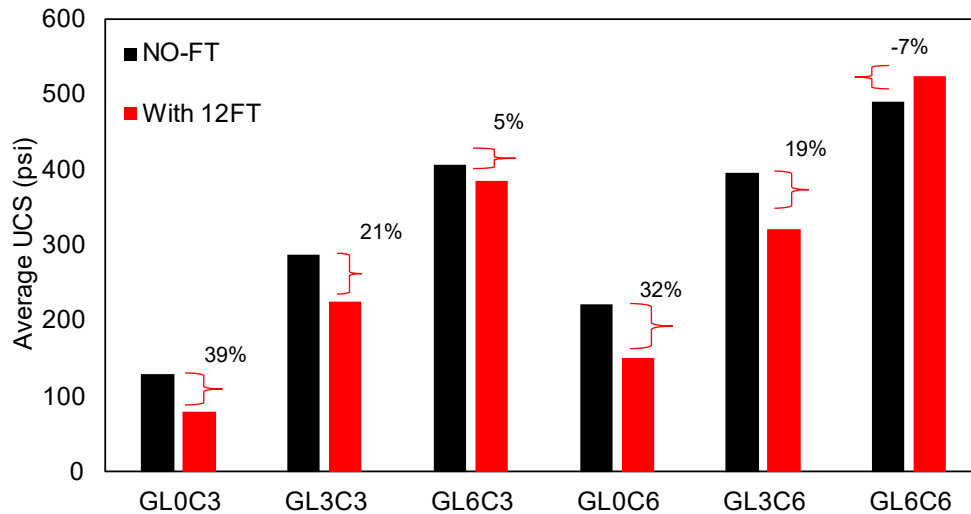


Figure 5.19 Comparison of UCS for grey shale soil stabilized with lime-cement after 28 days of curing and 28 days of curing, followed by 12 FT cycles.

The UCS results for clay soil stabilized with lime and cement after 12 FT cycles are summarized in Figure 5.20. The UCS of the sample with 0% lime and 3% cement (BL0C3) dropped by 21.1%, from 204.4 psi to 161.3 psi. The sample with 3% lime and 3% cement (BL3C3) had a minor UCS reduction of 2.5%, from 211.2 psi to 205.9 psi. In contrast, the sample with 6% lime and 3% cement (BL6C3) showed a 3.9% increase, from 244.1 psi to 253.7 psi. For samples with 6% cement, the UCS of the sample with 0% lime (BL0C6) dropped by 4.3%, from 287.1 psi to 274.6 psi. The sample with 3% lime (BL3C6) showed an increase of 10.2%, from 294.2 psi to 342.4 psi, while the BL6C6 samples exhibited a reduction of 3%, from 379.2 psi to 367.5 psi. For clay soil combined with lime and cement, it is recommended 6% lime and 3% or 3% lime and 6% cement is added, as these mixtures demonstrated strong performance against freezing-thawing cycles.

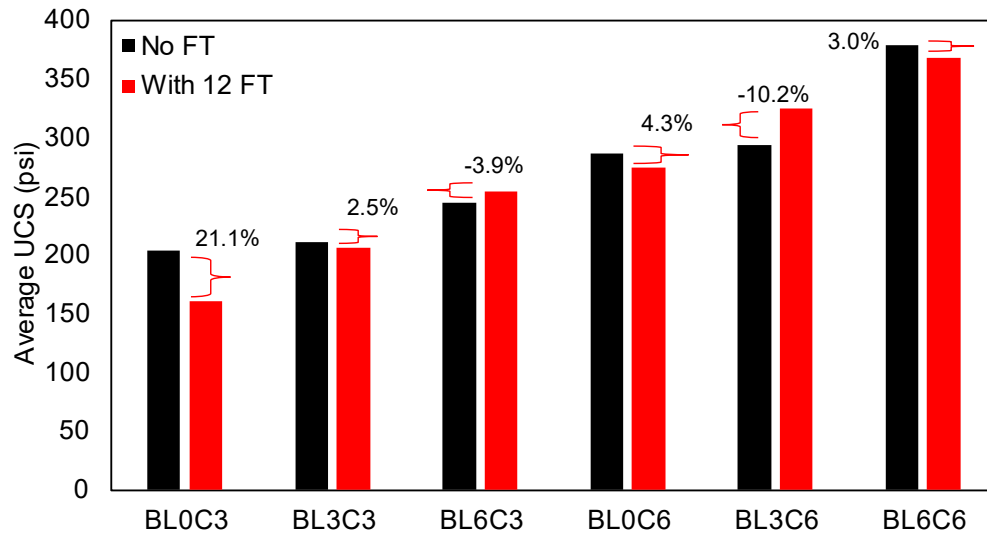


Figure 5.20 Comparison of UCS for clay soil stabilized with lime-cement after 28 days of curing and 28 days of curing, followed by 12 FT cycles.

5.3.6 Discussion of UCS Results for Grey Shale and Clay Soil Stabilized with Lime and Lime-Fiber After 12 FT Cycles

The UCS results for fiber-stabilized and lime-fiber stabilized samples (GL0F1, GL6F1, BL0F1, BL3F1) after 12 FT cycles are presented in Figure 5.21. For grey shale, GL0F1 without freeze-thaw treatment initially had a UCS of 57.7 psi. After 12 FT cycles, the UCS reduced to 23.9 psi, resulting in a 58.5% decrease. For GL6F1 (lime and fiber), the UCS reduced from 250.2 psi to 142.4 psi after 12 freeze-thaw cycles, which corresponds to a 43.1% decrease. In the case of clay soil, BL0F1 without freeze-thaw treatment initially had a UCS of 51.0 psi, which dropped to 24.0 psi after 12 FT cycles, resulting in a 53.0% reduction. For BL3F1 (lime and fiber), the UCS decreased from 137.4 psi to 91.2 psi after 12 FT cycles, representing a 33.6% decrease. The results show that fiber alone does not provide significant resistance against freeze-thaw cycles, as it exhibits substantial reductions in UCS, particularly in grey shale.

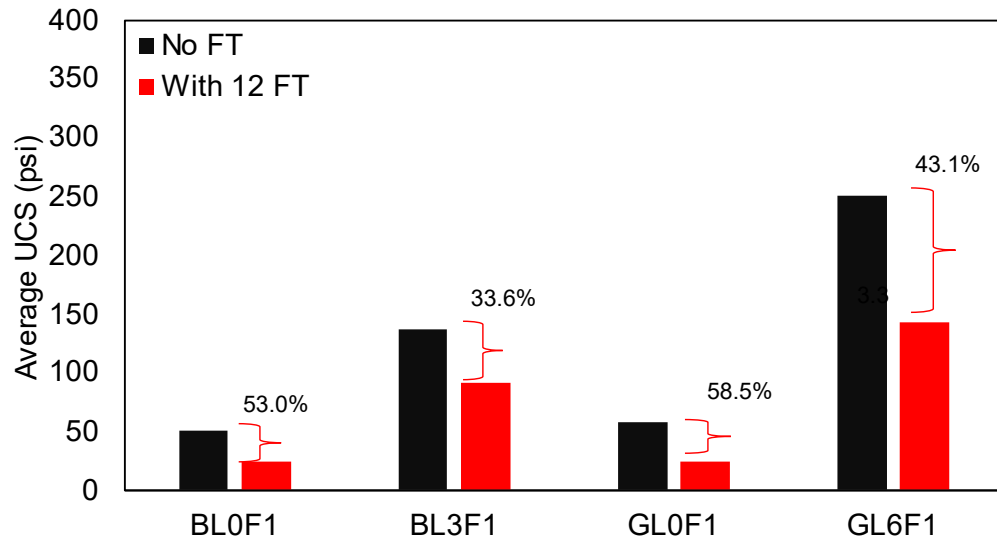


Figure 5.21 Comparison of UCS for grey shale and clay soil stabilized with Fiber and lime-fiber after 28 days of curing and 28 days of curing, followed by 12 FT cycles.

The application of FT cycles modifies the soil microstructure at the aggregate scale, reducing the UCS strength of both stabilized and untreated grey shale and clay. FT cycles induce physical changes in the soil matrix, including increased voids due to ice lens formation and water flow. These changes propagate cracks within the soil matrix as repeated cycles exacerbate crack growth and expansion (Hohmann-Porebska, 2002; Svensson & Hansen, 2010; Nguyen et al., 2019; Olgun, 2013). Heating and freezing change soil particle orientation and overall structure, potentially altering and further reducing the soil's strength and stability (Jaradat et al., 2017).

When comparing the UCS reduction of two types of soils stabilized with lime, cement, and fly ash, the observed differences are primarily driven by the soil's mineralogical composition, plasticity index, and the chemical reactivity of the stabilizing agents curing period. Hotineanu et al. (2015) and Nguyen et al. (2019) observed a similar phenomenon in their studies on lime-stabilized soils, noting that higher plasticity soils are more vulnerable to FT cycles due to significant structural damage at the aggregate scale.

5.4 Empirical Model for Estimating the UCS of Cementitious-Stabilized Soil

As discussed previously, the UCS of stabilized soil is influenced by the stabilizer content, curing period, and number of freeze-thaw cycles. These three factors play a critical role in determining the UCS. To account for these effects, an empirical model for estimating the UCS was proposed:

$$UCS = (a_1 \cdot L + a_2 \cdot C + a_3 \cdot FA + a_4 \cdot UCS_{un})(1 - RDF) \quad (2)$$

$$RDF = \left(\frac{b_1 N_{FT}}{(L + C + FA + C_u)^{b_2}} \right)^{b_3} \quad (3)$$

where L, C, and FA are the lime content, cement content, and fly ash content, respectively. N_{FT} is the number of freeze-thaw cycles, C_u is the curing period (in days), and UCS_{un} is the UCS of untreated soil. a_1 , a_2 , a_3 , b_1 , b_2 , and b_3 are the regression coefficients of the empirical formulas.

This model integrates the combined effects of stabilizer contents and environmental conditions to predict the UCS of treated soils under various scenarios. The parameters can be calibrated using experimental data to reflect site-specific soil and stabilization characteristics.

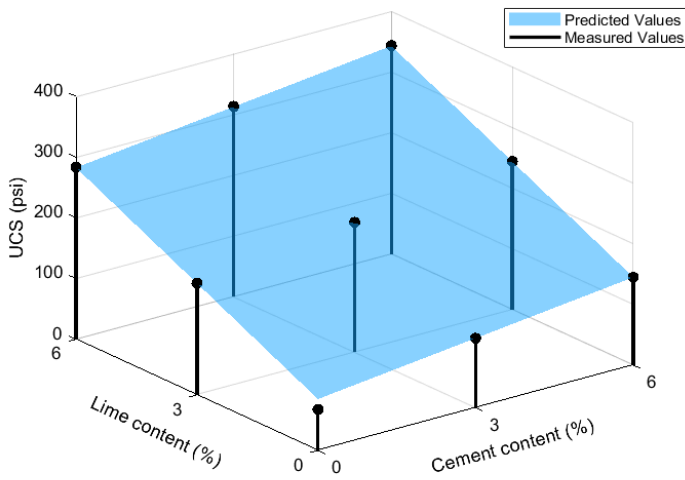
The UCS of stabilized clay consists of four main components: the contributions from lime, cement, fly ash, and the initial UCS values. These components exhibit a linear relationship, as represented in Equation (2). The reduction in UCS due to freeze-thaw cycles is described by a composite function, as shown in Equation (3). The reduction factor demonstrates a positive relationship with the number of freeze-thaw cycles and an inverse relationship with stabilizer content and curing period.

After calibrating the parameters using MATLAB software, all the regression coefficients for the empirical model and the correlation coefficients were obtained and are summarized in Table 5.5. Notably, a_1 in grey shale soil is four times higher than in clay, which means that lime is more effective in enhancing the strength of grey shale soil. This significant increase in a_1 can be attributed to the mineralogy of grey shale. a_2 is similar for both types of soil, indicating consistent stabilization behavior across different mineralogical compositions for this parameter.

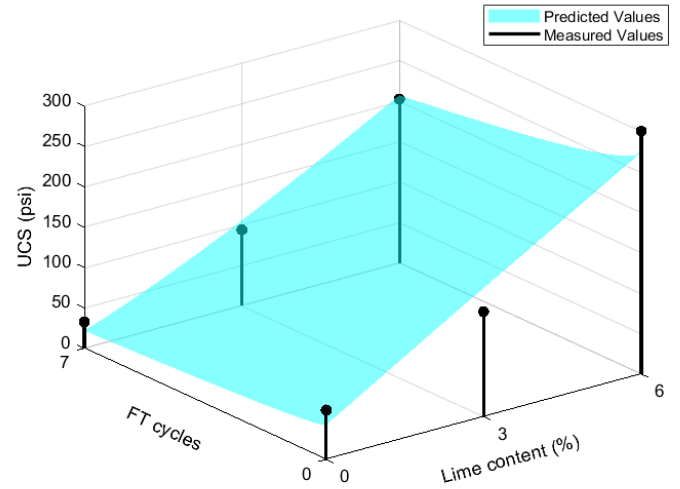
Figure 5.22 illustrates the comparison between the measured and predicted UCS values. In Figure 5.22 (a), (b), and (c), the tested UCS values are represented as lines, while the predicted UCS values, calculated using Equation (2) and (3), are shown as surfaces. Figure 5.22 (d) plots the predicted results against the tested results. The comparison highlights that the predicted UCS values from the empirical model align closely with the tested results, with an R^2 value of 0.935, indicating a strong agreement between the predicted and measured UCS values.

Table 5.5 Regression coefficient for empirical model of UCS cementitious-stabilized soil.

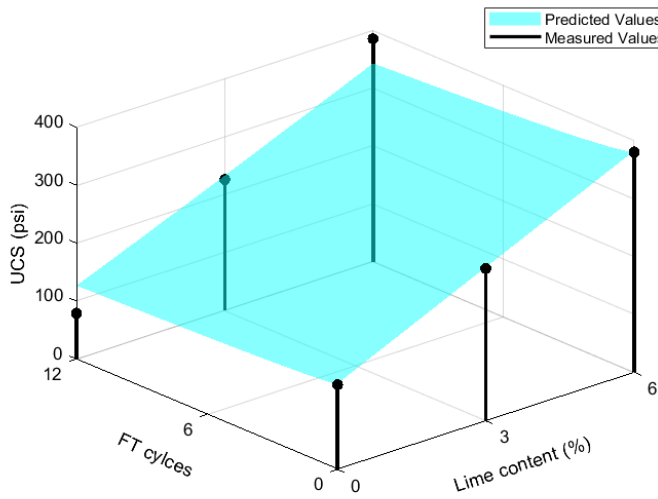
Regression coefficient	Grey shale	Clay
a_1	39	10
a_2	35.1	33
a_3	5.37	1
a_4	0.7	1.25
b_1	400	450
b_2	3.5	3.33
b_3	0.545	0.54



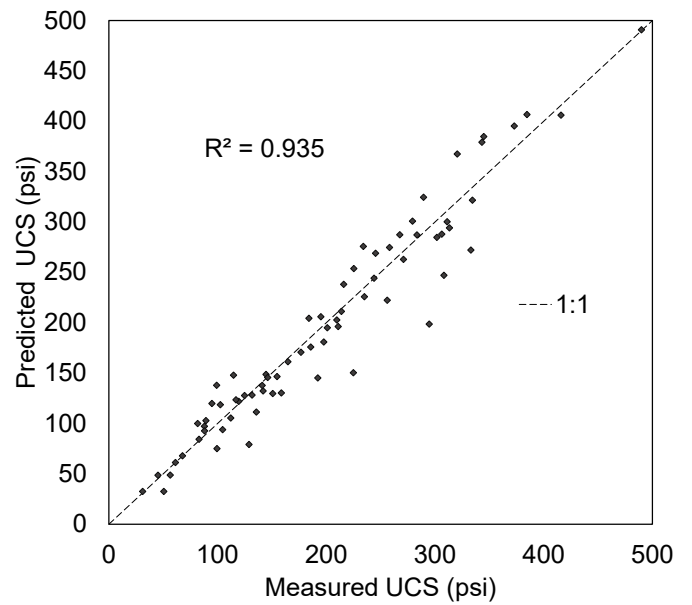
(a) Grey shale soil stabilized by lime-cement



(b) Clay stabilized by 3% of cement with vary lime content



(c) Caly stabilized with vary lime content



(d) Measured and predicted UCS samples

Figure 5.22 Comparison of measured and predicted UCS.

5.5 Analysis of LSTW test results

Three key parameters were assessed across the three cases to understand the impact of the use of fiber with clay soil and the effect of lime with grey shale. The parameters assessed included strength/stiffness, as reflected by DCP, DPI, permanent deformation across soil layer surface, and pressure distribution changes.

5.5.1 Evaluation of Fiber Reinforced Clay using LSTW Test

5.5.1.1 Evaluation of Pavement Strength/Stiffness

The evaluation of pavement strength/stiffness using the DCP provided valuable insights into the effects of fiber reinforcement on clay soils. The DPI served as an indicator of pavement stiffness, measured both before and after traffic loading. For the pre-traffic load condition, DCP tests were conducted away from the wheel path to evaluate the initial soil condition. For the post-traffic load condition, the DCP tests were performed directly on the wheel path following the LSTW test to assess soil densification.

As shown in Table 5.6, the addition of 1% fiber slightly improved the strength of clay. The DPI of the control soil in the pre-traffic load condition was 59.7 mm/blow, which decreased to 27 mm/blow after traffic loading. In contrast, the soil with 1% fiber exhibited a lower DPI of 51.3 mm/blow in the pre-traffic load condition, further decreasing to 21.6 mm/blow in the post-traffic load condition. The change in DPI for both unreinforced and fiber reinforced cases is summarized in Figure 5.25. The graphs of depth versus number of blows (Figure 5.23) and DCP index versus depth (Figure 5.24) clearly illustrate the impact of fiber reinforcement on the clay soil.

Table 5.6 Summary of DPI for unreinforced and fiber reinforced cases.

Case		Control	Fiber reinforced
DPI (mm/blow)	Before	59.7	51.3

Case		Control	Fiber reinforced
	After	27	21.6

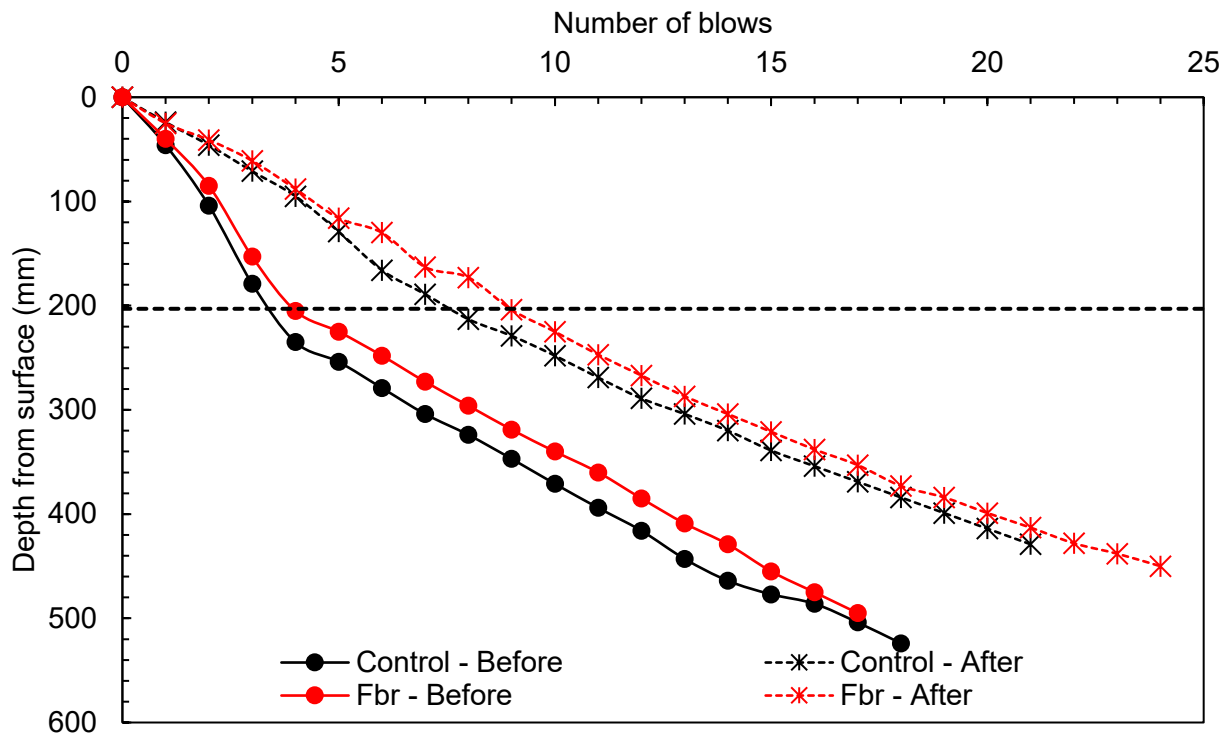


Figure 5.23 Comparison of cumulative blows versus depth for unreinforced and fiber-reinforced clay layers during DCP testing.

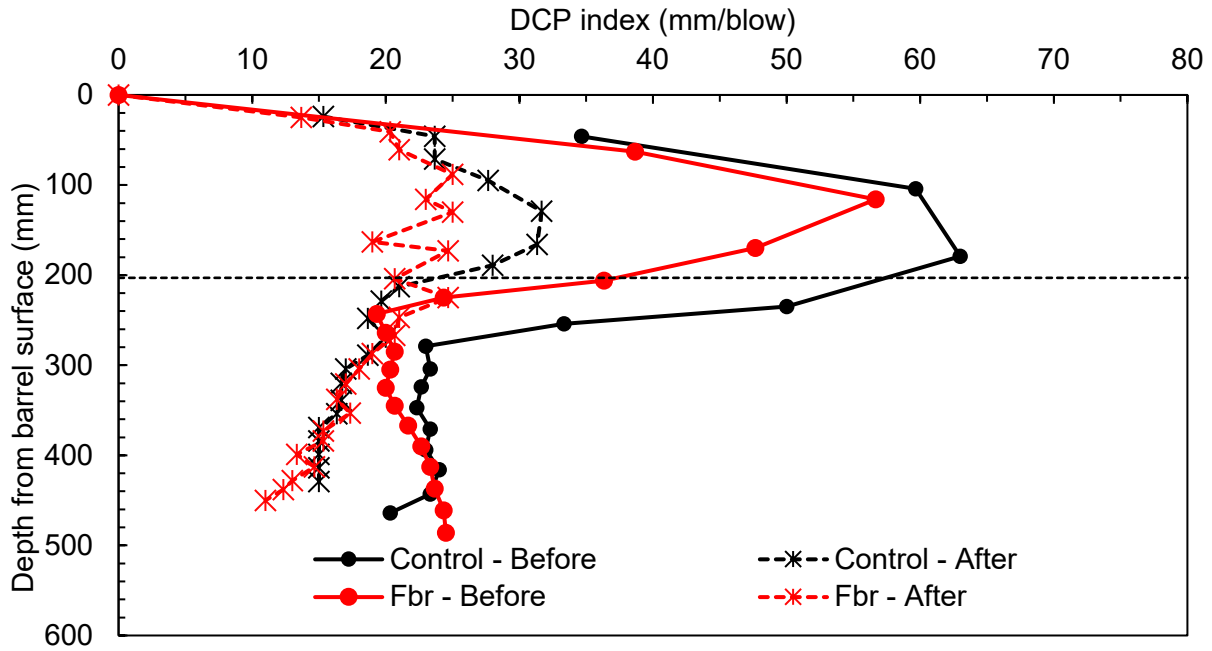


Figure 5.23 Comparison of DPI versus depth for unreinforced and fiber-reinforced clay layers.

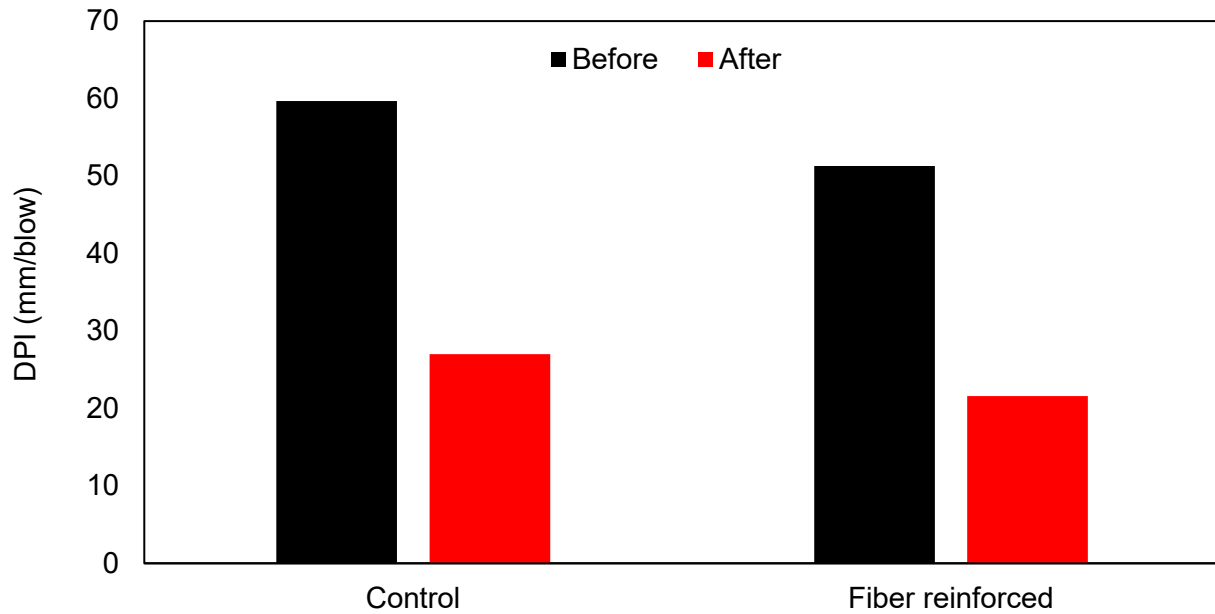


Figure 5.24 DPI comparison for unreinforced and fiber reinforced cases before and after rolling wheel loading.

5.5.1.2 Correlation between DPI and Resilient Modulus

Using correlations by Herath et al. (2005), the Resilient Modulus (M_r) of the clay soil was computed from the DPI for the control and fiber reinforced soil cases as shown in Table 5.7. Figure 5.26 shows a higher resilient modulus of 8% for the fiber reinforced soil than for the control case before the rolling wheel load was applied. This increase in resilient modulus for fiber reinforced soil can be attributed to the interaction between the soil and fiber creating a stronger bond. After the rolling wheel load application, the resilient modulus of the fiber reinforced soil as compared to the control case increased by 17%. This further increase can be attributed to densification of the clay layer from the rolling wheel load application and the higher residual strength of the fiber reinforced case as compared to the control.

Table 5.6 Correlation between Resilient Modulus (M_r) with Dynamic Penetration Index.

Case	DPI (mm/blow)		Mr (MPa)	
			Herath et al (2005)	
	Before	After	Before	After
Control 1 (Clay)	59.7	27	31.8	50.7
Fiber reinforced (Clay + 1% Fiber)	51.3	21.6	34.4	59.3

Table 5.7 Changes in M_r for unreinforced and fiber-reinforced cases in pre- and post-rolling wheel load conditions.

Case	Mr (MPa)		Percentage change (%)
	Herath et al. (2005)		
	Before	After	
Control 1 (Clay)	31.8	50.7	59.2%
Fiber reinforced (Clay + 1% Fiber)	34.4	59.3	72.4%
Percentage change (%)	8.0%	17.0%	

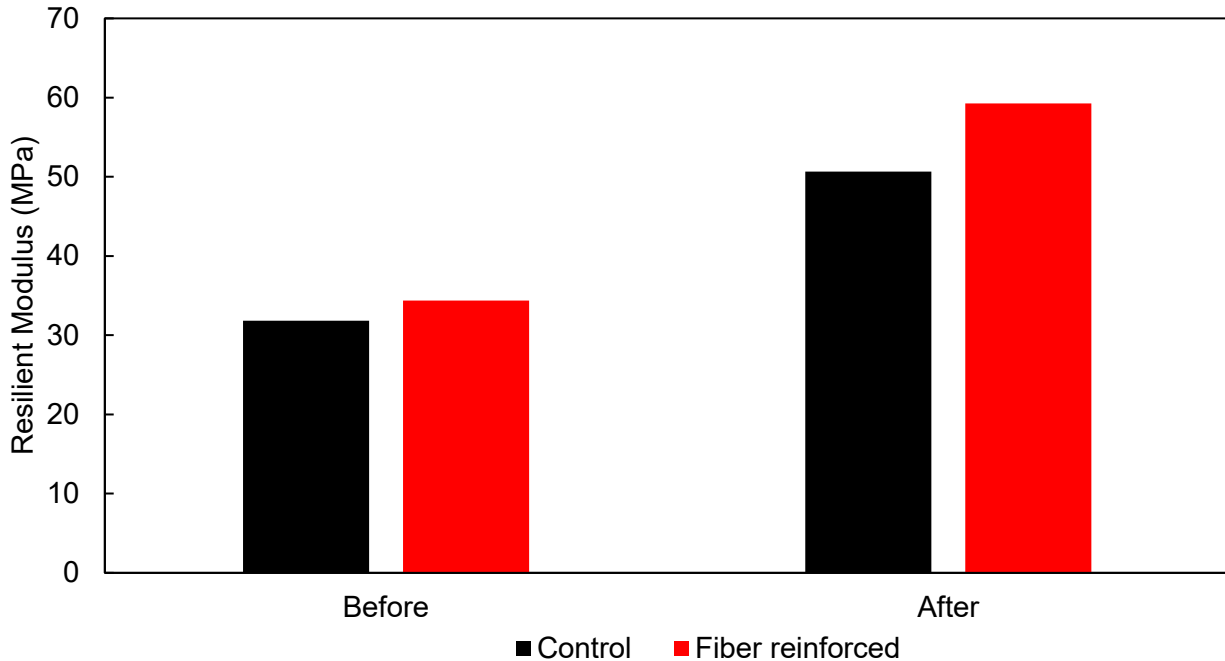


Figure 5.25 Comparison of resilient modulus for clay soil pre- and post-rolling wheel loads in unreinforced and fiber-reinforced cases.

5.5.1.3 Evaluation of Permanent Deformation (Rutting)

The total vertical deformation that occurred at the top surface of the clay layer was obtained after the rolling wheel load was applied for the two cases using the string potentiometer. The deformation was directly recorded using a measuring tape for confirmation (Figure 5.27). Figure 5.28 shows the total deformation recorded for both unreinforced and fiber reinforced cases. The test was terminated after the total deformation stabilized. A reduction in total deformation by 14.7% was observed for the fiber reinforced cases as compared to the control case. No clear trend in LVDT readings were seen for both unreinforced and fiber reinforced cases.



Figure 5.26 Rutting measurement using a measuring tape for the fiber-reinforced case.

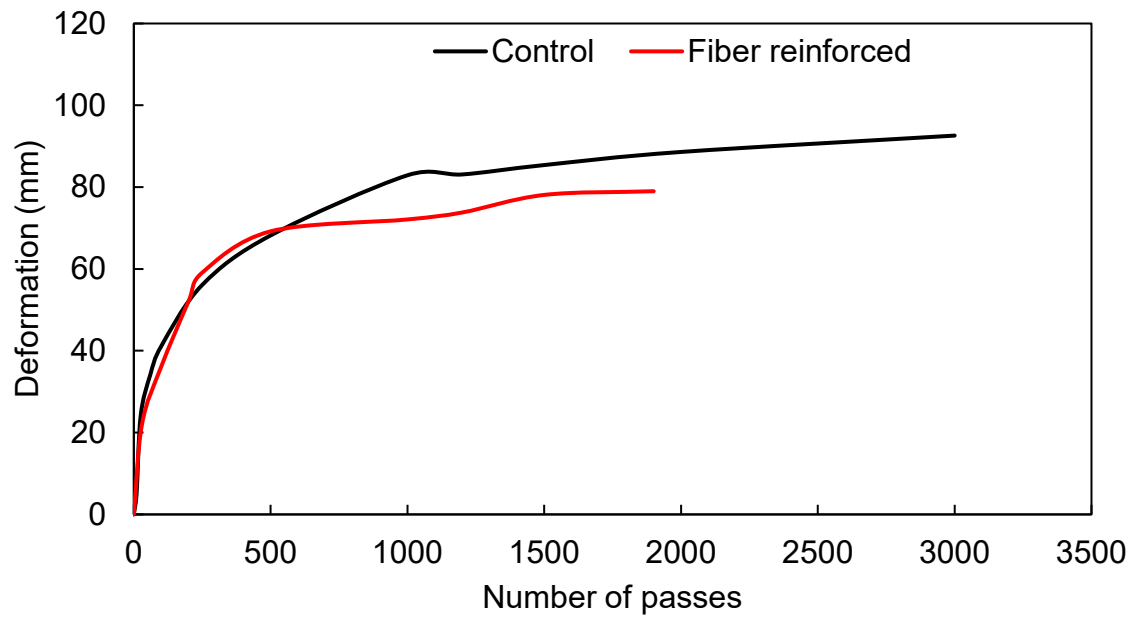


Figure 5.27 Comparison of rutting recorded from string potentiometer for unreinforced and fiber-reinforced cases.

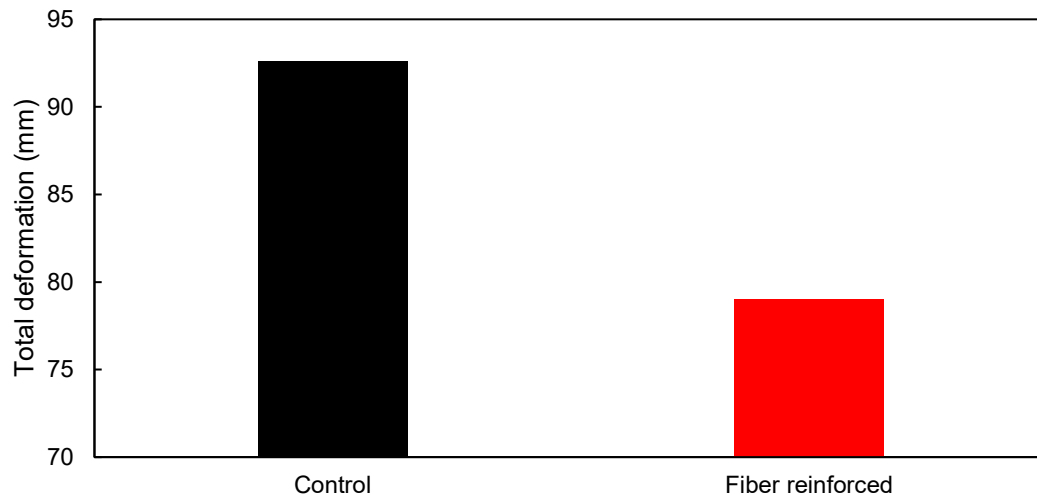


Figure 5.28 Comparison of total rutting in fiber-reinforced and unreinforced cases under applied wheel loads.

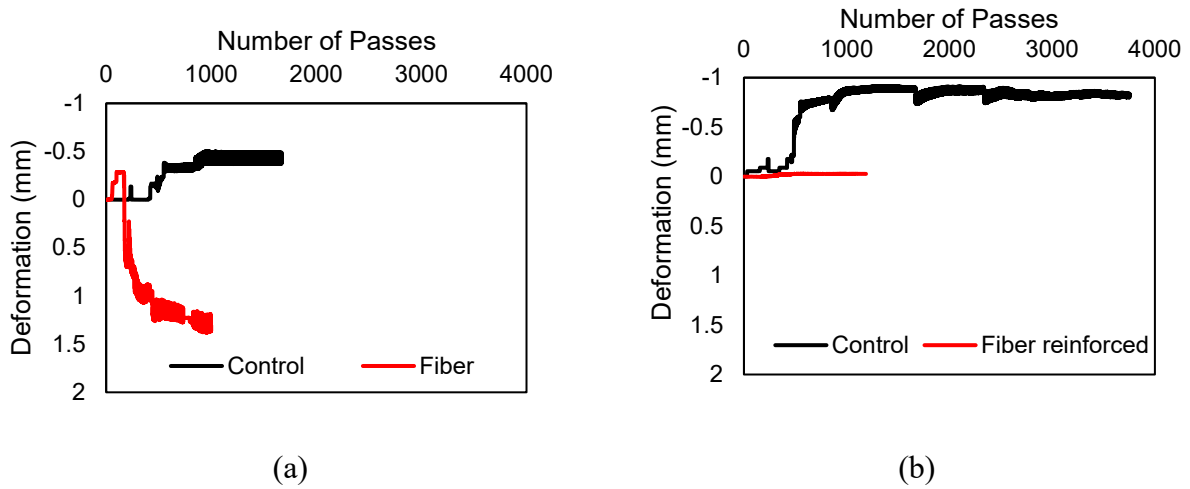


Figure 5.29 LVDT deformation readings for fiber-reinforced and control cases: (a) LVDT 1 deformation readings, (b) LVDT 2 deformation readings.

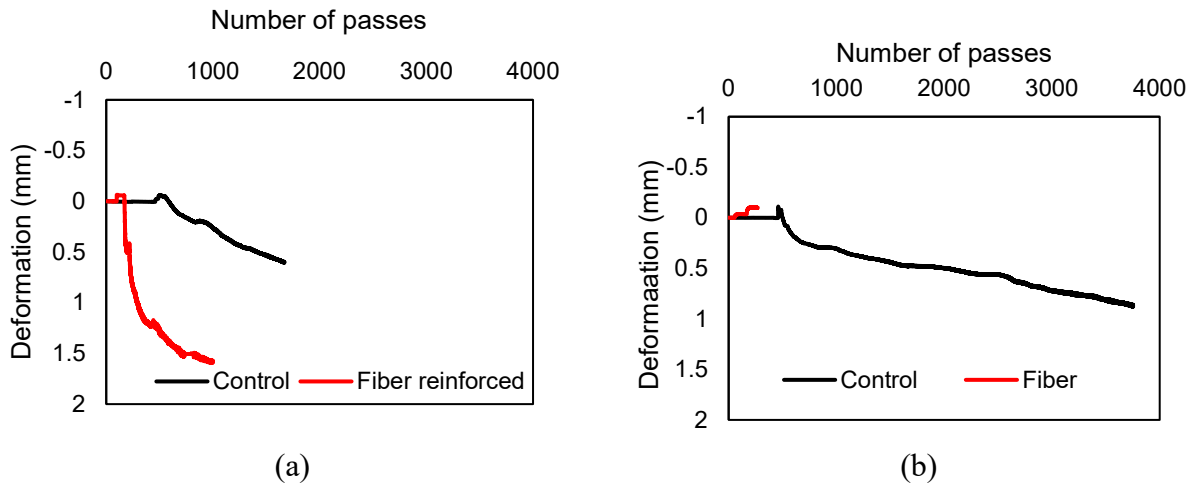


Figure 5.30 LVDT deformation readings for fiber-reinforced and control cases: (a) LVDT 3 deformation readings, and (b) LVDT 4 deformation readings.

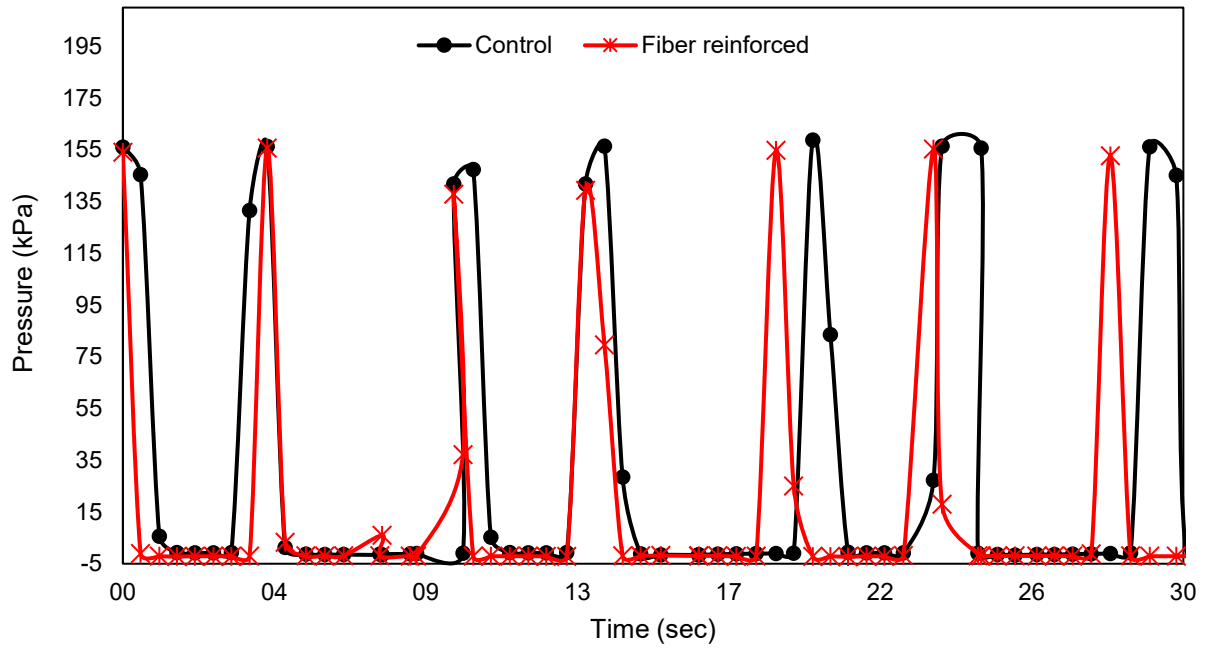
5.5.1.4 Pressure Distribution Effect

Figure 5.32 shows a pressure distribution profile for the top, middle, and bottom pressure cells taken over a 30 second period respectively. The peaks in the pressure cells reading show the point at which the wheel is directly above the pressure cells. Table 5.9 and Figure 5.33 show a summary of the pressure cell readings for the top, middle, and bottom pressure cells. For the top

pressure cell, the average maximum reading obtained in both the control and fiber reinforced cases are approximately equal. The bottom pressure cell for the fiber reinforced case had a lower peak pressure cell reading of 67.5 kPa as compared to the control case with an average peak pressure of 71.7 kPa. This represents a 5.8% pressure reduction recording in the bottom pressure cell for the fiber reinforced case. This can be attributed to the enhancement the fiber provides that distributes stress across the soil layer.

Table 5.8 Average peak pressure for top, middle, and bottom pressure cells in both unreinforced and fiber-reinforced cases.

Case	Pressure (kPa)		
	Top	Middle	Bottom
Control	152.1	119.4	71.7
Fiber reinforced	151.3	129.0	67.5
Percentage change	0.5%	-8.0%	5.8%



(a)

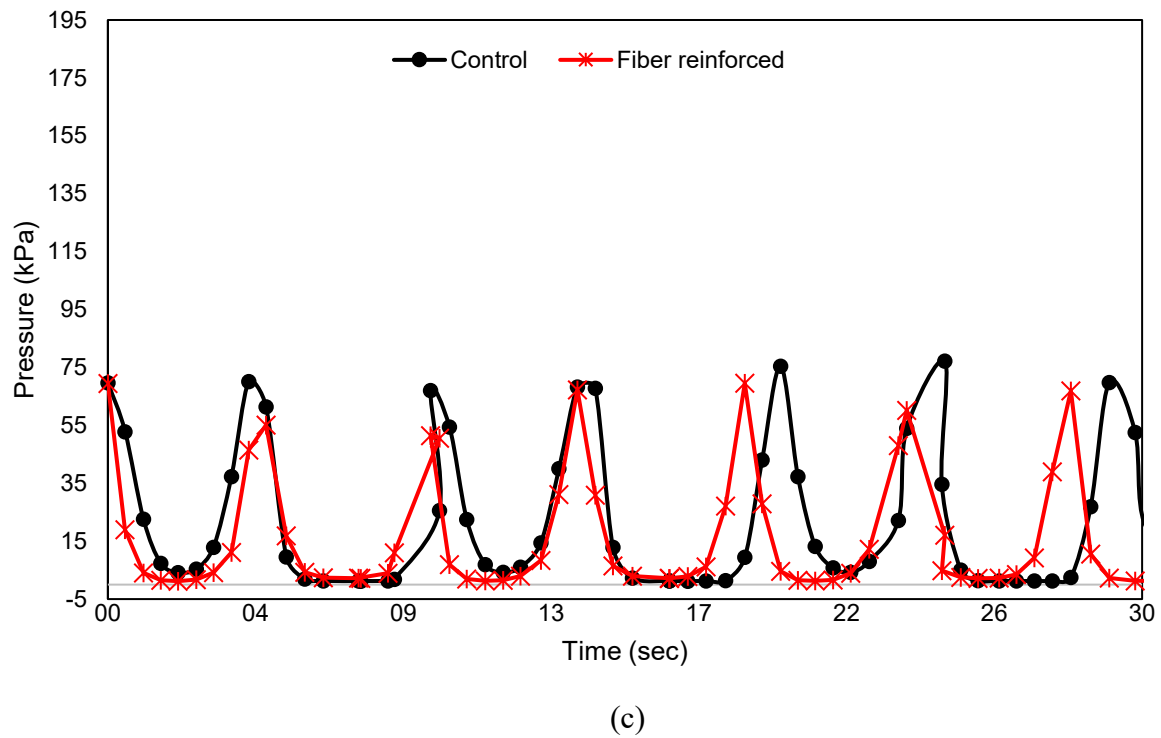
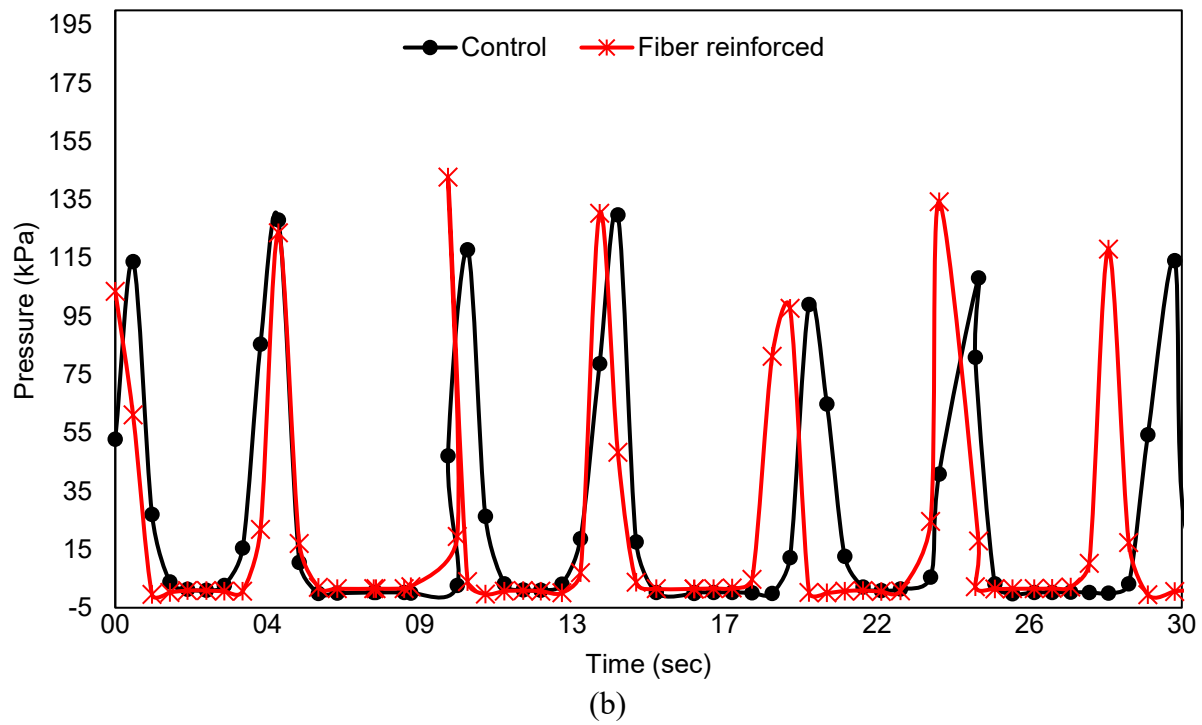


Figure 5.31 Pressure cell readings over a 30-second period for both unreinforced and fiber-reinforced cases: (a) top pressure cell, (b) middle pressure cell, and (c) bottom pressure cell.

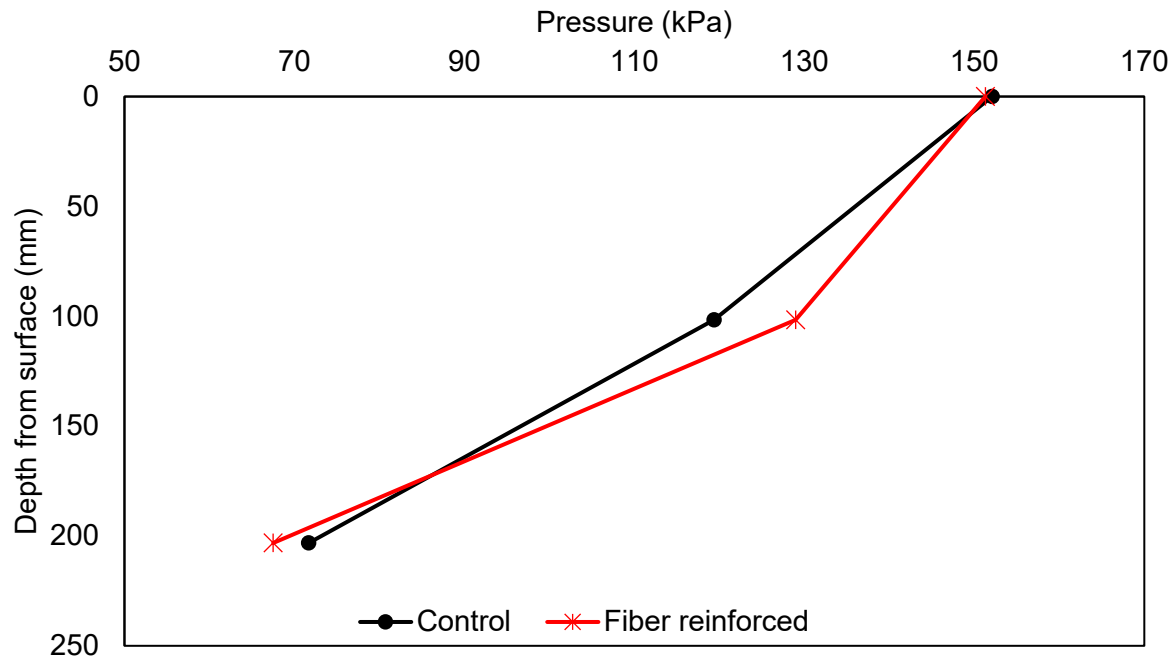


Figure 5.32 Comparison of pressure distribution across the clay layer for unreinforced and fiber-reinforced cases.

5.5.2 Evaluation of Stabilized Grey Shale Soil under LSTW Test

5.5.2.1 Evaluation of Pavement Strength/Stiffness

The evaluation of pavement strength and stiffness using the DCP provided insights into the impact of lime stabilization on grey shale soils. The DCP penetration index was used as an indicator of pavement stiffness, both before and after traffic load. The DCP tests in the pre-traffic load case were performed away from the wheel path to assess the initial condition of the soil. For the post-traffic case, the DCP tests were conducted at the wheel path following the LSTW test to assess soil densification. DCP test for the lime stabilized case was performed after 7 days of curing of the soil sample placed and compacted in the steel box of the LSTW test.

From Table 5.10, it is evident that adding 6% lime significantly improved the strength of grey shale soils. The DPI of the control soil in the pre-traffic load was 50.5 mm/blow, which decreased to 15 mm/blow in the post-traffic load. In comparison, for the soil treated with 6% lime,

the DPI in the pre-traffic load condition was much lower, at 15 mm/blow, and further reduced to 13 mm/blow in the post-traffic load condition. This minimal reduction in DPI indicates that the lime-stabilized case effectively enhanced subgrade stability.

The graphs depicting depth versus number of blows (Figure 5.34) and DCP index versus depth (Figure 5.35) show the positive impact of lime stabilization on grey shale soils. Control samples, both in pre-traffic and post-traffic load conditions, exhibited greater depth per number of blows and higher DCP index values compared to lime-stabilized subgrade, indicating weaker resistance. In contrast, the soil stabilized with 6% lime showed significantly higher resistance and lower DCP index values, demonstrating increased stiffness, reduced deformation, and enhanced load-bearing capacity due to lime stabilization.

Table 5.9 Summary of DPI for untreated and soil + 6% lime cases.

Case		Control	Soil + 6% Soil
DPI (mm/blow)	Before	50.5	15
	After	28	13

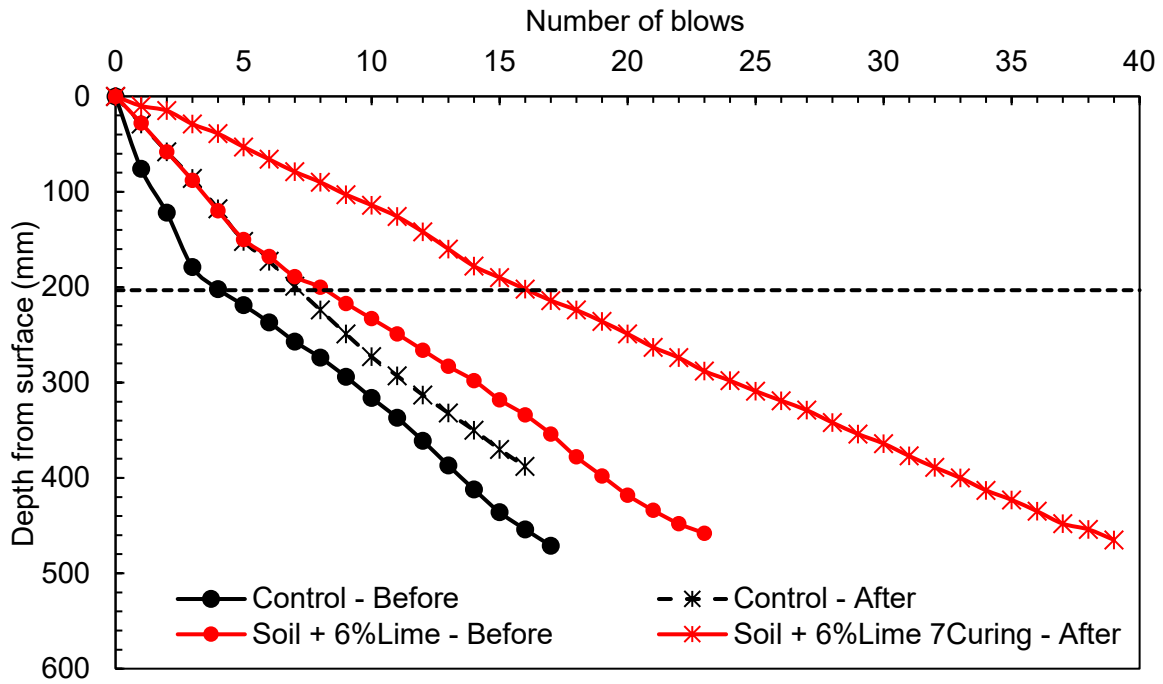


Figure 5.33 Cumulative blows vs depth for grey shale and lime stabilized cases.

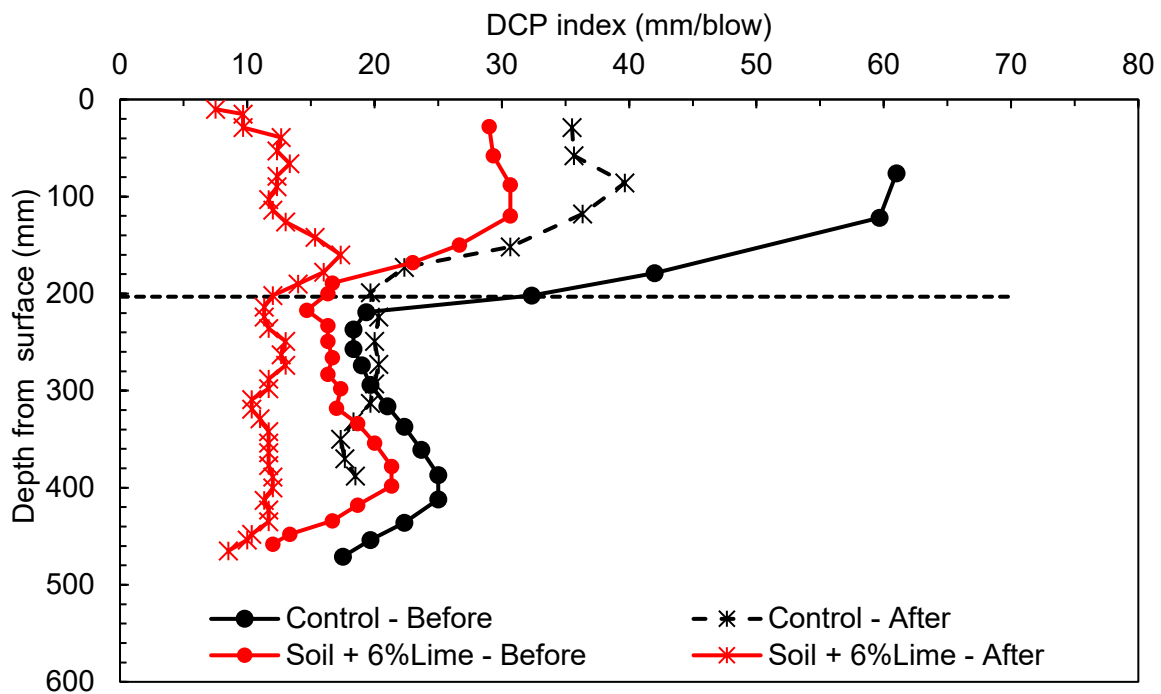


Figure 5.34 DPI vs depth for grey shale and lime stabilized cases.

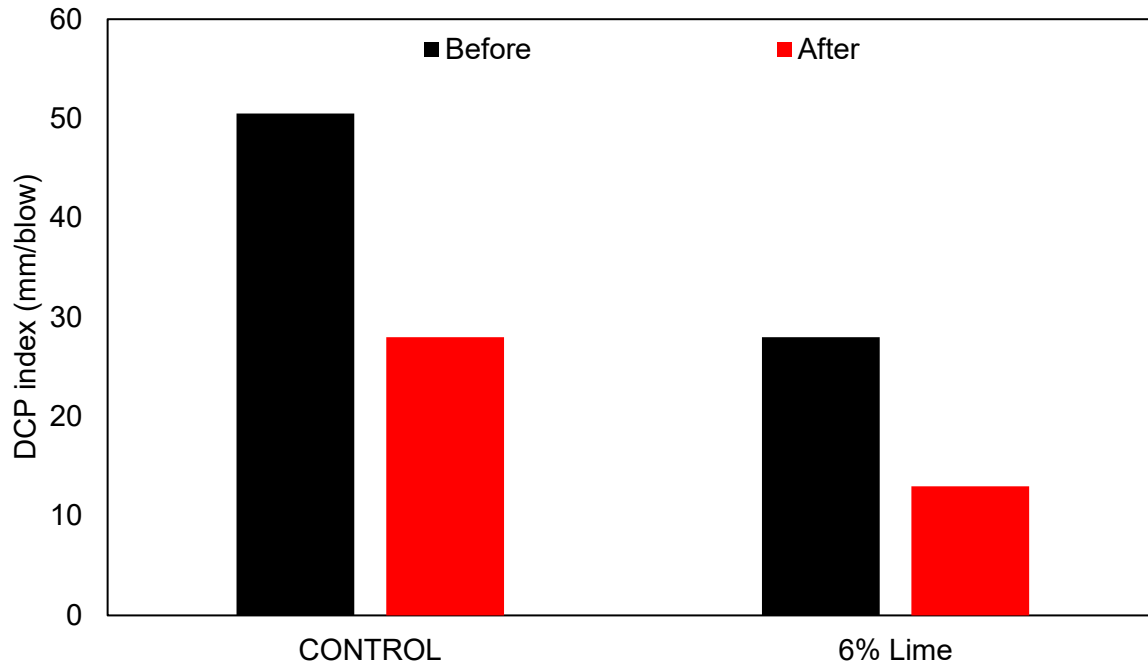


Figure 5.35 DPI comparison for control (grey shale) and stabilized lime cases before and after rolling wheel loading.

5.5.2.2 Correlation between DPI and Resilient Modulus

Using correlations by Herath et al. (2005) the Resilient Modulus of the grey shale soils were computed from the DPI for both control and lime-stabilized cases as shown in Table 5.11 and Table 5.12. This evaluation helps in understanding how lime stabilization influences the stiffness of the soil layer. . Mr increased from 34.7 MPa to 53.0 MPa, a 52.8% increase, demonstrating the significant impact of lime stabilization on Mr.. After traffic load , the Mr of the lime-stabilized soil further increased from 49.4 MPa to 87.7 MPa, a 77.4% increase compared to the control. The increase in Mr is likely due to densification from traffic loading and enhanced soil-particle interaction from lime stabilization.

Table 5.10 Resilient modulus of the control and lime stabilized cases.

Case	Mr (MPa)		Percentage change (%)
	Herath et al (2005)		
	Before	After	
Control 2 (Grey Shale)	34.7	49.4	42.6%
Lime stabilized (7 days curing)	53.0	87.7	65.5%
Percentage change (%)	52.8%	77.4%	

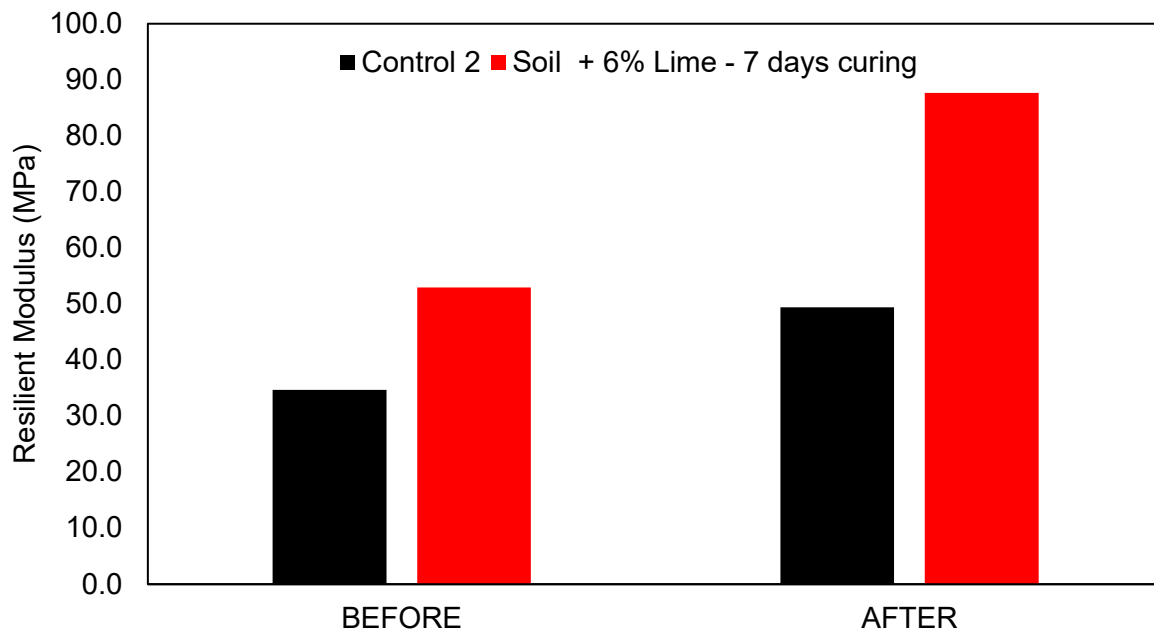


Figure 5.36 Resilient Modulus for control and lime stabilized cases.

5.5.2.3 Evaluation of Permanent Deformation (Rutting)

The evaluation of permanent deformation was conducted using the LSWT test to determine the performance of grey shale soil, for both the control and lime stabilized (6% lime) cases. Figure 5.38 illustrates the deformation recorded from the spring potentiometer for both untreated and lime-stabilized grey shale under rolling wheel loading from the LSWT test. For the untreated grey shale (control), deformation rapidly increases in the initial phases, and continued to grow steadily,

reaching approximately 93 mm by the end of the test (after approximately 2,500 cycles). For the lime stabilized case, the deformation was limited to 5 mm after 2,500 cycles, representing a reduction of about 94.6%, demonstrating significantly improved resistance to permanent deformation. This behavior demonstrates that untreated grey shale lacks sufficient structural stability to resist deformation, making it unsuitable for use in high-load applications without stabilization.

Figure 5.39 shows the deformation readings from LVDTs 1 to 4. The LVDTs were installed in the order of LVDT 4, LVDT 3, LVDT 2, and LVDT 1 from left to right. LVDTs 3 and 2 were positioned closest to the wheel on the left and right respectively. . For the control case (unstabilized grey shale), the results indicated significant deformation, particularly in the areas closer to the wheel (as recorded by LVDTs 2 and 3). Positive readings indicate downward deformation, while negative readings indicate heave or upward movement. The deformation accumulated quickly, with large values observed under the load path. LVDTs 2 and 3, being closer to the wheel, recorded higher deformation compared to LVDTs 4 and 1, which were further away. This pattern is consistent with the expected distribution of deformation under wheel loading, where the highest stresses occur directly beneath the wheel path. The control case also showed some negative readings, indicating heave in certain areas, highlighting the instability of the untreated grey shale under repeated loading. In contrast, the lime-stabilized grey shale showed minimal deformation across all LVDTs, demonstrating the effectiveness of lime treatment in stabilizing the surface. The lime-stabilized case exhibited consistently lower deformation, with negligible heave recorded by any of the LVDTs. This indicates that lime stabilization effectively reduced both surface deformation and uplift, not only under the wheel but also in the surrounding areas, enhancing both the lateral and overall stability of the treated grey shale.

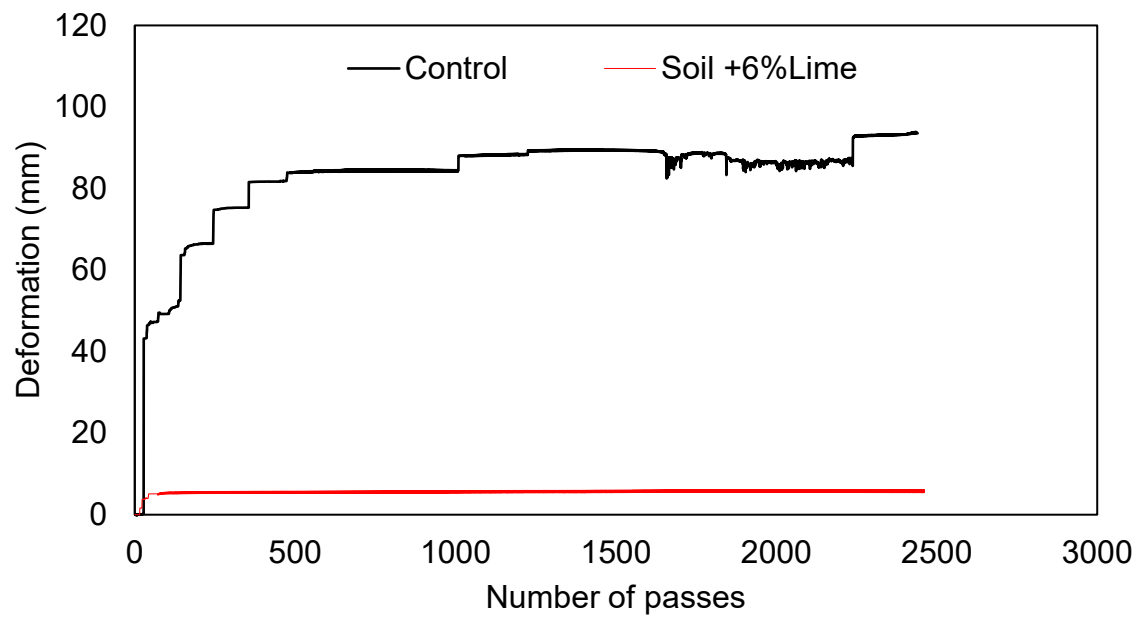


Figure 5.37 Comparison of rutting recorded from string potentiometer for grey shale and lime stabilized case.

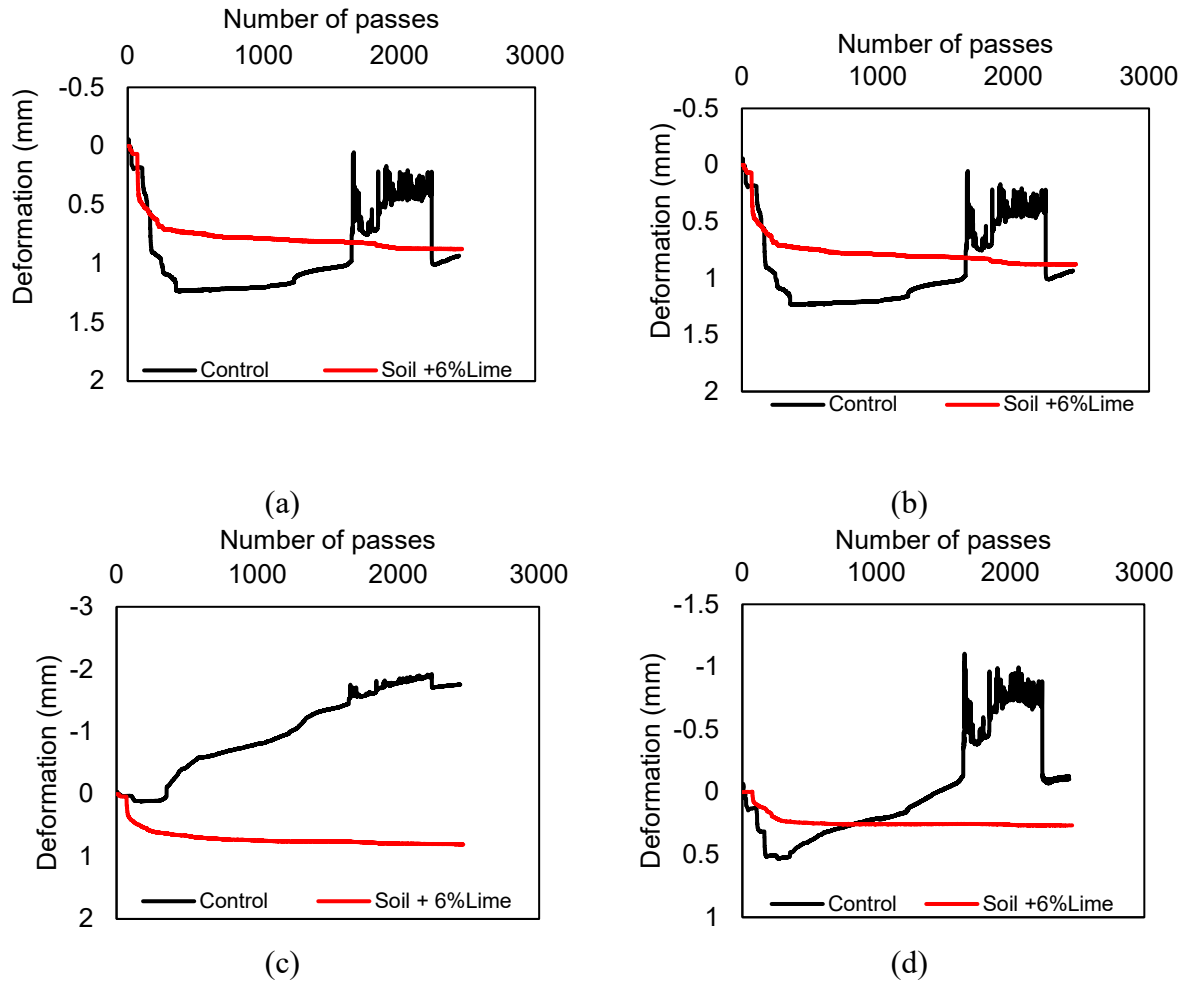


Figure 5.38 Comparison of LVDT deformation readings for control and lime-stabilized cases: (a) LVDT 1 deformation readings, (b) LVDT 2 deformation readings, (c) LVDT 3 deformation readings, and (d) LVDT 4 deformation readings.

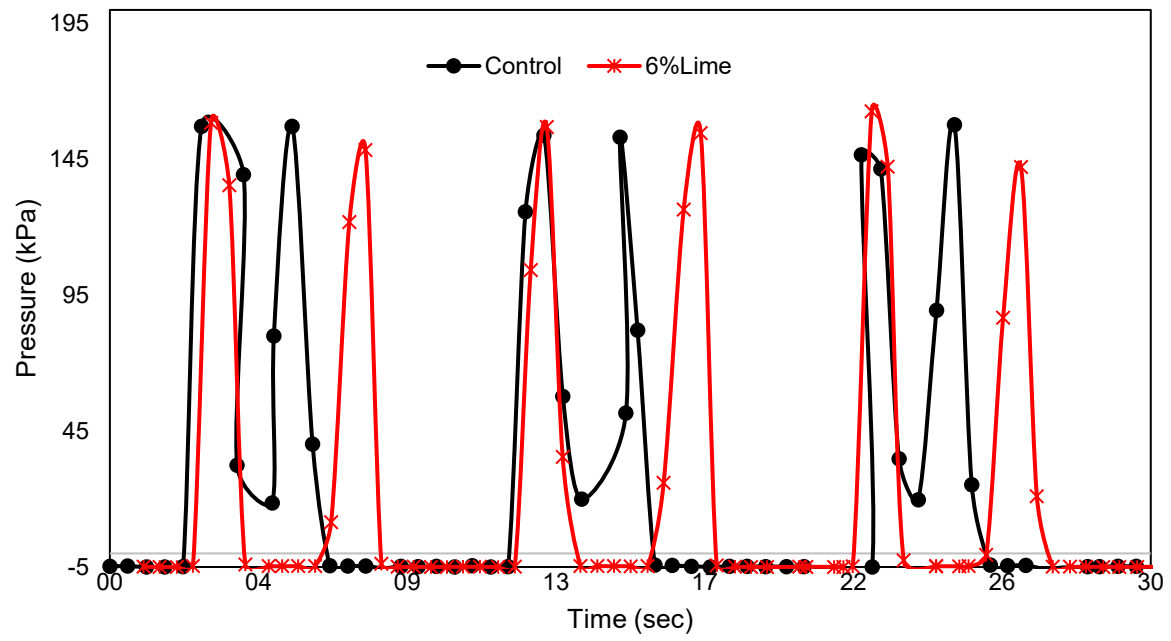
5.5.2.4 Pressure Distribution Effect

Figure 5.40 shows the pressure distribution profile for the top, middle, and bottom pressure cells taken over a 30-second period, respectively. The peaks in the pressure cell readings indicate the point at which the wheel is directly above the pressure cells. Table 5.12 and Figure 5.41 show a summary of the pressure cell readings for the top, middle, and bottom pressure cells. For the top pressure cell, the average peak readings in both the grey shale (control) and grey shale + 6% lime cases are approximately equal, with values of 153 kPa and 154 kPa, respectively, indicating that

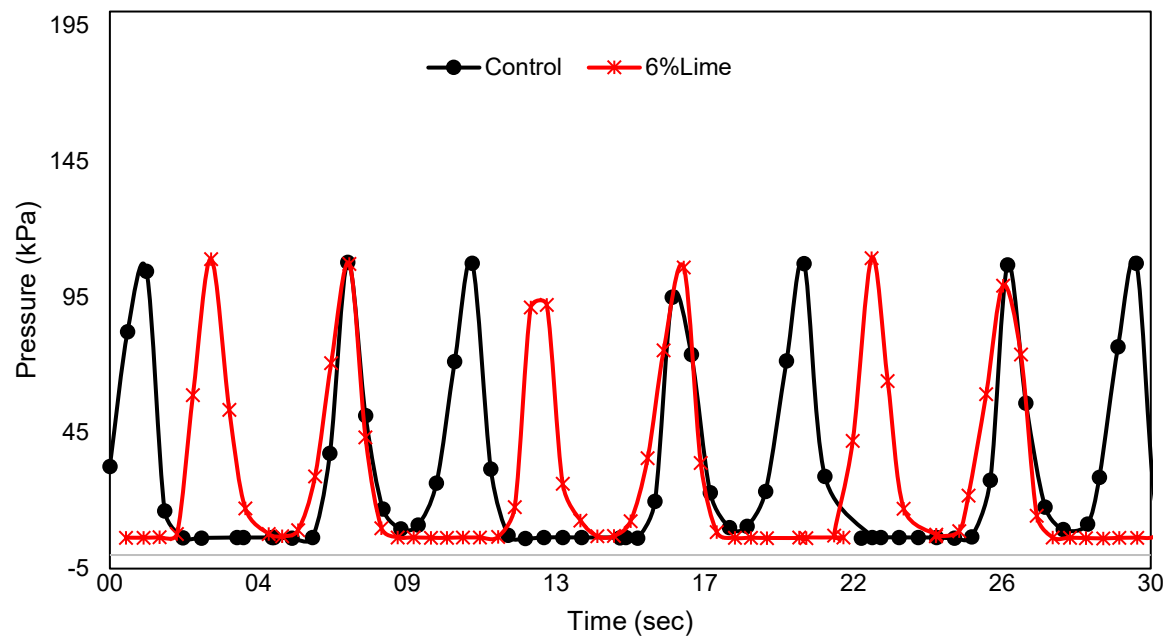
both cases were subjected to the same rolling wheel load. The bottom pressure cell for the grey shale + 6% lime case had a lower peak pressure reading of 50.48 kPa compared to 68.1 kPa for the control case. This represents a 26% pressure reduction recorded in the bottom pressure cell for the grey shale + 6% lime case. This reduction can be attributed to the enhanced ability of lime to distribute stress across the soil layer, resulting in less pressure on the subbase layer, which leads to increased stability of the road.

Table 5.11 Average peak pressure for top, middle, and bottom pressure cells for both control and lime-stabilized cases.

Case	Pressure (kPa)		
	Top	Middle	Bottom
Control	153	107.9	68.1
6%Lime stabilized soil	154	107.8	50.48
Percentage change	-1%	0%	26%



(a)



(b)

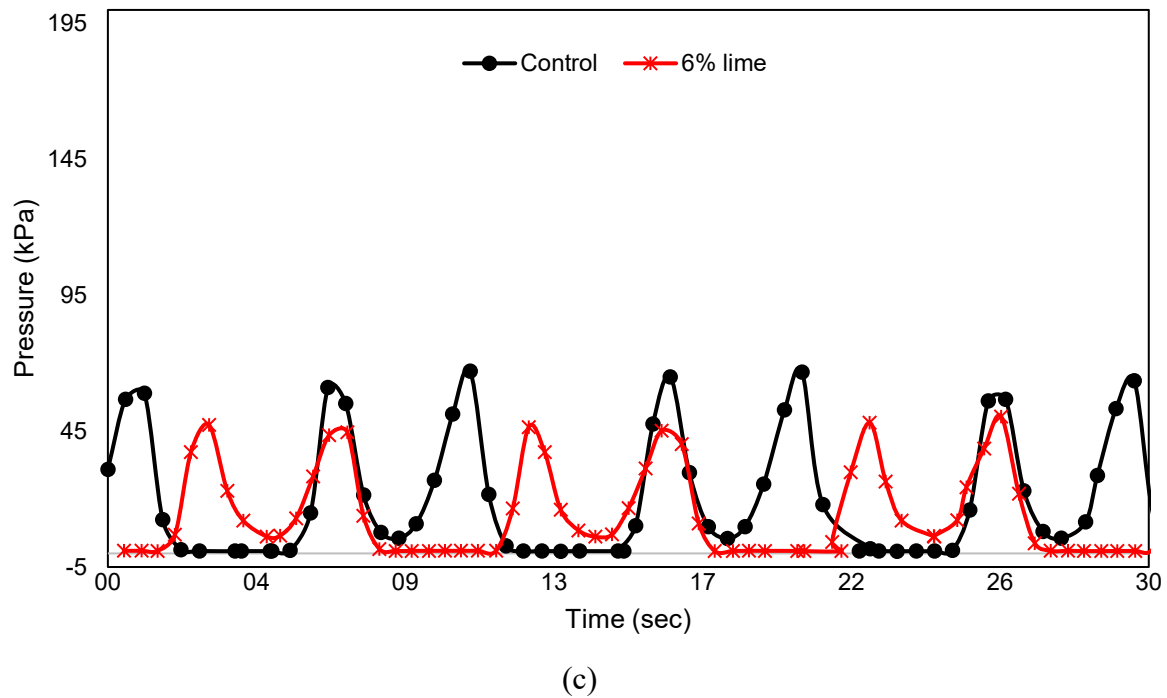


Figure 5.39 Pressure cell readings over a 30-second period for both control and lime-stabilized cases: (a) top pressure cell, (b) middle pressure cell, and (c) bottom pressure cell.

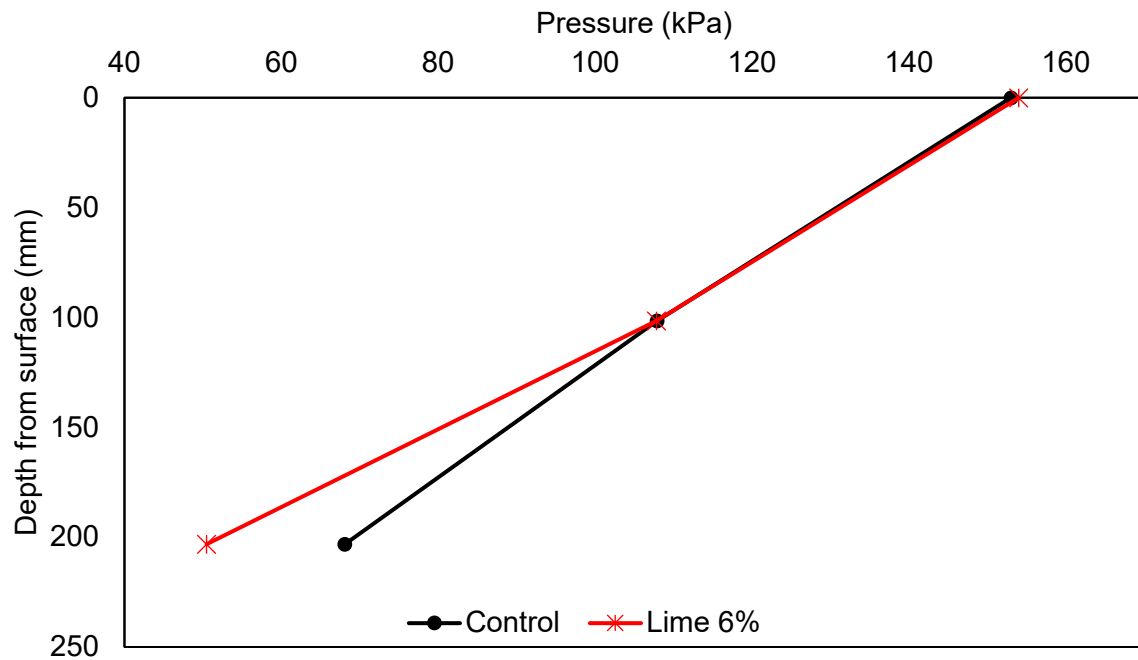


Figure 5.40 Comparison of pressure distribution across the grey shale layer for control and lime stabilized case.

Chapter 6 Conclusion

From the laboratory tests and analysis of data presented in the preceding chapters, the following conclusions can be drawn:

The Proctor results on all soils showed an increase in OMC and a decrease in MDD with increasing amounts of lime for both soil types. For fiber cases, the OMC did not change significantly, but a reduction in MDD was observed.

The plasticity index of grey shale soil reduced significantly with the addition of lime and fly ash, transforming it from a high plastic to low plastic soil. An 82% reduction in plasticity index was achieved using a combination of 3% lime and 10% fly ash. Increasing the lime content was beyond 3% while maintaining 10% fly ash did not yield further improvement. However, for the clay soil, the combined use of fly ash and lime did not provide significant reduction in the plasticity index compared to lime alone.

The direct shear test results demonstrated that both fiber reinforcement and lime stabilization significantly improved the shear strength parameter of grey shale soil and clay. For the control sample, the peak cohesion and internal friction angle were observed to be lower compared to the reinforced and stabilized samples. The inclusion of fiber increased the peak cohesion of grey shale, while lime stabilization further increased it. Similarly, the residual cohesion also showed improvements, with fiber-reinforced and lime-stabilized soils exhibiting higher values than the control. Lime stabilization, in particular, resulted in a significant increase in the internal friction angle.

The UCS results for grey shale and clay soils stabilized with lime and lime-fly ash indicated significant improvements. For grey shale, the UCS increased substantially with the addition of lime. Each 3% increment in lime content from 0% to 6% resulted in approximately a 200% increase in UCS. Specifically, there was a 113% increase from 0% to 3% lime, a 391% increase

from 0% to 6% lime, and a 150% improvement with the addition of 10% fly ash compared to 3% lime alone. Adding fly ash at higher lime contents had a limited effect, with UCS values for grey shale ranging from 61.2 to 300.7 psi for lime stabilization and 137 to 272 psi for lime and fly ash stabilization. For clay soil, the UCS increased by approximately 118% with 3% lime. However, increasing the lime content to 6% did not yield a further increase with the UCS. The addition of fly ash showed a limited impact on enhancing clay soil strength compared to lime-only stabilization, with UCS values ranging from 68 to 149 psi for lime stabilization and 119 to 146 psi for lime and fly ash stabilization.

The UCS results for grey shale and clay soils stabilized with lime and cement showed substantial improvements. For grey shale, the strength gains compared to the untreated sample showed an increasing trend with both lime and cement additions, reaching a maximum of 702% for 6% lime and 6% cement, with UCS values ranging from 129 to 490.8 psi. For clay soil, the initial UCS was 67.9 psi, and it increased significantly with the addition of cement and lime. The strength gains for BL0C3, BL3C3, BL6C3, BL0C6, BL3C6, and BL6C6 were approximately 201%, 211%, 259%, 323%, 333%, and 458%, respectively, compared to the untreated sample, with UCS values ranging from 204 to 379.2 psi. This trend demonstrates that the combined use of lime and cement significantly improves the strength of both grey shale and clay soils, particularly at higher lime and cement contents.

The UCS results for grey shale soil stabilized with lime and lime-fly ash after seven FT cycles showed that stabilization improved the resistance to freeze-thaw effects in the short term, but some reduction in strength was observed. Unstabilized grey shale experienced a significant reduction of approximately 47% after seven FT cycles. For grey shale stabilized with 3% lime, the UCS decreased by 28%. For samples stabilized with 6% lime, the UCS decreased by 32%, which

was higher than other combinations. The addition of 10% fly ash alongside lime also resulted in UCS reductions of 27% for 0% lime and 10% fly ash, 26% for 3% lime and 10% fly ash, and 27% for 6% lime and 10% fly ash. Among these combinations, 3% lime and 10% fly ash exhibited the least reduction in UCS.

The UCS results for clay soil stabilized with lime and lime-fly ash after seven FT cycles demonstrated the impact of different stabilization combinations. The UCS for unstabilized clay decreased by approximately 28%. For clay soil stabilized with 3% lime, the UCS decreased by 34%, indicating that lime alone resulted in a higher reduction compared to other combinations. Similar trends were observed for grey shale, where lime stabilization alone showed higher reductions in UCS after freeze-thaw cycles, suggesting that lime alone is less effective against freeze-thaw conditions. For samples stabilized with 6% lime, the UCS reduced by 18%. The addition of 10% fly ash alongside lime also resulted in UCS reductions: 30% for 10% fly ash, 17% for 3% lime and 10% fly ash, and 10% for 6% lime and 10% fly ash.

For grey shale, the UCS values ranged from 61.2 psi to 300.7 psi for lime-stabilized samples, 137 psi to 272 psi for lime and fly ash-stabilized samples, and 129 psi to 490.8 psi for samples stabilized with a combination of lime and cement, highlighting significant strength improvements with each stabilization method. Similarly, for clay soil, the UCS values ranged from 68 psi to 149 psi for lime-stabilized samples, 119 psi to 146 psi for lime and fly ash-stabilized samples, and 204 psi to 379.2 psi for samples stabilized with a combination of lime and cement, demonstrating notable enhancements in strength across all treatments.

The UCS results for grey shale stabilized with various combinations of cement and lime showed differences in resistance to freeze-thaw cycles. Grey shale stabilized with 3% cement experienced a significant reduction in UCS of 42%, highlighting the vulnerability of cement

stabilization alone. When 3% lime and 3% cement were used together, the UCS decreased by 32%, indicating an improvement in freeze-thaw resistance compared to cement alone. The combination of 6% lime and 3% cement resulted in a 26% reduction in UCS, showing better performance. The best resistance was observed with 6% lime and 6% cement, which demonstrated the highest UCS retention after seven freeze-thaw cycles, with a reduction of only 17%. This suggests that increasing lime content in combination with cement can effectively enhance the durability of grey shale under freeze-thaw conditions.

The UCS results for clay soil stabilized with various combinations of cement and lime showed different levels of resistance to freeze-thaw cycles. Clay soil stabilized with 3% cement exhibited a significant reduction in UCS of 32%, indicating vulnerability to freeze-thaw conditions. The combination of 3% lime and 3% cement showed a smaller decrease in UCS of 19%, suggesting improved resistance compared to cement alone. With 6% lime and 3% cement, the UCS reduction was 20%, showing moderate resistance. The best performance was observed with 6% cement, which had the lowest reduction of 4%, demonstrating the highest UCS retention among the tested combinations. This suggests that cement stabilization, especially at higher contents, is effective in improving the freeze-thaw durability of clay soil.

The UCS results for grey shale stabilized with lime and lime-fly ash after 12 freeze-thaw cycles demonstrated varying levels of resistance to strength degradation. Unstabilized grey shale experienced a significant reduction of 47%, which is similar to the reduction observed after seven freeze-thaw cycles, suggesting that the reduction impact becomes consistent after a certain number of cycles. Grey shale stabilized with 3% lime exhibited a UCS reduction of 14%, while the sample with 6% lime showed a reduction of only 10.5%, indicating that higher lime content improved resistance to freeze-thaw degradation. The addition of fly ash also enhanced resistance, with the

combination of 6% lime and 10% fly ash demonstrating the least reduction of 9%. These results indicate that incorporating both lime and fly ash, particularly at higher lime content, significantly enhances the freeze-thaw resistance of grey shale.

The UCS results for clay soil stabilized with lime and lime-fly ash after 12 freeze-thaw cycles demonstrated the varying levels of resistance to strength degradation. Unstabilized clay soil experienced a reduction of 28.3%, which is similar to the reduction observed after seven FT cycles, suggesting that the reduction in UCS for unstabilized soil may reach a stable level after a certain number of cycles. The sample stabilized with 3% lime showed a UCS reduction of 19%, while the sample with 6% lime showed a reduction of 13.8%, indicating that higher lime content effectively improved the soil's resistance to freeze-thaw degradation. The incorporation of fly ash with lime further enhanced resistance, with 0% lime and 10% fly ash resulting in a 22% reduction, while the combination of 3% lime and 10% fly ash exhibited a reduction of only 3.3%. The best performance was observed for the sample stabilized with 6% lime and 10% fly ash, which showed a negligible reduction of 0.6%, highlighting the effectiveness of this combination in enhancing the freeze-thaw resistance of clay soil.

The UCS results for grey shale stabilized with lime and cement after 12 freeze-thaw cycles demonstrated varying levels of resistance to strength degradation. The sample with 0% lime and 3% cement experienced a significant reduction of 39%. For the sample stabilized with 3% lime and 3% cement, the UCS decreased by 21%. The combination of 6% lime and 3% cement showed the smallest reduction of 5%, indicating that 6% lime and 3% cement is an effective combination for enhanced stability under freeze-thaw conditions. The sample with 0% lime and 6% cement exhibited a reduction of 32%, while the sample with 3% lime and 6% cement showed a decrease of 19%. Interestingly, the sample with 6% lime and 6% cement demonstrated a unique behavior,

with a 7% increase in UCS, likely due to ongoing pozzolanic reactions and cement hydration, which enhanced soil strength even under freeze-thaw conditions.

The UCS results for clay soil stabilized with lime and cement after 12 freeze-thaw cycles demonstrated different levels of resistance to strength degradation. The sample with 0% lime and 3% cement exhibited a reduction of 21.1%. The sample with 3% lime and 3% cement had a minor UCS reduction of 2.5%. In contrast, the sample with 6% lime and 3% cement showed a 3.9% increase, indicating improved resistance. For samples with 6% cement, the sample with 0% lime exhibited a reduction of 32.3%, while the sample with 3% lime showed a reduction of 10.2%. The sample with 6% lime demonstrated an increase of 7%, highlighting the effectiveness of this combination in enhancing freeze-thaw resistance. These results suggest that using 6% lime in combination with either 3% or 6% cement provides the best performance against freeze-thaw cycles for clay soil.

Fiber reinforcement slightly improved the strength, stiffness, and resistance to deformation of the clay subgrade under the LSTW test.. Additionally, fiber reinforcement led to a 14.7% reduction in total deformation which can be attributed to the increased residual strength of fiber reinforced soils.

Lime stabilization significantly improved strength, stiffness, and deformation resistance of grey shale soil under the LSTW test. The addition of 6% lime resulted in enhanced subgrade stability, as indicated by reduced DCP penetration values before and after traffic load application. Additionally, lime stabilization led to a 94.6% reduction in total deformation.

Chapter 7 Recommendations

Based on the findings of this study, the following recommendations are made in alignment with best practices for soil stabilization:

- The combined application of lime and fly ash is recommended to effectively reduce the plasticity index, ensuring it meets the specified requirements for highway construction.
- The use of fiber reinforcement is recommended for side works, including embankments and shoulders, particularly on slope construction, to enhance the friction and stability of the stabilized material, in accordance with NDOT guidelines.
- The Dynamic Cone Penetrometer is recommended for verifying site compliance and ensuring the stabilization strength and thickness meet project specifications.
- Considering the reduction in unconfined compressive strength due to freeze-thaw cycles after two sites of testing, it is recommended to use the minimum specified combination of lime, cementitious materials, and soil type as indicated in Table 7.1, to comply with NDOT stabilization requirements.

Table 7.1 Summary of soil stabilization recommendations for lime, fly ash, cement, and their combination applications.

Minimum Stabilizer Dosage (% by weight)	Soil Group Classification (AASHTO)	
	A7-6 (Grey Shale) ^a	A7-5 (Clay) ^a
Lime	6% ^b	3% ^b
Cement	-	6%
Lime- Fly ash	3%-10%	3%-10%
Lime-Cement	6%-3%	3%-6%

The blank table indicates the additives are not recommended.

The recommendations are based on the findings of this research and are specifically applicable to the soil types investigated in this study.

a: Sulfate content < 3000 ppm.

b: Trial mix should be performed to achieve the target pH and UCS as recommended.

References

- AASHTO. (2020). Mechanistic-empirical pavement design guide: A manual of practice. Washington, DC: AASHTO.
- ASTM Committee D2166/D2166M. (2016). Test method for unconfined compressive strength of cohesive soil. ASTM International.
- ASTM Committee D4318-17e1 on Soil and Rock. (2018). Standard test methods for liquid limit, plastic limit, and plasticity index of soils. ASTM International.
- ASTM International. (2022). Standard Test Methods for Unconfined Compressive Strength of Compacted Soil-Lime Mixtures (ASTM D5102/D5102M-22). Retrieved from <https://standards.iteh.ai/catalog/standards/astm/80ab502f-7af2-47ee-acd5-61c54acb6300/astm-d5102-d5102m-22>.
- ASTM International. (2023). Standard test method for direct shear test of soils under consolidated drained conditions (ASTM D3080/D3080M-23). Retrieved from https://www.astm.org/d3080_d3080m-23
- ASTM International. (2024). Standard test methods for freezing and thawing compacted soil-cement mixtures (ASTM D560/D560M-24). Retrieved from https://www.astm.org/d0560_d0560m-24.html
- ASTM, D. (2021). Standard Test Methods for Laboratory Compaction Characteristics of Soil Using Standard Effort (12 400 ft-lbf/ft³). D698-12.
- Akula, P., Hariharan, N., Little, D. N., Lesueur, D., & Herrier, G. (2020). Evaluating the long-term durability of lime treatment in hydraulic structures: Case study on the Friant-Kern Canal. *Transportation Research Record*, 2674(6), 431–443. <https://doi.org/10.1177/0361198120919404>
- Bagshaw, S. A., Herrington, P. R., Kathirgamanathan, P., & Cook-Opus International Consultants LTD. (2015). Geosynthetics in basecourse stabilization. Research Report 574, Wellington, New Zealand: New Zealand Transportation Agency.
- Basma, A. A., & Tuncer, E. R. (1991). Effect of lime on volume change and compressibility of expansive clays. *Transportation Research Record*, (1295).
- Bell, F. G. (1996). Lime stabilization of clay minerals and soils. *Engineering Geology*, 42(4), 223–237. [https://doi.org/10.1016/0013-7952\(96\)00028-2](https://doi.org/10.1016/0013-7952(96)00028-2)
- Bhattacharja, S., & Bhatta, J. I. (2003). Comparative performance of Portland cement and lime stabilization of soils. *Portland Cement Association Research and Development Bulletin*.

- California Department of Transportation. (2021). Guidelines for the Stabilization of Subgrade Soils in California. California Department of Transportation.
- Consoli, N. C., Casagrande, M. D., Prietto, P. D., & Thomé, A. N. (2003). Plate load test on fiber-reinforced soil. *Journal of Geotechnical and Geoenvironmental Engineering*, 129(10), 951–955.
- Consoli, N. C., Zortéa, F., de Souza, M., & Festugato, L. (2011). Studies on the dosage of fiber-reinforced cemented soils. *Journal of Materials in Civil Engineering*, 23(12), 1624–1632.
- Cui, Z. D., Huang, M. H., Hou, C. Y., & Yuan, L. (2023). Seismic deformation behaviors of the soft clay after freezing-thawing. *Geomechanics and Engineering*, 34(3), 303. <https://doi.org/10.12989/gae.2023.34.3.303>
- Elseifi, M., & Dhakal, N. (2017). Lime Utilization in the Laboratory, Field, and Design of Pavement Layers (No. FHWA/LA. 16/575). Louisiana State University. Department of Civil and Environmental Engineering.
- Eun, J., Kim, S., Ibdah, L., & Owusu, K. (2024). Application of Microfiber Reinforcement to Weak Soils for Alternative Road Stabilization Strategy. Mid-America Transportation Center, University of Nebraska-Lincoln.
- Eun, J., Kim, S., Robertson, D., Alhowaidi, Y., Van, H., Ibdah, L., & Owusu, K. (2024). Development of Guideline for the Use of Geosynthetics in Different Roadway Layered System in Nebraska (No. PR-FY21 (002)). Nebraska Department of Transportation.
- Ferguson, G., & Levorson, S. M. (1999). Soil and pavement base stabilization with self-cementing coal fly ash. American Coal Ash Association.
- Georgia Department of Transportation. (2021). Standard Specifications for the Construction of Transportation Systems. Georgia Department of Transportation. Retrieved from <https://www.dot.ga.gov/PartnerSmart/Business/Source/specs/ss225.pdf>.
- Halsted, G. E., Adaska, W. S., & McConnell, W. T. (2008). Guide to Cement-Modified Soil (CMS). Portland Cement Association.
- Herath, A., Mohammad, L. N., Gaspard, K., Gudishala, R., & Abu-Farsakh, M. Y. (2005). The use of dynamic cone penetrometer to predict resilient modulus of subgrade soils. In *Advances in pavement engineering* (pp. 1-16).
- Hohmann-Porebska, M. (2002). Microfabric effects in frozen clays in relation to geotechnical parameters. *Applied Clay Science*, 21(1-2), 77-87. doi: [https://doi.org/10.1016/S0169-1317\(01\)00094-1](https://doi.org/10.1016/S0169-1317(01)00094-1).
- Hoover, J., Moeller, D., Pitt, J., Smith, S., & Wainaina, N. (1982). Performance of randomly oriented fiber-reinforced roadway soils: A laboratory and field investigation. Iowa DOT Project HR-211, Iowa State University, Department of Civil Engineering, Ames, Iowa.

- Hotineanu, A., Bouasker, M., Aldaood, A., & Al-Mukhtar, M. (2015). Effect of freeze–thaw cycling on the mechanical properties of lime-stabilized expansive clays. *Cold Regions Science and Technology*, 119, 151-157. doi: <https://doi.org/10.1016/j.coldregions.2015.08.008>
- Jaradat, K. A., Darbari, Z., Elbakhshwan, M., Abdelaziz, S. L., Gill, S. K., Dooryhee, E., & Ecker, L. E. (2017). Heating-freezing effects on the orientation of kaolin clay particles. *Applied Clay Science*, 150, 163-174. doi: <https://doi.org/10.1016/j.clay.2017.09.028>
- Kakroudi, H. A., Bayat, M., & Nadi, B. (2024). Static and dynamic characteristics of silty sand treated with nano-silica and basalt fiber subjected to freeze-thaw cycles. *Geomechanics and Engineering*, 37(1), 085. <https://doi.org/10.12989/gae.2024.37.1.085>
- Kaniraj, S. R., & Havanagi, V. G. (2001). Behavior of cement-stabilized fiber-reinforced fly ash-soil mixtures. *Journal of Geotechnical and Geoenvironmental Engineering*, 127(7), 574–584.
- Kim, S. S., Frost, J. D., Durham, S. A., Geum Chorzepa, M., Hanumasagar, S. S., & Wright, J. (2019). Development of geosynthetic design and construction guidelines for pavement embankment construction in North Georgia (No. FHWA-GA-19-1611). Georgia Department of Transportation.
- Kumar, A., Singh, R., & Patel, S. (2024). Assessment of durability of chemically stabilized soils using different moisture-susceptible methods. *Journal of Geotechnical Engineering*.
- Kumar, A., Walia, B. S., & Bajaj, A. (2007). Influence of fly ash, lime, and polyester fibers on compaction and strength properties of expansive soil. *Journal of Materials in Civil Engineering*, 19(3), 242–248.
- Li, J. (2003). Experimental investigations on mechanical behavior of unsaturated subgrade soil with lime stabilization and fiber reinforcement (No. MD-03-SP107B4J). Maryland State Highway Administration, Research Division.
- Li, S., Lai, Y., Pei, W., Zhang, S., & Zhong, H. (2014). Moisture–temperature changes and freeze–thaw hazards on a canal in seasonally frozen regions. *Natural Hazards*, 72, 287–308. <https://doi.org/10.1007/s11069-013-1021-3>
- Little, D. N. (1999). Evaluation of structural properties of lime stabilized soils and aggregates. National Lime Association.
- Louisiana Department of Transportation. (2016). Standard specifications for roads and bridges: Part 3, Section 305. Louisiana Department of Transportation.
- Maher, M. H., & Ho, Y. C. (1994). Mechanical Properties of Kaolinite/Fiber Soil Composite. *Journal of Geotechnical Engineering*, 120(8), 1381-1393.

- McDowell, C. (1959). Stabilization of soils with lime, lime-flyash, and other lime reactive materials. Highway Research Board Bulletin, 231(1), 60–66.
- National Lime Association. (2004). Lime treated soil construction manual. Arlington, VA: NLA.
- National Weather Service. (2022). 2022 Climate Summary. Retrieved from <https://www.weather.gov/oax/2022climatesummary>.
- Nebraska Department of Transportation. (2018). NDOT Pavement Design Manual. Nebraska Department of Transportation.
- Negi, A. S., Faizan, M., Siddharth, D. P., & Singh, R. (2013). Soil stabilization using lime. International Journal of Innovative Research in Science, Engineering and Technology, 2(2), 448-453.
- Nguyen, T. T. H., Cui, Y. J., Ferber, V., Herrier, G., Ozturk, T., Plier, F., & Tang, A. M. (2019). Effect of freeze-thaw cycles on mechanical strength of lime-treated fine-grained soils. Transportation Geotechnics, 21, 100281. doi: <https://doi.org/10.1016/j.trgeo.2019.100281>
- Newman, J. K., & White, D. J. (2008). Rapid assessment of cement and fiber-stabilized soil using roller-integrated compaction monitoring. Transportation Research Record, 2059(1), 95–102.
- North Carolina Department of Transportation. (2018). Standard specifications for roads and structures. North Carolina Department of Transportation.
- Olgun, M. (2013). The effects and optimization of additives for expansive clays under freeze–thaw conditions. Cold Regions Science and Technology, 93, 36-46. doi: <https://doi.org/10.1016/j.coldregions.2013.06.001>
- Padmaraj, D., & Arnepalli, D. N. (2023). Carbonation in lime-stabilized clays: Mechanism, effects, and future prospects. Bulletin of Engineering Geology and the Environment, 82(7), 258. <https://doi.org/10.1007/s10064-023-03273-6>
- Rabab’ah, S. R., Taamneh, M. M., Abdallah, H. M., Nusier, O. K., & Ibdah, L. (2021). Effect of adding zeolitic tuff on geotechnical properties of lime-stabilized expansive soil. KSCE Journal of Civil Engineering, 25, 4596-4609. doi: <https://doi.org/10.1007/s12205-021-1603-7>
- Ramsey, W. S., Haliburton, T. A., & Walker, J. W. (1957). Lime stabilization for highways. Highway Research Board Bulletin, 128, 1–13.
- Sadiq, M. F., Naqvi, M. W., Cetin, B., & Daniels, J. (2023). Role of temperature gradient and soil thermal properties on frost heave. Transportation Research Record. <https://doi.org/10.1177/03611981221147261>

- Santoni, R. L., & Webster, S. L. (2001). Airfields and roads construction using fiber stabilization of sands. *Journal of Transportation Engineering*, 127(2), 96–104.
- Sargent, P. (2015). The development of alkali-activated mixtures for soil stabilisation. In *Handbook of Alkali-Activated Cements, Mortars and Concretes* (pp. 555–604). Woodhead Publishing.
- Sharma, N. K., Swain, S. K., & Sahoo, U. C. (2012). Stabilization of a clayey soil with fly ash and lime: A micro level investigation. *Geotechnical and Geological Engineering*, 30, 1197–1205. <https://doi.org/10.1007/s10706-012-9531-y>
- Sirivitmaitrie, C., Puppala, A. J., Chikyala, V., Saride, S., & Hoyos, L. R. (2008). Combined lime and cement treatment of expansive soils with low to medium soluble sulfate levels. *GeoCongress 2008: GeoSustainability and GeoHazard Mitigation*. [https://doi.org/10.1061/40971\(310\)42](https://doi.org/10.1061/40971(310)42)
- Sirivitmaitrie, C., Puppala, A. J., Saride, S., & Hoyos, L. (2011). Combined lime–cement stabilization for longer life of low-volume roads. *Transportation research record*, 2204(1), 140–147.
- Solanki, P., Zaman, M., & Laguros, J. G. (2013). Effect of freeze-thaw cycles on performance of stabilized subgrade. *Journal of Materials in Civil Engineering*, 25(10), 1419–1427. [https://doi.org/10.1061/\(ASCE\)MT.1943-5533.0000697](https://doi.org/10.1061/(ASCE)MT.1943-5533.0000697)
- Svensson, P. D., & Hansen, S. (2010). Freezing and thawing of montmorillonite—A time-resolved synchrotron X-ray diffraction study. *Applied Clay Science*, 49(3), 127–134. doi: <https://doi.org/10.1016/j.clay.2010.04.015>
- Texas Department of Transportation. (2019). Treatment guidelines for soils and base in pavement structures. Texas Department of Transportation. Retrieved from <https://ftp.txdot.gov/pub/txdot/mtd/treatment-guidelines.pdf>
- Ural, N. (2021). The significance of scanning electron microscopy (SEM) analysis on the microstructure of improved clay: An overview. *Open Geosciences*, 13(1), 197–218.
- Virginia Department of Transportation. (2020). Road and Bridge Specifications. Virginia Department of Transportation. Retrieved from <https://www.vdot.virginia.gov/doing-business/technical-guidance-and-support/technical-guidance-documents/road-and-bridge-specifications>
- White, D. J., & Vennapusa, P. K. R. (2013). Cement stabilization with fiber reinforcement of subbase. Iowa State University, Institute for Transportation. Retrieved from https://intrans.iastate.edu/app/uploads/2018/03/cement_fibers_tb1.pdf

Appendix A

A.1 Soil preparation



Figure A.1 Air drying the wet soil.



Figure A.2 Grinding clay soil.



Figure A.3 Clay soil after grinding.



Figure A.4 Breaking down clay soil clumps using a rubber mallet to achieve finer particles for testing.

A.2 UCS samples preparation and testing



Figure A.5 Grey shale divided into three equal layers for consistent compaction and testing.



Figure A.6 Pouring Grey shale soil into the UCS mold for sample preparation and compaction.



Figure A.7 Extracting UCS samples from the mold using a hydraulic jack.



Figure A.8 Prepared UCS sample of grey shale soil, ready for UCS testing.

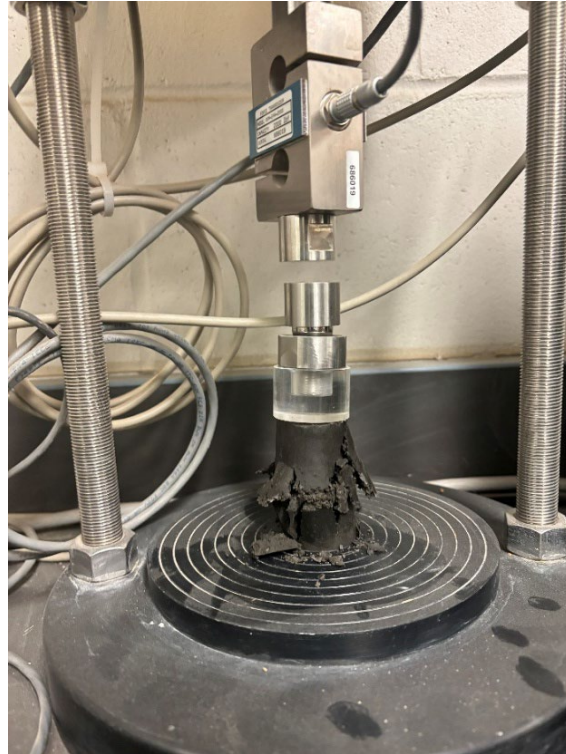


Figure A.9 UCS sample after testing.



Figure A.10 Mixing clay soil with fiber reinforcement



Figure A.11 Fiber-reinforced clay sample under the testing machine.

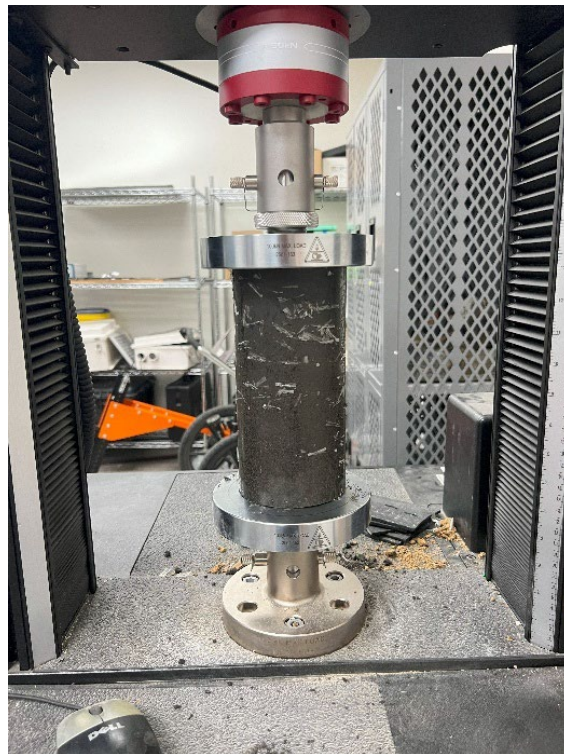


Figure A.12 Fiber-reinforced grey shale sample under the testing machine.



Figure A.13 Fiber-reinforced clay sample after testing.

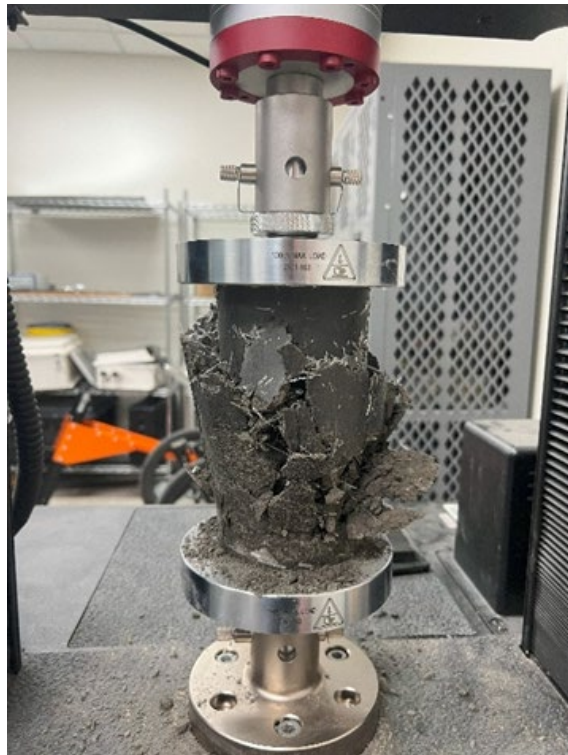


Figure A.14 Fiber-reinforced grey shale sample after testing.

A.3 LSTW preparation and sensor installation

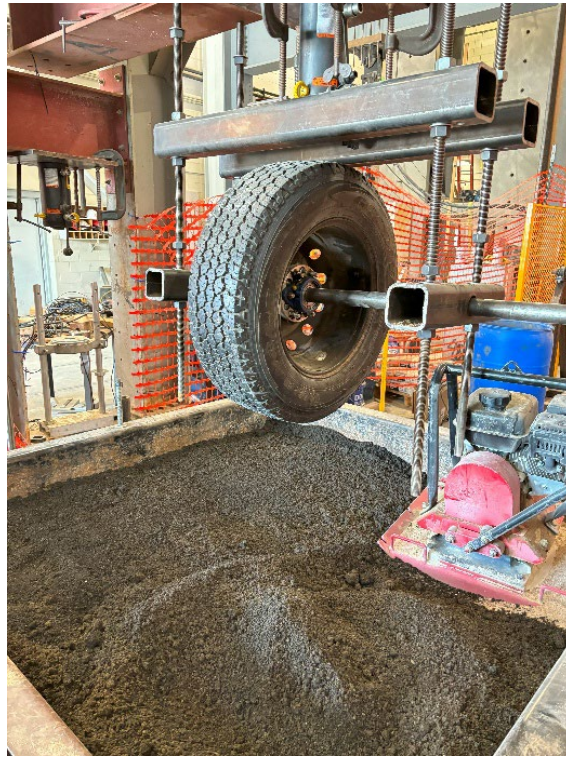


Figure A.15 Pouring grey shale soil to prepare the first lift of the grey shale base layer for testing.



Figure A.16 Installing the middle pressure cell after compacting the first lift of the grey shale base layer to measure stress distribution.



Figure A.17 Leveling the surface after compacting the second lift of the grey shale.



Figure A.18 This picture was taken during the test, capturing the deformation during the test.



Figure A.19 Measuring permanent rutting depth using a tape measure after terminating the test on the grey shale base layer.



Figure A.20 Pour 0000the mixed fiber and clay soil to prepare the first lift of the fiber-reinforced clay base layer.



Figure A.21 Installing pressure sensors within the fiber-reinforced clay layer.



Figure A.22 Performing a sand cone test to measure the density of the compacted fiber-reinforced clay layer.

Appendix B

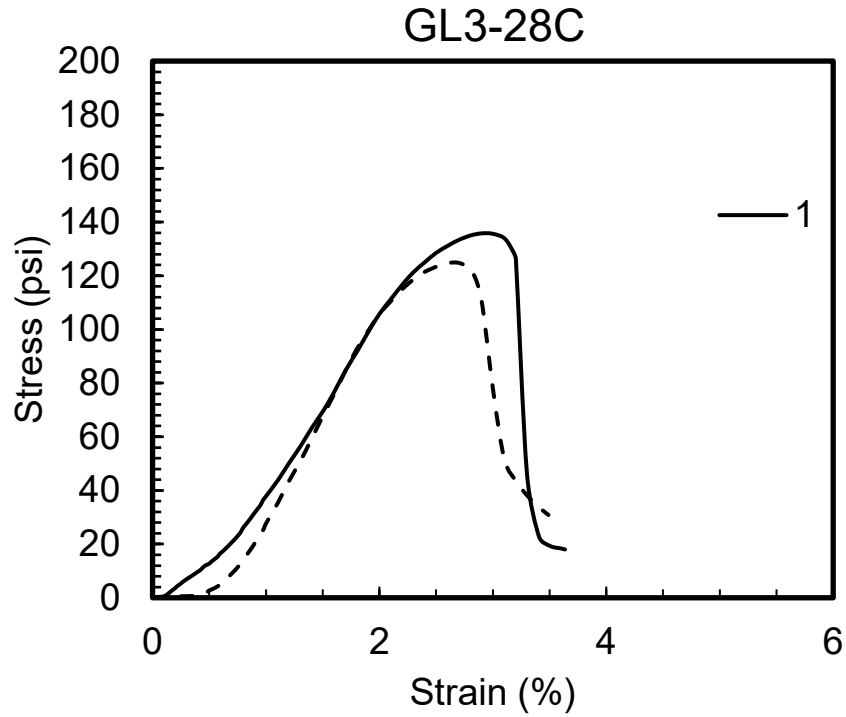


Figure B.1 Stress vs. strain curves for two samples of grey shale stabilized with 3% lime.

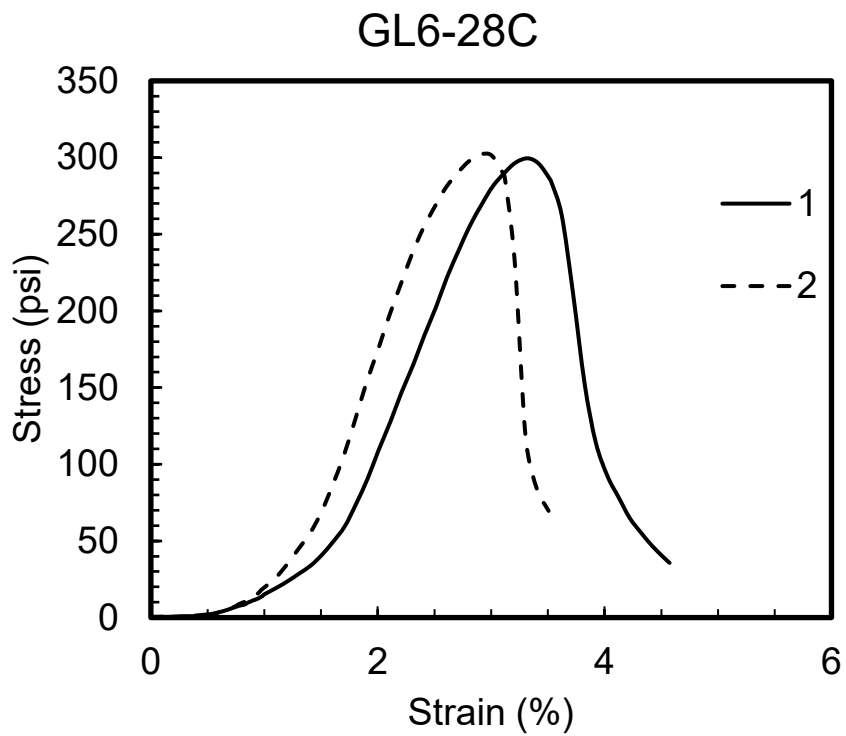


Figure B.2 Stress vs. strain curves for two samples of grey shale stabilized with 6% lime.

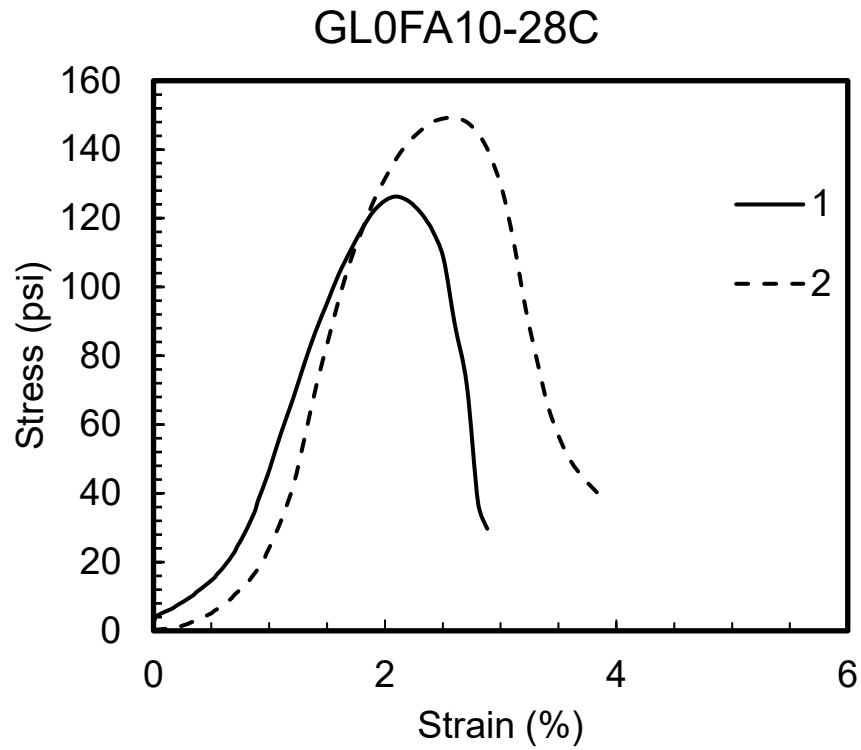


Figure B.3 Stress vs. strain curves for two samples of grey shale stabilized with 10% fly ash.

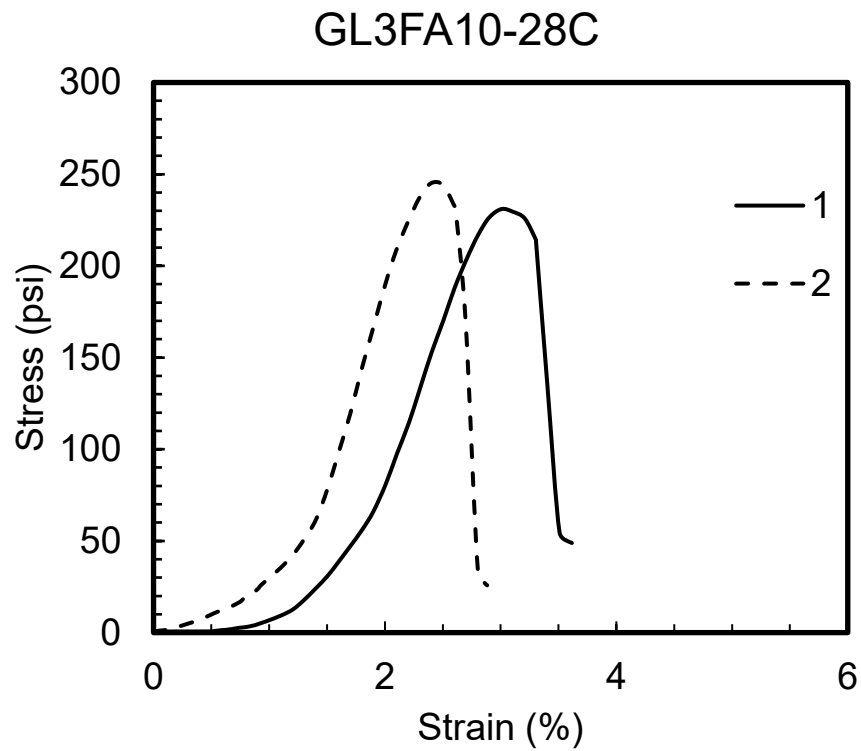


Figure B.4 Stress vs. strain curves for two samples of grey shale stabilized with 3% lime and 10% fly ash.

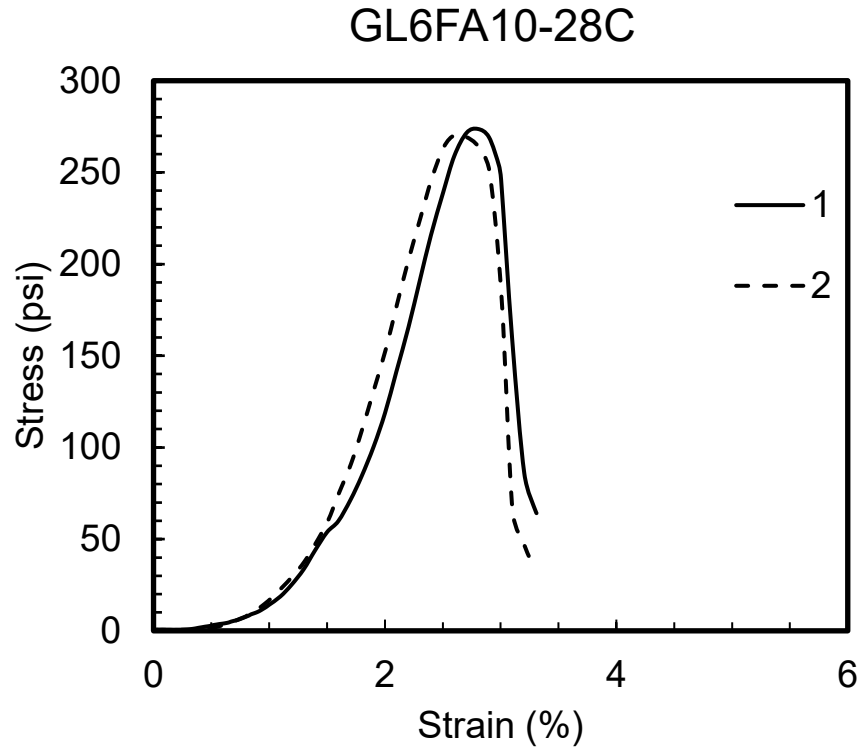


Figure B.5 Stress vs. strain curves for two samples of grey shale stabilized with 6% lime and 10% fly ash.

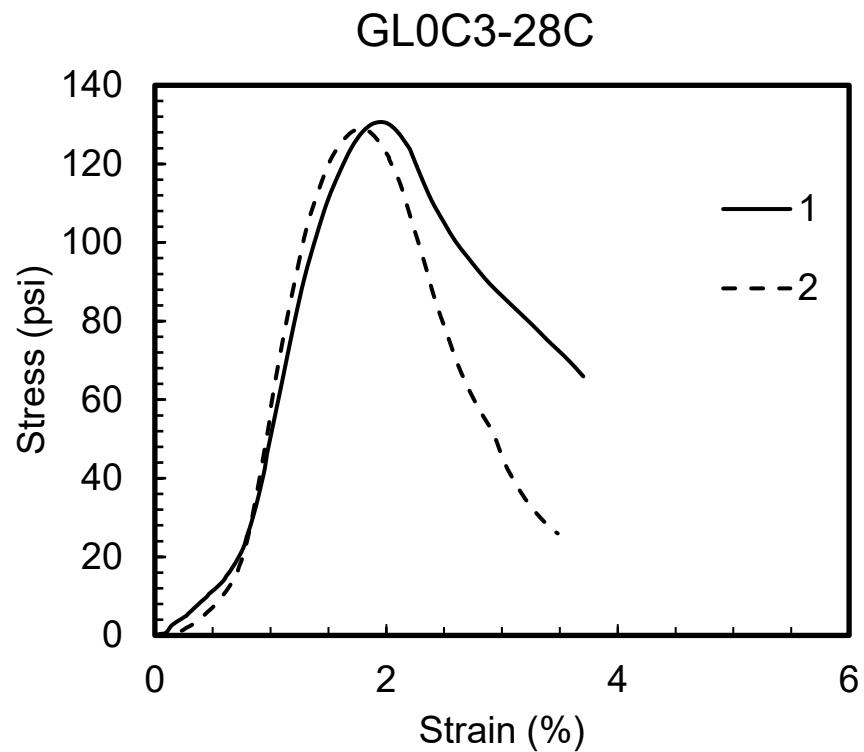


Figure B.6 Stress vs. strain curves for two samples of grey shale stabilized with 3% cement.

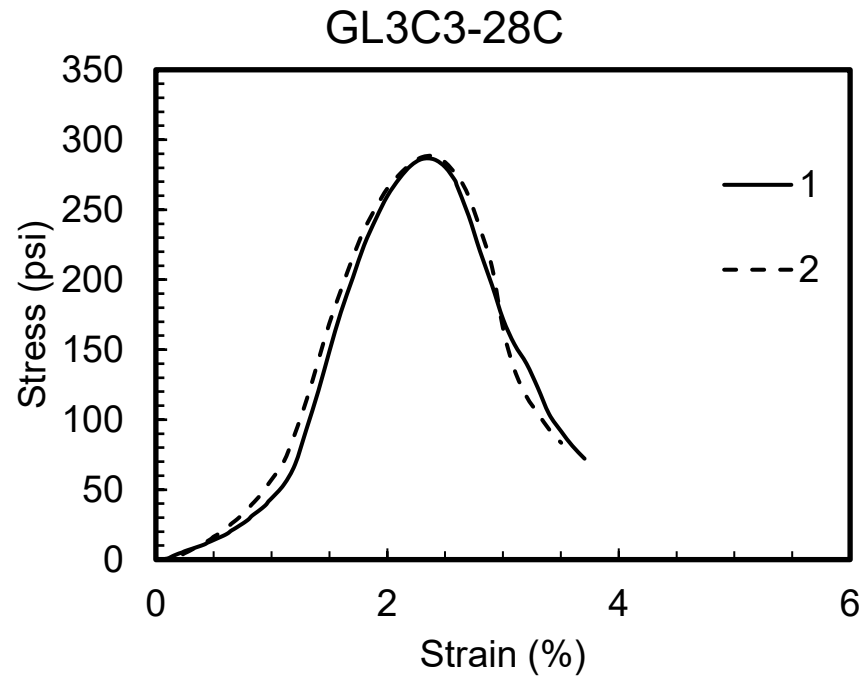


Figure B.7 Stress vs. strain curves for two samples of grey shale stabilized with 3% lime and 3% cement.

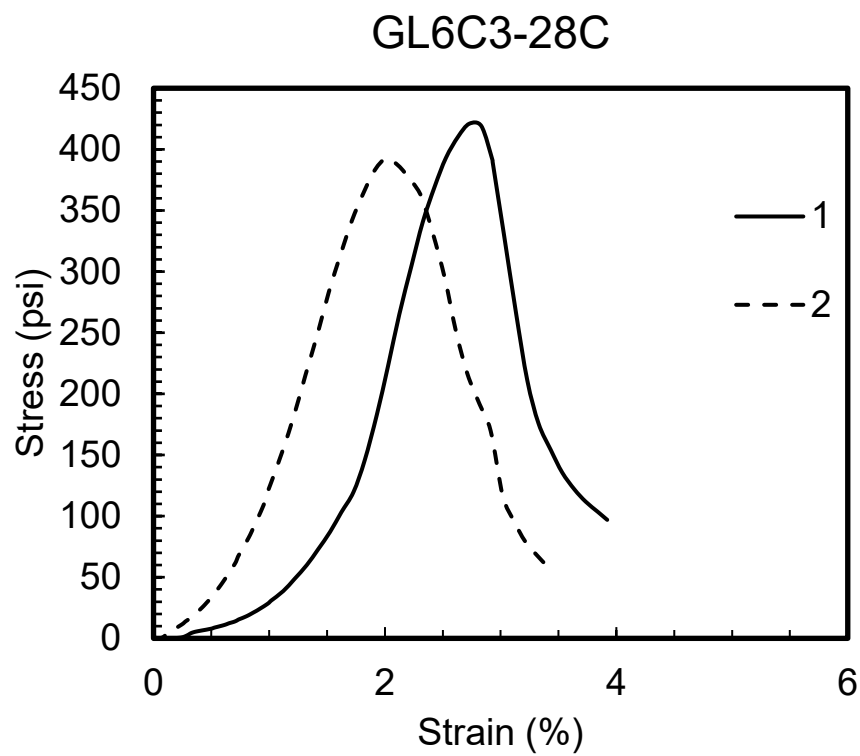


Figure B.8 Stress vs. strain curves for two samples of grey shale stabilized with 6% lime and 3% cement.

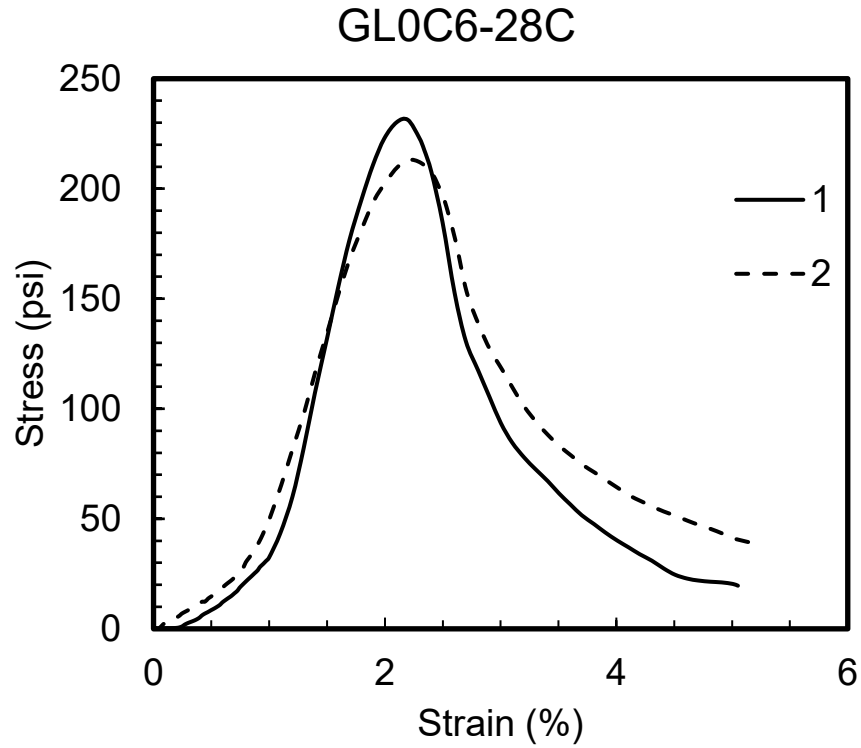


Figure B.9 Stress vs. strain curves for two samples of grey shale stabilized with 6% cement.

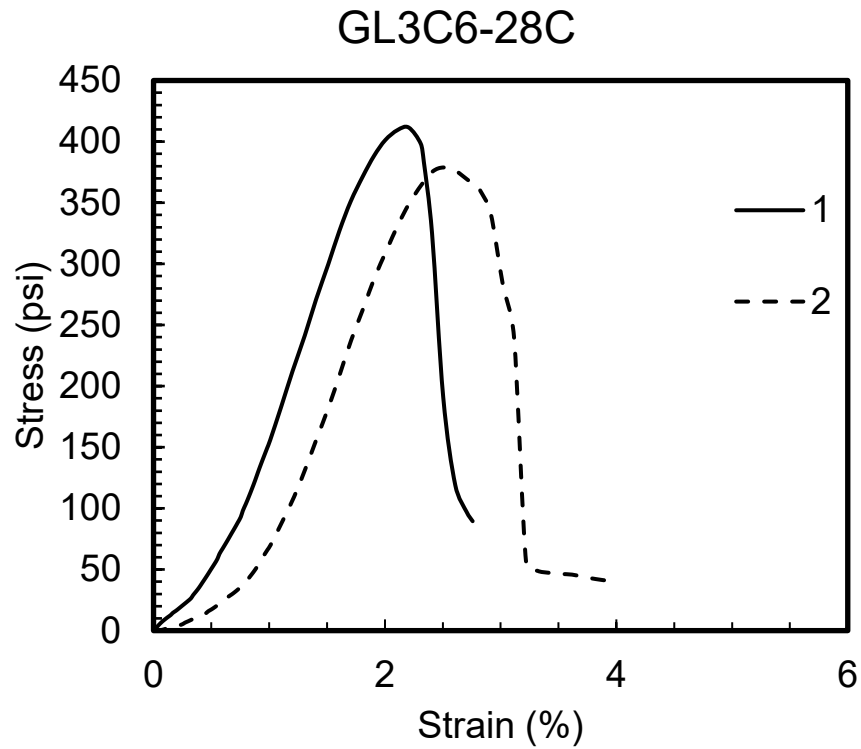


Figure B.10 Stress vs. strain curves for two samples of grey shale stabilized with 3% lime and 6% cement.

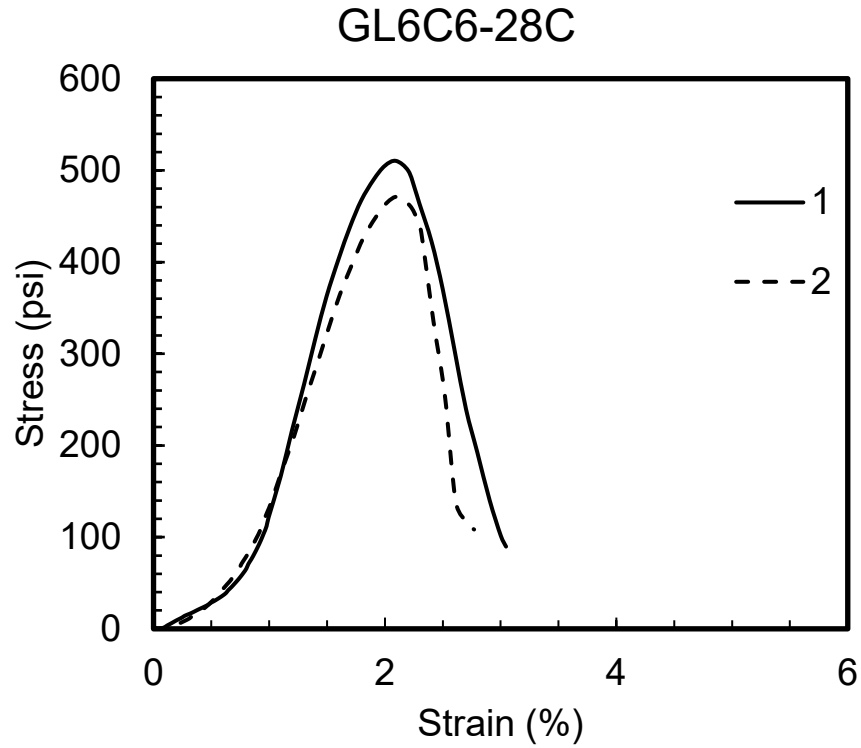


Figure B.11 Stress vs. strain curves for two samples of grey shale stabilized with 6% lime and 6% cement.

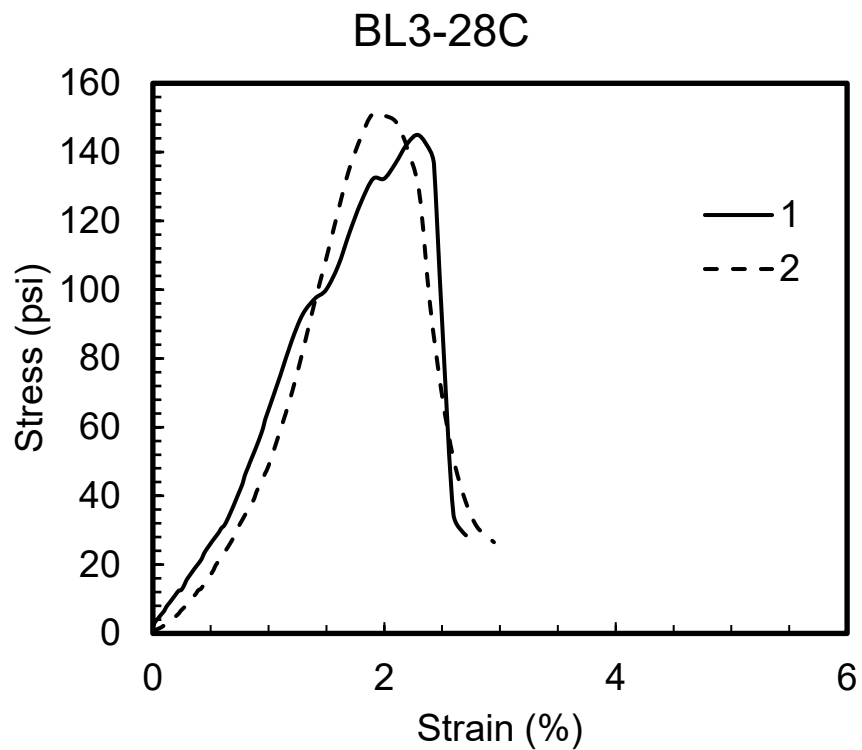


Figure B.12 Stress vs. strain curves for two samples of grey shale stabilized with 3% lime .

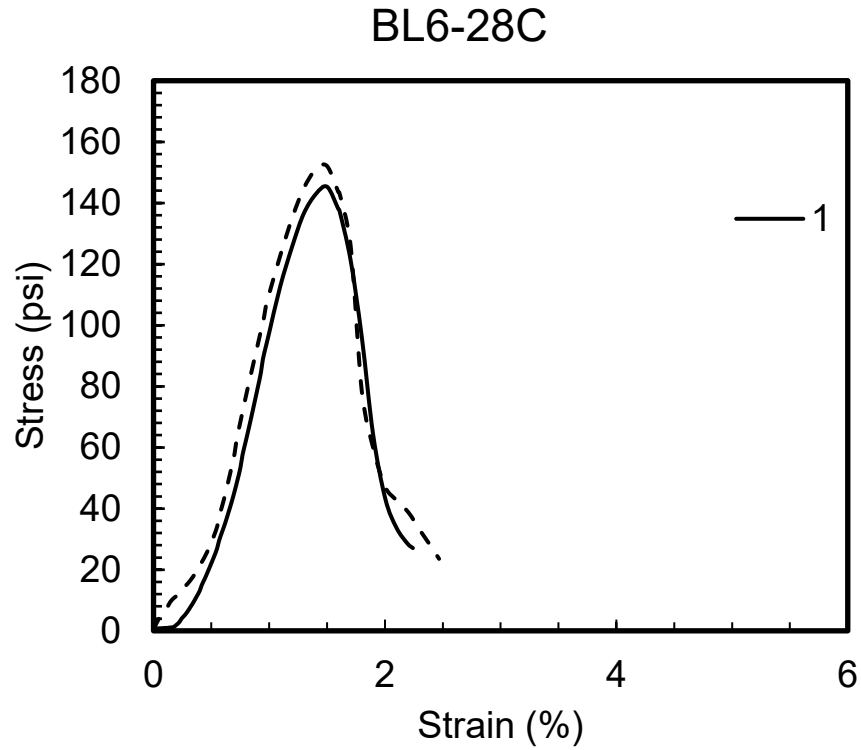


Figure B.13 Stress vs. strain curves for two samples of grey shale stabilized with 6% lime.

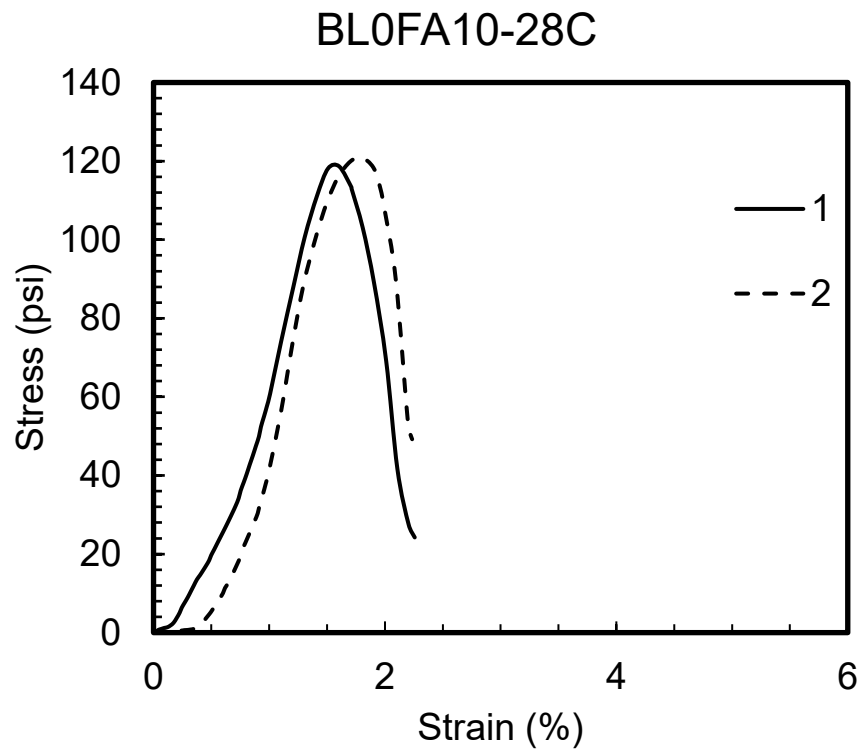


Figure B.14 Stress vs. strain curves for two samples of grey shale stabilized with 0% lime and 10 fly ash.

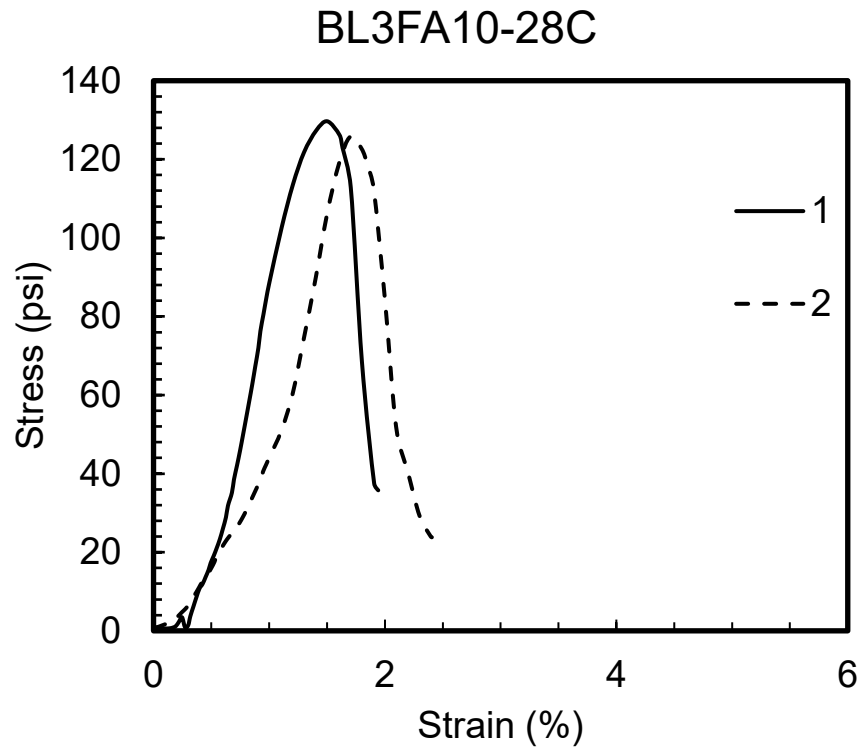


Figure B.15 Stress vs. strain curves for two samples of grey shale stabilized with 3% lime and 10 fly ash.

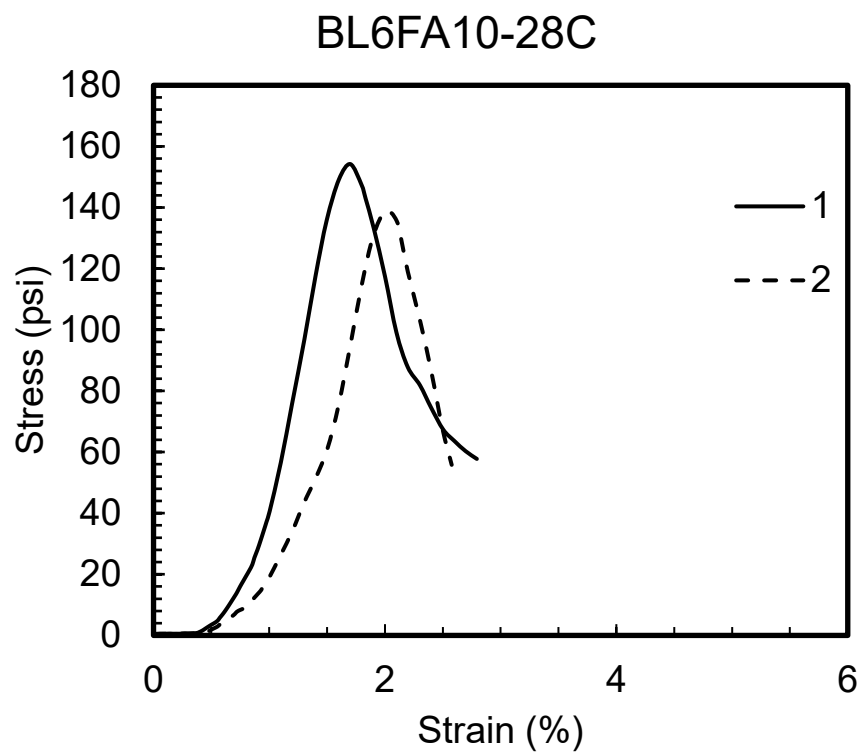


Figure B.16 Stress vs. strain curves for two samples of grey shale stabilized with 6% lime and 10 fly ash

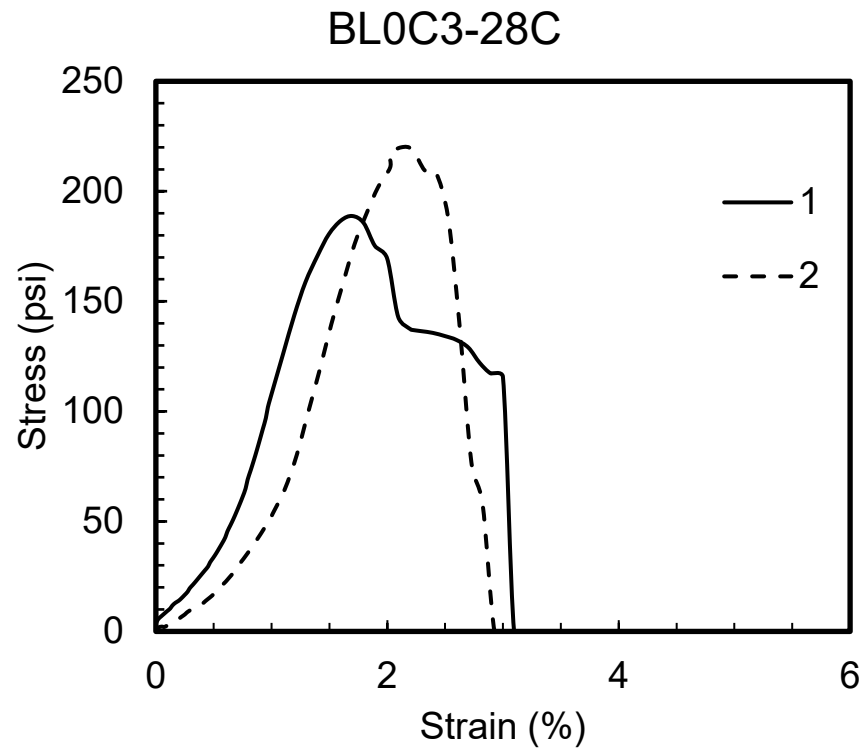


Figure B.17 Stress vs. strain curves for two samples of grey shale stabilized with 3% cement.

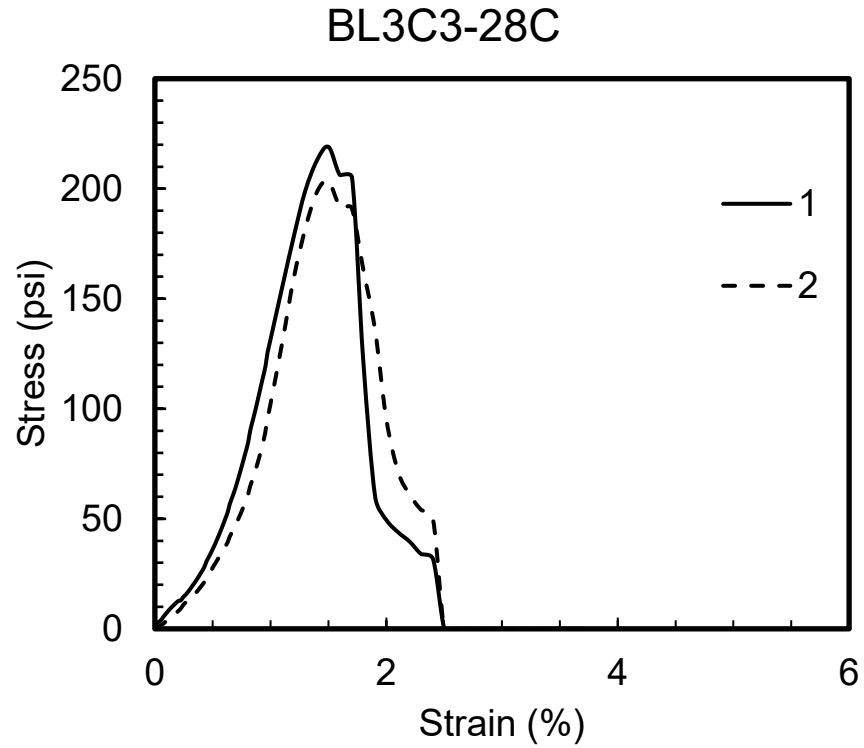


Figure B.18 Stress vs. strain curves for two samples of grey shale stabilized with 3% lime and 3% cement

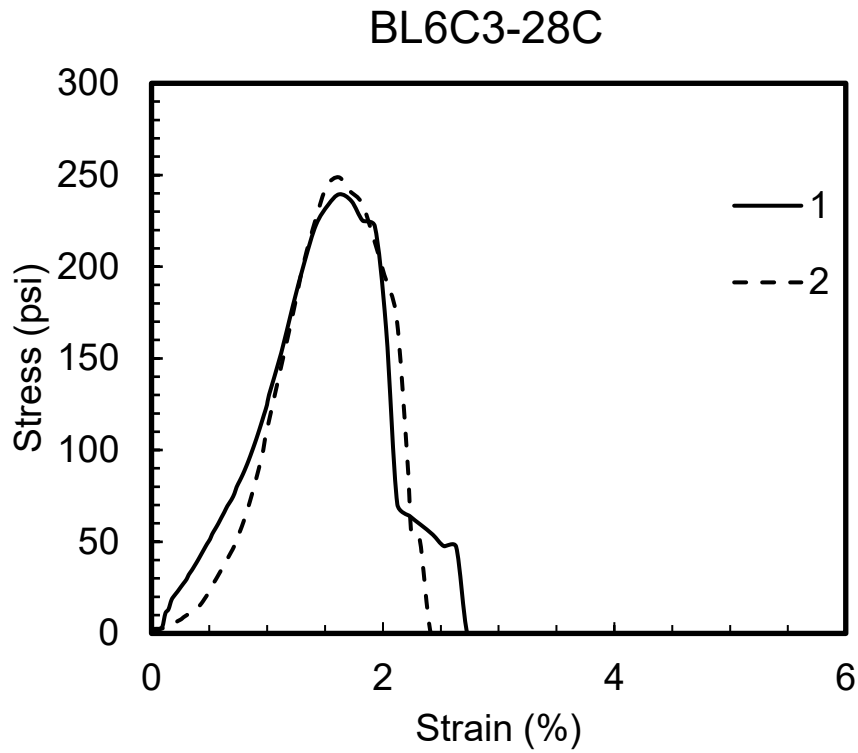


Figure B.19 Stress vs. strain curves for two samples of grey shale stabilized with 6% lime and 3% cement.